NUMERICAL SIMULATIONS OF COASTALLY TRAPPED DISTURBANCES

By

Hai Fu

B.S., Nanjing University, 1993

A THESIS SUBMITTED IN PARTIAL FULFILLMENT OF

THE REQUIREMENTS FOR THE DEGREE OF

MASTER OF SCIENCE

in

ENVIRONMENTAL SCIENCE

THE UNIVERSITY OF NORTHERN BRITISH COLUMBIA

March 1999

Abstract

Coastally trapped disturbances (CTDs) are trapped horizontally by the Coriolis force and vertically by a subsidence temperature inversion to propagate along coastal mountains. There are sudden temperature drops and wind reversals in CTD events. CTDs are initiated as gravity currents in a 3 dimensional mesoscale numerical model in this research by cooling the model lower atmosphere near the shore. The RAMS model is used in a sensitivity testing mode to examine the influences of the following factors on the evolution of CTDs:

1. different initial synoptic wind speeds
2. initial cooling amount and cooling area
3. topography that descends in the direction of propagation
4. different valleys that dissect coastal mountains
5. sea surface temperature
6. the presence of a near-shore island such as Vancouver Island

The results show that:

1. The larger the initial northerly wind is, the smaller the offshore scale of a CTD is.

2. CTDs are very sensitive to initial cooling conditions by which they are created. The larger the cooling amount is, the stronger a CTD is. The effect of cooling area depends on initial cooling amount. The influence of different cooling areas can be the opposite with different initial cooling amount.

3. The propagation speed of CTDs is greatly reduced in the case of descending topography.

4. Valleys which dissect the coastal mountains greatly reduce the off-shore scales of CTDs.

5. When the sea surface temperature is close to the potential temperature of the lower atmosphere after cooling, a front comes into being in the lower atmosphere and the propagation speed of CTDs is enhanced.

6. Simulations show that near-shore islands may split a CTD with trapped disturbances propagating along both the island and mainland.

Table of Contents

List of Tables

List of Figures

Chapter 1

Introduction

1.1 What are Coastally Trapped Disturbances?

Coastally Trapped Disturbances(CTDs) are meteorological phenomena propagating along coastal mountains. In the northern hemisphere they propagate with the coast on the right while in southern hemisphere the coast is on the left. CTDs can be either troughs of low pressure or ridges of high pressure, depending on the nature of the initial disturbance. They are trapped vertically by a marine inversion which inhibits vertical motion, and trapped horizontally by the Coriolis force which pushes them against the coastal mountains. In North American CTDs there can be sudden wind reversals from northerly to southerly, a temperature drop and a dramatic increase of low clouds and fog when a CTD reaches a coastal region (Reason, 1989). Sea surface air pressure increases with the arrival of CTDs in North America and Australia while pressures decrease in South African CTDs (i.e. they are troughs). The length scales for mid-latitude CTDs are usually a Rossby radius (around 300 km) in the across-shore direction, around 1000 km in the alongshore direction, and 0.2-1 km vertically. They have a time scale of 1 day or more and occur 4-5 times a summer along the U.S. west coast. In winter there are usually no observations of CTD in North America (Reason, 1989).

See Fig. 1.1 for a schematic picture of a CTD (Dorman, 1987). Fig. 1.2 illustrates the

topography of North American Pacific coast where CTDs occur (Mass and Albright, 1987).

1.2 Where and how do CTDs occur?

CTDs have been observed in many areas of the world (Reason, 1989). The CTDs in South Africa, Southern Australia and the west coast of North America are the best known. In South Africa the coastally trapped lows usually originate in southwest Africa and propagate eastward around the subcontinent, generally as far as Durban (Reason, 1989). In Southeast Australia the coastally trapped ridges originate in the marine layer in Southern Victoria, near the western end of the Great Dividing Range, and sometimes can propagate 2000 km along the coastal mountains. Along the North American west coast the coastally trapped ridges propagate in the marine layer from California to the Pacific North West. Sometimes they can propagate as far as Vancouver Island (Reason and Dunkley, 1993). There is evidence that CTDs also exist in South America and Northwest Africa (Reason, 1989). CTDs have been observed occasionally along the Beaufort Sea coastline (Kubu, 1997). Large land-sea temperature differences can be observed on both the meso- and synoptic scales in each case (Reason, 1989). In a region where a large land-sea temperature difference exists the chances of observing a disturbance are increased. A change of wind direction may bring cold marine air to the coastal region originally occupied by warm continental air and cause an aberration from the original state (Mass and Albright, 1987). For the CTDs to propagate, steep mountains along the coast are important because the CTDs are trapped horizontally by these mountains. A temperature inversion below the mountain crest is also an important factor for a CTD to propagate in a region.

1.2.1 How CTDs are trapped along the coastal mountains

Horizontal trapping mechanism

The Coriolis force is important for topographic trapping of CTDs because these disturbances are restricted inside a certain zone offshore of the mountains. The Coriolis force is an "imaginary" force that must be applied in a rotating system so that Newton's second law remains valid (e.g. Holton(1979)). In other words, Coriolis is the way of compensating for the earth based coordinate system. In the northern hemisphere, the Coriolis force acts to the right of the velocity. The Coriolis force makes CTDs propagate with the continent on the right in the northern hemisphere and on the left in the southern hemsiphere (Reason, 1989). Thus northward moving air along the North American west coast is pushed against the coastal mountains by the Coriolis force. Gill (1977) found the offshore size of the trapping zone to be the internal Rossby radius, which for mid-latitude CTDs is around 300 km. The Rossby radius is a scale length in the study of rotating stratified fluids, when the Coriolis force becomes as important as the stratification.

The formula for Rossby radius is $R = (g'H/f^2)^{1/2}$, where $g' = g(\theta_1 - \theta_2)/\theta_2$ is reduced gravity, θ_2 is the potential temperature of the marine boundary layer; and θ_1 is the potential temperature of the upper air above the marine boundary layer; H is the scale height of the marine boundary layer; f is the Coriolis parameter, and g is gravity (e.g. Holton(1979)).

1.2.2 Vertical trapping mechanism

CTDs are trapped vertically by a temperature inversion (e.g. Holton (1979)) which is a region where the temperature increases with height, below the coastal ridge. The atmosphere

is stable and vertical motion is suppressed when there exists a temperature inversion. This inversion is due to large scale subtropical subsidence (Reason, 1989). For example, there is usually a high pressure zone near the west coast of North America in the summer. This high pressure zone causes subsidence, or downward vertical motion. In subtropical areas there is usually subsidence and this can cause warming above the cool marine boundary layer (hereafter MBL) resulting in an inversion. The inversion decreases vertical motion and prevents CTDs from dissipating upwards.

1.3 Observation of CTD

There have been many observations of North American CTDs. Dorman (1985) and Mass and Albright (1987) used buoys and meteorological stations to observe the May 1982 CTD event. A synoptic scale low was observed to migrate across the southern California coast. The marine boundary layer depth then increased in the Southern California Bight from which a CTD initiated. The CTD caused wind reversal and propagated northward from south of Point Conception to Cape Mendocino. Soundings taken in the Southern California Bight at San Diego and Point Mugu revealed that the depth of the marine boundary layer was between 1-2 km. A significant temperature drop was observed with the arrival of the CTD. The CTD propagated as far as Cape Mendocino and a cyclonic eddy came into being (Dorman, 1985). The sharp bends in the coastal mountains at Cape Mendocino are thought to have stopped the CTD from propagating further (Reason and Steyn, 1992).

Reason and Dunkley (1993) discuss a CTD event along Vancouver Island which occured in September 1988. A synoptic scale low was observed to move toward the California coast.

Coastal stratus formed due to the interaction of this migrating low with the coastal topography. The CTD propagated northward and the coastal stratus was observed to be along the entire west coast of Vancouver Island. Surface pressure increase and wind reversal accompanied the propagation of the CTD.

In the summer of 1994 field observations were made along the U.S. west coast to explore the vertical and offshore structure of the CTD event in June 1994 (Ralph et al., 1998). Vertical wind profiles were obtained with boundary layer radar wind profilers. An instrumented Piper aircraft was used to document the offshore structure with surface and ship observations providing a complementary data set. A warming of 10-15 ^{0}C was observed in northern California. Persson et al. (1995) suggested that this warming is caused by the increased frictional generation of potential vorticity. Deep southerly flow (>2km) and a cooling of 2-3 ^{0}C which was related to the wind reversal were observed. At the surface stations, a pressure trough was first observed, then the northerly flow slowly reversed into southerly flow. The low clouds in this event were not coincident with the region of southerly flow but lagged the transition. The coastally trapped disturbance propagated to the north with a speed of about 11.9 m/s on 10 June. It stalled for 11-12 hour due to the enhanced northerly flow as a part of the diurnal cycle. Then it propagated again with a speed of 11.6 m/s. Anticyclonic eddies were observed when the CTD progressed around headlands and it is speculated (Ralph et al., 1998) that seabreeze effects are important in the evolution of these eddies. The flights performed by a research aircraft showed that the southerly flow extended at least 100 km offshore and appeared first within the marine boundary layer inversion as the inversion thickened upward. However, the height of the inversion's base (the MBL depth) changes very

little, until 12-14 hours after the southerly wind begins. This is inconsistent with the two-layer, shallow water idealizations. The aircraft data indicate that the MBL height doesn't increase southward during the transition to southerly flow, as suggested by earlier studies. At some buoys the air temperature increases after the arrival of the CTD. The maximum southerly wind speed is less than the propagation phase speed. The above two features are inconsistent with those of gravity current. Dorman et al. (1998) studied observed data for the 1994 case and proposed an explanation of cloud formation based on the growth of the sea surface mixed layer (hereafter SSML). The winds at the coastal stations were found to reverse earlier than the corresponding coastal buoys offshore. The overcast stratus cloud developed after the wind reversal. The cloud behavior can be explained by a SSML model which begins at the time of wind reversal and grows with the square root of time. The sea surface is colder and heat is transfered from the SSML to the sea surface. When the temperature of the SSML is below the dewpoint temperature, clouds come into existence. The observed cloud structure had the features of undular bores observed in the atmosphere (Simpson 1987) and on rivers (Tricker 1964). This was consistent with the surface winds, pressure and temperature structure at some coastal stations. The bore is suggested to develop at the top of SSML and propagate with a speed of 8 m/s. North of Monterey Bay the bore evolved into a gravity current. The strong northerly wind at Point Arena prevented the disturbance from propagating further, forming a cyclonic eddy in the lee of the point.

In the summer of 1996, a research group at the Naval Postgraduate School conducted an experiment to observe the CTDs from June to August (Nuss, 1997). Drifting buoys and aircrafts were used to study the coastal surges. A very short-lived CTD was observed around

June 5, 1996. This propagating disturbance lasted less than 24 hours and traveled a very short distance compared to other CTDs (Nuss, 1997). In observation, the typical length scale of CTDs is 1000 km in alongshore direction (Reason, 1989).

Bond, Mass and Overland (1996) document the climatology and composite temporal evolution of coastally trapped wind reversals along the U.S. west coast. Moored coastal buoys and Coastal-Marine Automated Network stations are used to obtain hourly data. It was found that there were two types of wind reversals, one a coastally trapped reversal and the other caused by synoptic factors. The frequency, magnitude and timescale of the CTDs were analyzed and their synoptic evolution was studied. Grided Prediction synoptic analyses of National Center for Environmental Prediction are used to obtain the average synoptic condition during CTD events. Their results show that all of the coastally trapped wind reversals are linked to the creation of higher sea level pressure to the south and are actually downgradient ageostrophic flow. Their study is very useful for idealised simulations of CTDs since idealised simulation results should be able to reveal climatological values of CTDs.

1.4 Theoretical approaches in CTD study

Shallow water equations are widely used in theoretical study of CTDs. These equations were first used to study CTDs by Gill (1977). Gill suggests that the features of the CTDs in South Africa are similar to those of coastally trapped waves in the ocean. He used nonlinear shallow water equations on the f plane (The Coriolis force is constant on the f plane) and obtained a Kelvin wave as the solution. A nonlinear advection term is found

to steepen the wave front and make the wind speeds and direction change abruptly. Since then many meteorologists have used shallow water equations to study CTDs. The shallow water equations are used in fluid dynamics when the hydrostatic approximation and a 2-layer fluid are assumed. When the horizontal scale is far larger than the vertical scale, the hydrostatic approximation is usually valid. The hydrostatic approximation means that the vertical pressure gradient balances gravity and there is no vertical acceleration. As the vertical structure of the coastal atmosphere in all three regions roughly consists of two parts: a homogeneous marine boundary layer and a less dense upper layer, there is a direct analogy to shallow water. Thus in the study of CTDs, shallow water equations are widely used. The shallow water equations used by Reason and Steyn (1992) are as follows:

$$u_t + uu_x + vu_y - fv = -g'h_x + F_1 \tag{1.1}$$

$$v_t + uv_x + vv_y + fu = -g'h_y + F_2 \tag{1.2}$$

$$g' = g(\theta_1 - \theta_2)/\theta_2 \tag{1.3}$$

$$h_t + (hu)_x + (hv)_y = 0 \tag{1.4}$$

Equations (1.1) and (1.2) are the u, v momentum equations; equation (1.3) is the reduced gravity; equation (1.4) is conservation of mass. Note that in these equations, the notation u_t means $\partial u/\partial t$, and similarly for u_x, u_y, v_x etc.

The axes used in the equations are as follows:

- y co-ordinate is to measure distance alongshore.
- x co-ordinate is to measure distance offshore.

The side boundary representing the coastal mountains is an infinitely long wall.

The symbols used in the equations are as follows:

- u: horizontal component of the velocity in the x direction.
- v: horizontal component of the velocity in the y direction.
- h: the perturbation height.
- h_t: the change rate of perturbation height with time.
- f: the Coriolis parameter.
- g': the reduced gravity of the two layer atmosphere.
- θ_1: the potential temperature of the upper layer.
- θ_2: the potential temperature of the lower layer.
- F_1 and F_2: forcing terms. For example, synoptic pressure gradients.

See Fig. 1.3 for a schematic picture showing the axis and symbols used in the shallow water equations.

The shallow water equations are partial differential equations. General analytical solutions cannot be obtained. In order to get an analytical solution, most existing models omit the nonlinear advection terms to simplify the equations since they are smaller terms compared to other terms such as the Coriolis force. The equations can then be solved analytically. A linear Kelvin wave or a gravity current can be obtained as the solution, depending on the boundary conditions. This is the coarsest simplification of the shallow water equations. This approach can be used when the following conditions are met (Reason, 1989):

1. The across-shore velocity in the marine layer is small (in comparison with the across-shore velocity in nonlinear Kelvin waves) for a linear Kelvin wave.

2. The alongshore length scale is much greater than the across-shore length scale.

A gravity current is caused by a horizontal density difference in the atmosphere. It requires a continual influx of denser air and causes a long-term displacement of the marine layer and corresponding drops in temperature and changes in the windfield. The flow is unsteady, often spurting. A density front exists between the gravity current and ambient fluid. Kelvin waves are a type of gravity wave that propagates along the interface between two fluids of different density and can only exist at the vertical side boundary of a rotating fluid. They do not necessarily require a fluid reservoir of different density. Propagation of a Kelvin wave is progressive (Reason, 1989).

Besides the coarsest approach mentioned above, there are at least three other ways which have been used to solve the shallow water equations:

1. Various special forms of the forcing terms are applied to the equations. For example, periodic and isolated pressure forcing terms (Rogerson and Samelson, 1995), and vertical velocity, to represent the synoptically driven off-shore and onshore flow in the marine layer (Reason, 1989). The shallow water equations still assume the linear form.

2. Nonlinear alongshore advection terms have been added to the equations, assuming the across-shore flow is negligible (Reason, 1989). In a nonlinear relationship, the variables can compound each other.

3. In the nonlinear semigeostrophic theory of CTD, the solutions are separated into semigeostrophic and ageostrophic parts (e.g. Holton (1979))(Reason and Steyn, 1992).

Reason (1989) and subsequently, Reason and Steyn (1992) is a comprehensive theoretical study on CTD. In his thesis the CTDs in North America, Southern Africa and southeastern Australia are examined. It was found that the dynamical features of these disturbances are the same (hydrostatic and semigeostrophic). The differences in the CTDs are due to different forcing and boundary conditions in each area. Shallow water equation theory is developed based on the similar dynamics in these three cases. Three types of solutions are found, a Kelvin wave, a steady coastal gravity current and a non-linear gravity current with an associated nonlinear (either solitary or shock) Kelvin wave. The relative importance of nonlinearities is discussed by studying different forcings and boundary conditions. The results are as follows:

- Southern African case is consistent with a continuously forced, linear Kelvin wave.
- North American and Australian disturbances show characteristics of both gravity current and nonlinear Kelvin wave.

In each case the theoretical propagation speed is compared with the observed speed and it is found that they are very close.

1.5 Current idealised numerical simulation methods in CTD research

An idealised simulation approach is numerical modelling in which parameters are a summarization of real observations. This will be discussed in detail in the Methodology section.

Currently there are two approaches in the numerical simulation of CTD: one of them uses shallow water equations; the other uses a 3-dimensional mesoscale numerical model.

1.5.1 Shallow water equations approach

In Klemp, Rotunno and Skamarock's (1995) work, 2-D nonlinear shallow water equations were used. Their work is similar to method 3 mentioned above. Their model parameters are summarized in Table 1.1.

Parameter	value
alongshore distance	2000 km
across-shore distance	1000 km
horizontal resolution	10 km
initial inversion height	500 m
initial wind field	undisturbed

Table 1.1: Parameters used in Klemp et al.'s (1995) simulation of coastally trapped disturbances.

The pressure gradient which forced the coastally trapped disturbance was inserted over the first 10 h to avoid numerical problems with dramatically changing the pressure field. The magnitude of the total pressure gradient is 2 mb over a distance of 600 km and the direction is alongshore with lower pressure to the north in the simulations which were set in the northern hemisphere. Because of the imposed pressure gradient the marine air accelerated toward the north. After 10 hours of simulation the Coriolis force turns the flow to westerly. The westerly flow is blocked by the coastal barrier and raises the MBL (Marine Boundary Layer). A wave-like disturbance is formed in a later stage of the simulation.

Samelson and Rogerson (1995) also use the shallow water equation approach in the simulation of CTDs. In their approach, the coastal mountains are represented by a wall and

the CTD is initiated by a migrating low. When the low comes across the coastal mountains, there is onshore flow to the south of the low and offshore flow to the north of the low. The onshore flow in the south leads to convergence. The convergence causes the MBL height and surface pressure to increase; the offshore flow in the north leads to divergence. The divergence causes the MBL height and surface pressure to decrease. Thus, a pressure gradient with the lower pressure in the north is created. The alongshore pressure gradient leads to the creation and propagation of CTDs.

In their approach, convergence/divergence of the onshore/offshore flow is the only factor that leads to the initiation of CTDs. In the shallow water equations there is no thermal advection equation. The relative importance between thermal advection effect and warming/cooling might be resolved in the future when more detailed observations are available.

1.5.2 Three dimensional mesoscale modelling approach

The other approach is to use a three-dimensional (hereafter 3D and two-dimensional will be abbreviated as 2D) mesoscale numerical model such as the Regional Atmospheric Modeling System (hereafter RAMS) (Jackson and Reason, 1995). Actually the basic idea is the same as creating a high pressure system near the shore. In the RAMS approach, a certain area near the shore is cooled and a high pressure system is created. The advantages and disadvantages of the RAMS approach over the shallow water approach will be discussed in detail in the Methodology section. In the present simulations Jackson and Reason's (1995) approach is used in studying the influence of synoptic and topographic factors, and initial cooling amount and area on CTD propagation.

The Regional Atmospheric Modeling System (RAMS)

RAMS is a widely used 3D atmospheric model developed by the scientists at Colorado State University and the ASTER division of Mission Research Corporation (Pielke et al., 1992). Its major components are shown in Table 1.2. RAMS is a limited-area model which

1	an atmospheric model
2	a data analysis package to convert observed meteorological data into a format used by RAMS
3	a post-processing model visualization and analysis package

Table 1.2: The major components of RAMS

can also be used in simulation of the planetary-scale atmosphere. Sometimes a smaller area in a large domain becomes the focus of research. In this case nested grids can be used to increase resolution in that particular region. FORTRAN 77 is used for most of RAMS while C is also used to a lesser extent. The input data RAMS requires and the output data RAMS generates are 3D or 2D gridded pressure, temperature, humidity, wind, etc.

There are two ways of initializing RAMS. One of them is to input observed data on a 3D grid, converting them into the format that RAMS uses. The other way is to use a single vertical sounding from a certain spot and using this single profile to define the conditions across the entire grid resulting in horizontally homogeneous initial conditions. After several hours of simulation the initial homogeneous condition will be adjusted closer to reality. Homogeneous initiation is a widely used method in atmospheric numerical modelling. For example, in numerical modelling of global wind field (Fu, 1993), at the start of the simulation the wind is set to 0 everywhere. After some time the wind field adjusts to the global pressure field and becomes geostrophic (Fu, 1993).

The atmospheric model can be changed to insert certain forcing to initiate atmospheric phenomenon such as precipitation or a CTD. In Jackson and Reason's (1995) approach the forcing is a cooling condition. After the data that represents the state of the atmosphere are input at the start of the model, the model will calculate what the state of the atmosphere will become in the future.

The input parameters of atmospheric models must be set so that they can represent the real atmosphere. Their values must be in the range of atmospheric observations, otherwise the models may be meaningless. For example, if the temperature of the lowest level of the atmosphere is set as 5 K, it will not represent the atmosphere of the earth. The output of models must also be compared to real observations to ensure that other parameters such as computational schemes are correct, since different computational schemes can also have a large impact on the model output. For example, if the time step is set too large, the flow may become unstable and very large (such as 100 m/s) wind speeds can appear. The horizontal and vertical resolutions can also affect the model output. If both the input parameters and the output are consistent with observations, it is reasonable to conclude that the model is correct. Finally it is possible that there is an error in the model or in the way it is applied – comparison with observation will lend confidence that the model is correct and that it is used appropriately.

1.6 Realistic simulations of CTDs

A realistic simulation is a kind of numerical modelling in which observed data are used in the model. Since there are only a few buoys and aircraft routinely observing CTDs the

observations are usually sparse. Thus there are not enough data to reveal detailed structure of CTDs. The realistic simulation approach is an alternative way to examine the features of CTDs. Guan, Jackson and Reason's (1998) work carried out a realistic simulation of the May 1985 event using RAMS. The following features were found to be very consistent with observations:

- simulated sea level pressure and temperature fields near the surface
- mesoscale sea level pressure
- 6-hour pressure changes
- hourly time evolution of sea level pressure and the southerly transitions at a series of coastal stations and buoys

Thompson et al. (1998) made a realistic simulation of the 1994 case with the COAMPS model and studied the effect of coastal terrain on the initiation of CTDs. The following features were found to be consistent with observations:

- the relatively shallow boundary layer with a warm, nearly neutral layer above
- a tongue of coastal stratus/fog which lags behind the propagation of southerly flow
- a large reduction in CTD propagation speed caused by sea breeze

In their sensitivity study of the effect of coastal terrain on the initiation of CTDs was tested. In the control simulation, the coastal terrain in California was replaced by an idealised mountain. The results show that adiabatic warming due to offshore flow is necessary for the formation of an alongshore pressure gradient. In the second sensitivity test, the height of the

terrain was set as 0. Consequently, the downslope flow disappears and there is no mesoscale organization of the southerly flow.

1.7 Research questions

The main objective of this research is to find how different synoptic and topographic factors influence the evolution of CTDs. Specifically, the detailed objectives are to find how:

1. Across-shore and alongshore synoptic wind speeds affect CTD propagation.

2. Topographic configurations influence the structure and propagation of CTDs.

3. Cooling amount and cooling area affect CTDs.

4. Sea surface temperature affect CTDs.

5. Stability within the marine layer affect CTDs.

6. And to find the interaction between different factors, such as the interactions between cooling area and cooling amount; cooling area/cooling amount and synoptic wind speed; cooling amount and terrain height; cooling amount and gap width.

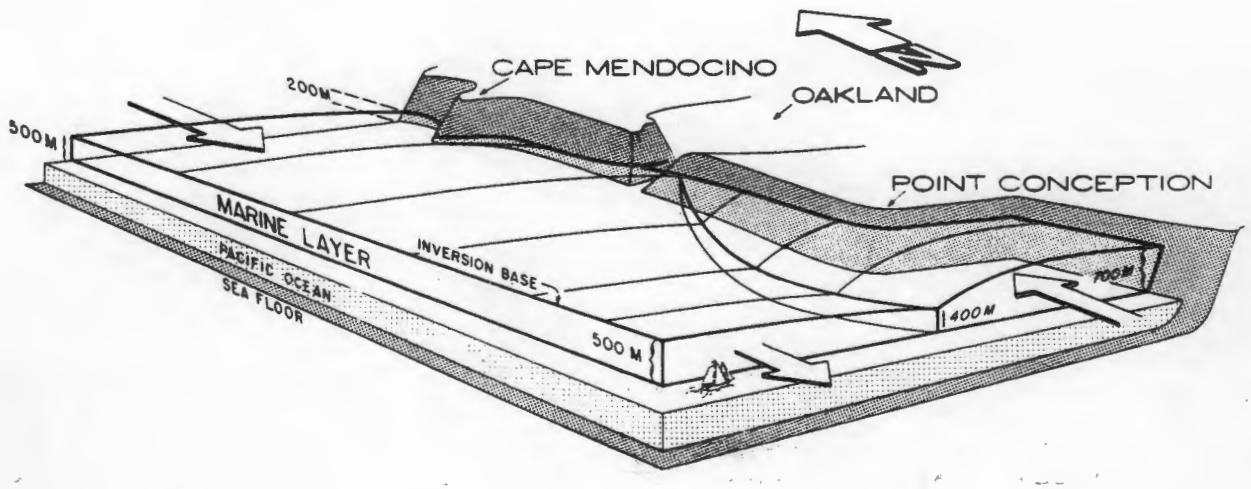

Figure 1.1: A schematic picture of a coastally trapped disturbance. Note the shallow zone of flow from the south which is trapped against the coastal mountains (reproduced from Dorman, 1987).

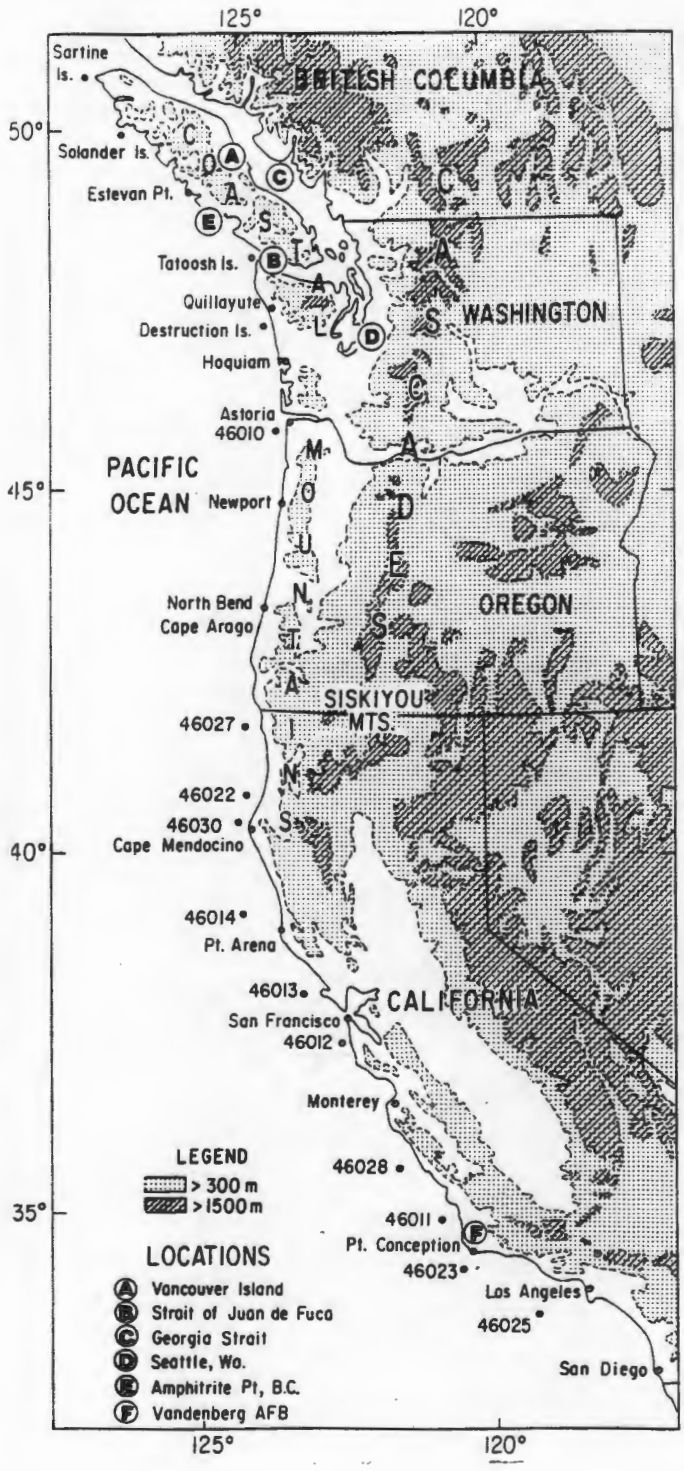

Figure 1.2: Topography of the North American West Coast (reproduced from Mass and Albright, 1987)

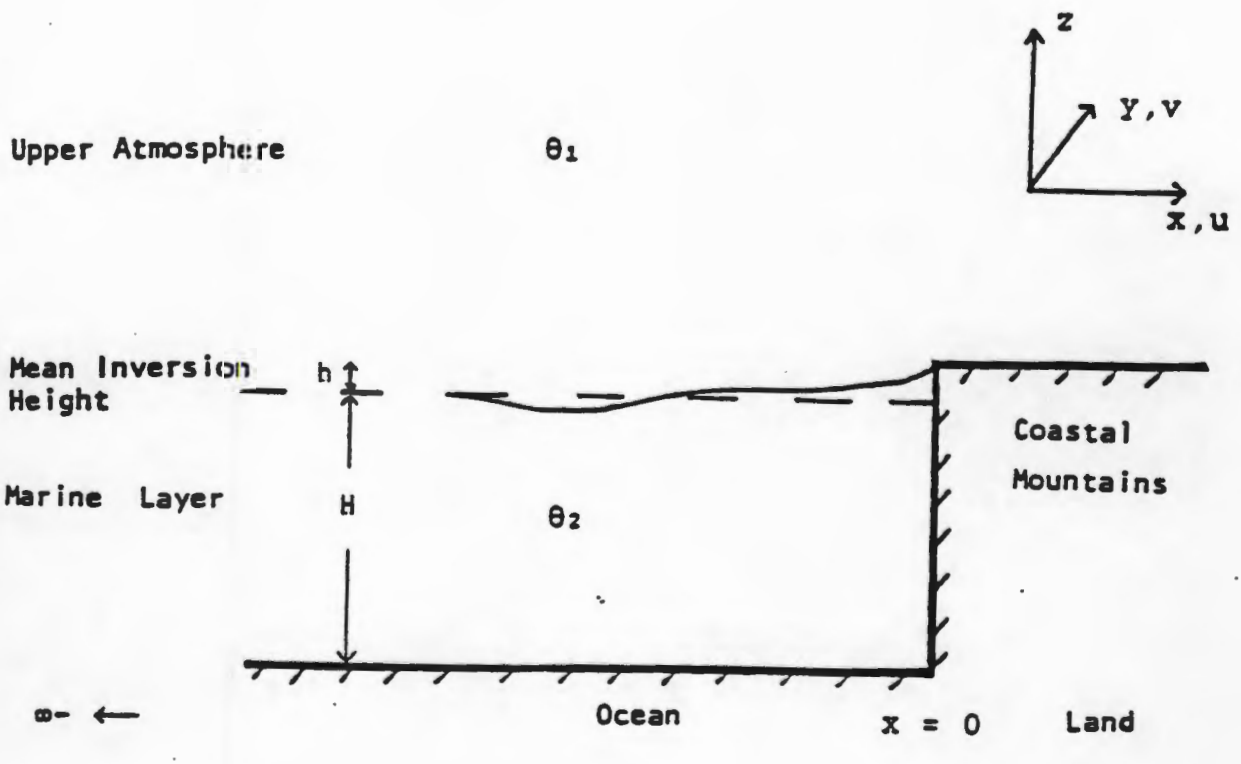

Figure 1.3: A schematic picture showing the axis and symbols used in shallow water equations (reproduced from Reason, 1989). H is the height of undisturbed marine boundary layer.

Chapter 2

Methodology

2.1 Study area

In this research the study area is the North American west coast from Southern California to British Columbia (Fig. 1.2), where many CTDs have been observed (e.g. Mass and Albright, 1987; Reason and Dunkley, 1993). This study tries to simulate the general features common to all CTDs that occur along the North American west coast. Since the forcing mechanisms are the same, the results could also apply to CTDs that are ridges of high pressure in other parts of the world such as in Australia.

2.2 Idealised 3D simulations using RAMS

In this section the following three questions will be addressed:

- Why use a modelling approach?
- Why use an idealised modelling approach rather than realistic modelling approach?
- Why use a 3D modelling approach rather than a 2D modelling approach?

An obvious distinction between atmospheric science and other disciplines of natural science is that it is difficult for meteorologists to experiment on the atmosphere. Numerical simulation is an alternative way to achieve this goal, because parameters in the model can

be adjusted to see how the model responds. Therefore modelling provides a means of understanding atmospheric processes.

In idealised simulations, observation of the real atmosphere, such as temperature, wind speed and air pressure are reasonably summarized and simplified into a model. In the process of summarization, random variations of the real atmosphere are omitted and only the general pattern common to all subjects remains to achieve the goal of a representative simulation. Otherwise the experiment will be affected by irrelevent factors if there are too many random variations. For example, the synoptic wind field of a real atmosphere is very complicated with winds in a wide range of directions. In every North American west coast CTD incident, the prevailing wind direction is northerly (Bond, et al., 1996). Thus we can summarize the wind field as uniformly northerly and omit random variations. The model parameters such as initial synoptic wind speed and sea surface temperature are based on observations and must be realistic. Thus the justification that the parameters are all considered possible and within the range found from observation in the real atmosphere is necessary. In an idealised simulation approach, it is easy to change only one parameter at a time while holding other parameters constant so that we can study the effect of a particular factor. In realistic simulations, real observations are used and there are many factors changing at the same time. It is more difficult to tell which factor causes what effect. Thus idealised simulations are used to find the effect of various parameters on CTD. To sum up, in an idealised modelling approach it is easier to control variables while in the realistic modelling approach, it is much more difficult.

In this research, RAMS is used. RAMS is better than the shallow water equations in many respects, because:

- A non-hydrostatic approach can be adopted in RAMS. Shallow water equations assume a hydrostatic atmosphere. When the hydrostatic approximation is assumed there will be no vertical acceleration. Actually the vertical speed changes with time and there should be vertical acceleration.

- In shallow water equations, the atmospheric stratification is oversimplified. Homogeneous potential temperatures are assumed in both the marine layer and overlaying air. Observed data show that there is continuous stratification in both layers.

- In RAMS it is easy to set various kinds of topography. A terrain smoothing function is used in RAMS to minimize the computational noise caused by sharp changes in topography, and we are not restricted to vertical wall mountain barriers.

- RAMS is based on a set of equations far more complex than the shallow water equations. More processes such as fluxes of heat, momentum, water vapor transfer between the atmosphere and the sea and land is considered. The shallow water equations used by Klemp, et al. (1995) are so simple that even viscous stress is not considered. Viscous stress is important because it decreases wind speed near the surface and it may affect CTD propagation.

The advantage of shallow water equations are that they are easy to understand while RAMS is very complicated and not as easy to manipulate.

RAMS can be used to do both 2D and 3D simulations. Since, in CTD simulations across-shore wind is insignificant compared with alongshore wind, $x - z$ 2D simulations can be used (the x axis is in the alongshore direction and the z axis is in the vertical direction). Two dimensional simulations were used previously to test some synoptic effects, and the 3D simulation approach is developed from the 2D approach. In 2D simulations there are only two ways of dealing with topography: one is to ignore topography and the other is to represent the coastal mountains as a wall. Coastal mountains are far less steep than a wall. Since topographic effects on CTD propagation is an important part of my work, a 3D model is necessary. Also, the initial cooling area is hard to study in 2D simulation.

The modeling results need to be compared with observed data to ensure that the modeling results are meaningful. The horizontal, vertical structure of the wind field, temperature field and pressure field and their evolution are compared with observations. Additionally, the alongshore and across-shore scales of CTDs, the vertical structure of the potential temperature field of CTDs will be compared with observations. The modeled propagation speed of CTDs along different coastal topography is also an important feature to be compared with observed data. For example, in the model the propagation speed of CTDs greatly decreases near coastal valleys, which is consistent with observations.

2.3 Model parameters

2.3.1 RAMS configuration

The following RAMS options are used in the simulations:

- Non-hydrostatic.
- Horizontally homogeneous initial conditions.
- Precipitation mechanisms are present.
- Rigid lid upper boundary condition.
- Solar and terrestrial radiation is permitted and the timestep for radiation update is 30 seconds.
- A terrain smoothing function is used to minimize computational noise.

2.3.2 Model domain, resolution and topography

In the CTD simulations the resolution and model size are set as shown in Table 2.3.

Dimension	Resolution	Number of grid points
Alongshore direction	16 km	80
Across-shore direction	16 km	40
Vertical direction	50 m at the first interval; stretching ratio is 1.15 until it reaches 1000m	25

Table 2.3: Parameters used in the simulations of coastally trapped disturbances.

In three general simulations concerning the cooling area the north-south distance is around 1200 km, about the distance from Southern California to Southern Washington State, which

is a typical CTD propagation area. In other sensitivity tests the north-south distance is smaller, about 600 km. This small domain is sufficient for the purpose of sensitivity testing. For example, in testing the effect of valleys on CTD propagation, a valley can be set in the middle of the domain and we can examine whether the CTD is terminated or slowed down by the valley. How CTDs propagate after they pass the valley is not important for the research question. It is the same with the sensitivity testing of synoptic factors. Six hundred km is large enough to study the propagation speed and structure of wind field. The resolution should not be a problem as in Guan, Jackson and Reason's (1998) realistic simulation their resolution is 100 km in grid 1 and 25 km in grid 2, much larger than the 16 km used here. Since their results compare reasonably with observation, there should not be major problem with the resolution used here. As will be shown in section 3.1, the simulation results compares well qualitatively with observation and this also shows that the resolution is feasible.

The topography in the simulations of different synoptic conditions is set as a steep 2000 m high escarpement running along the coast. Our coastline runs north-south along the eastern edge of the domain, meant to represent the coastline from California to Washington State. See Fig. 2.4 for the topography used and Fig. 1.2 for the real topography.

2.3.3 Sea surface temperature (SST)

In all the simulations, except SST sensitivity tests, the SST is uniformly set as 19 ^{0}C, which is 5 ^{0}C lower than the lowest level atmospheric temperature. Because the model starts

at 4:00 PM local time, air temperature and SST are both slightly above the seasonal average. This compares well with the SST in the NCEP reanalysis project (NOAA, 1997). In May the SST is usually lower than the atmospheric temperature along the west coast of North America.

2.3.4 Vertical sounding input data and initiation method

Atmospheric models such as RAMS must be provided a set of initial conditions describing the atmosphere, and are then integrated forward in time to make a forecast of the future atmospheric conditions. The initial conditions in the model to a large extent determine the end result of the forecast. For this reason the initiation method can have large impact on the evolution of CTDs. In observed CTD cases, a migrating low pressure system initiates the CTDs. In RAMS idealized simulations, it is not easy to represent a migrating low pressure system for initial and model boundary conditions. Thus a cooling condition, which is caused by the migrating low, is used to initiate the CTDs. In order to minimize the large pressure gradient between the initial cooling region and ambient air, the temperature inside the cooling region was set as decreasing gradually from the center of the cooling region. Otherwise if the pressure gradient near the edge of the cooling region is very large, shock waves can be created which will ruin the simulation.

The vertical sounding temperature and dew point temperature data are adopted from real observations of the May 1985 case (Mass and Albright, 1987). In my simulations the marine boundary layer (MBL) where potential temperature is homogeneous, is 400 metres high. The cooling condition was set in the southern edge of the domain in a zone near the shore to make the MBL expand to 1300 metres high. In this cooling condition there is a

maximum cooling location near the shore and the cooling tapers off evenly away from this location. The cooling condition is applied after 2 hours of simulation. See Fig. 2.5(a)(b) for a comparison of the potential temperature of the original cooling area before and after cooling 24.1 m above the sea surface in the horizontal cross-section. The horizontal extent of the cooling is varied to test the sensitivity of the flow to this parameter. See Fig. 2.6(a)(b) for a comparison of vertical cross-sections before and after the cooling. After the new MBL comes into being, the temperature of the original cooling area is held constant. The reason that observed data are used, is that this is the best way to avoid abnormal sea-land and mountain-valley local circulations. During the day the temperature is higher over the land than over the water. Because the air over water is more dense, there is high pressure over the ocean and wind direction is towards the land. During the night it is just the opposite. This is the sea breeze/land breeze circulation. During the day the air over the mountain is warmer than the air over the valley, similarly there is a high pressure over the valley and the wind direction is towards the mountain. During the night it is just the opposite. This is the mountain-valley circulation (e.g., Holton (1979)). If the air temperature is set too low or too high comparing to the radiation balance temperature, local circulations can become unnaturally dominant.

The May 1985 CTD is a very strong CTD event. There are some differences in the initiation mechanism between the simulated CTD and the observations. In the numerical modelling there is only cooling in the south while in a real CTD event there are both cooling in the south and warming in the north. Thus the simulated CTD is weaker than the observed one. If the observed cooling rate is used, the simulated CTD does not propagate.

Thus a cooling amount that is 4-6 K more than the observed amount was used. However the results reveal that the larger cooling amount still doesn't make up for the lack of a warming condition. For example, the observed CTD of May 1985 didn't stop at the Columbia river valley while the simulated CTD stops even at valleys whose depth is more than that of the Columbia river valley.

2.4 Sensitivity tests of factor interaction

In CTD study it is found that different factors may interact with each other. The interaction between different factors can be found as follows: first factor a will be set as $a0$ and the sensitivity of the CTD to factor b will be studied. Then factor a will be changed to $a1$ while holding all other factors constant to study the sensitivity of factor b under a different value of a. If the sensitivity of the CTD to b changes significantly under different values of a, we can say that there is interaction between factor a and b. This is applied when looking at the interaction between cooling amount and cooling area.

2.5 Model fields to be analysed

The model fields to be analysed include:

- Horizontal and vertical wind fields. What is the maximum wind? Where is it located? Where are the local maximum and minimum wind? What is the time evolution of wind fields? What is the off-shore scale of the CTD? How does the wind reversal expand northward? Does the wind reversal happen on the surface first or in the upper level first? What are the vertical profiles of the wind fields?

- The structure of potential temperature field. What are the maximum and minimum potential temperatures? Where are the maximum and minimum temperature located? What is the time evolution of potential temperature field? Is there any front in the potential temperature field? What is the height of the homogeneous marine boundary layer?

The propagation speed of CTD and time evolution are studied. As CTDs are 3D phenomena, wind and temperature fields in upper levels and in vertical cross-sections are also studied.

2.6 The method to compare the strength of two CTDs

In sensitivity tests very often CTDs in different simulations are compared with each other. The comparison criteria are as follows:

1. Time scale. The time scale is the length of time before the CTD ceases northward propagation. The average time scale of CTDs is 36 hours. The shorter a CTD's time scale, the weaker it is. The quicker a CTD retreats, the less effect it can have on the coastal weather. Time scale is the most important factor in the comparison of two CTDs. The CTD which retreats sooner is defined as the weaker CTD, even if other factors such as its maximum southerly wind speed and propagation speed in early stages are about the same as the other CTD.

2. Propagation speed. If the time scales of two CTDs are both around the average time scale of those simulated, propagation speed is the deciding factor as to which CTD is stronger.

3. Southerly wind speed. The CTD with a stronger southerly wind field is considered to be stronger even if the propagation speeds are similar.

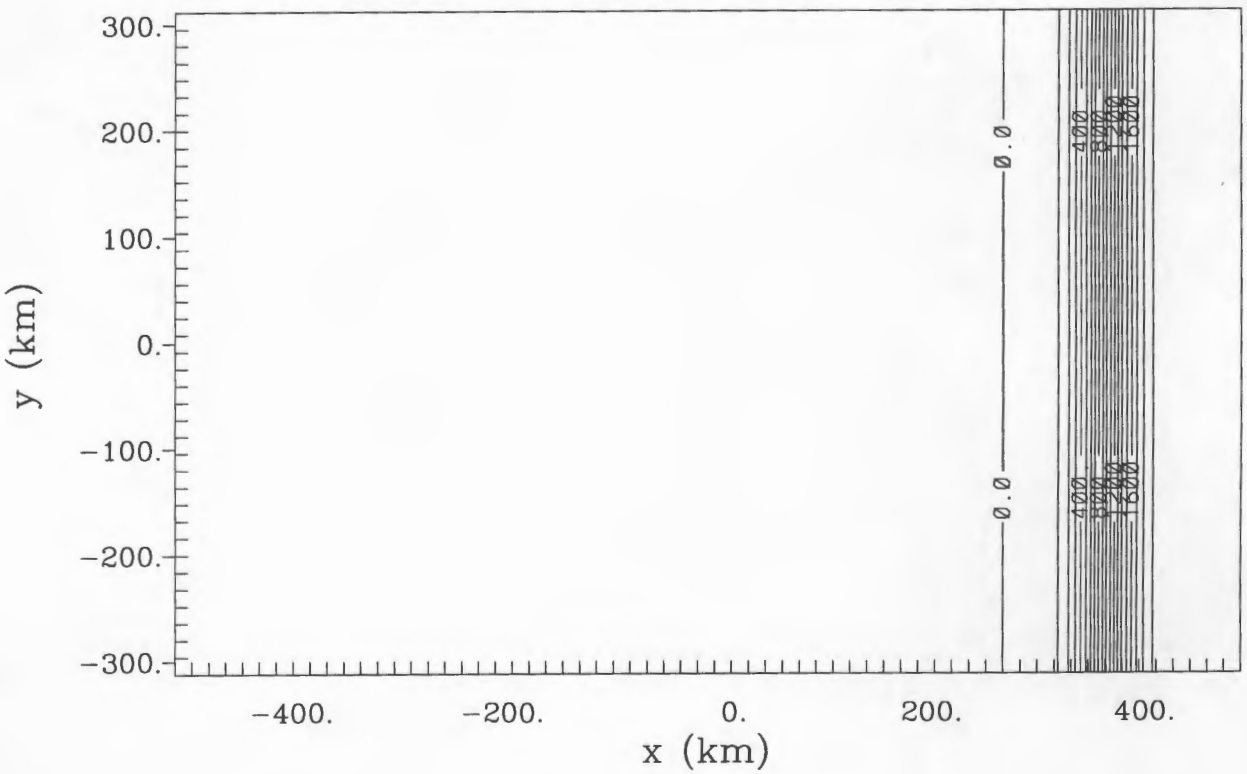

Figure 2.4: Contours of terrain height used in the sensitivity tests of cooling condition, initial wind speed and sea surface temperature. The shoreline is located at the 0 contour line. The ticks along the x, and y axes indicate grid spacing of 16 km. Values along each axis are distance from the domain center in kilometers. Axes are the same with most of the other horizontal cross-section plots.

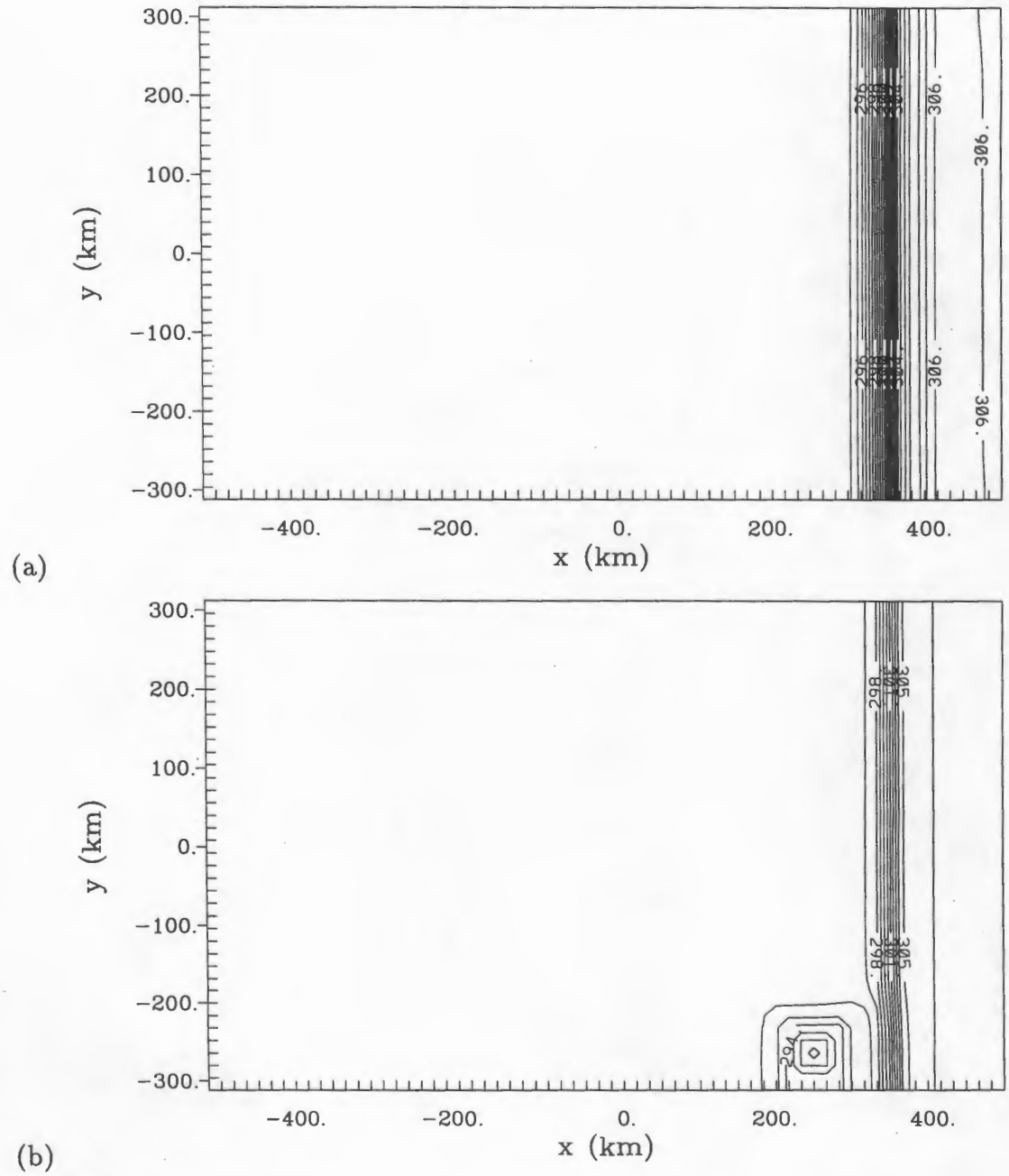

Figure 2.5: The atmospheric potential temperature in the horizontal cross-section 24.1 m above ground. (a) before the cooling. (b) after the cooling. The vertical cross-sections which follow are located in a south-north slice 160km west of the eastern boundary of the model domain (just offshore). Contour interval: 0.5K.

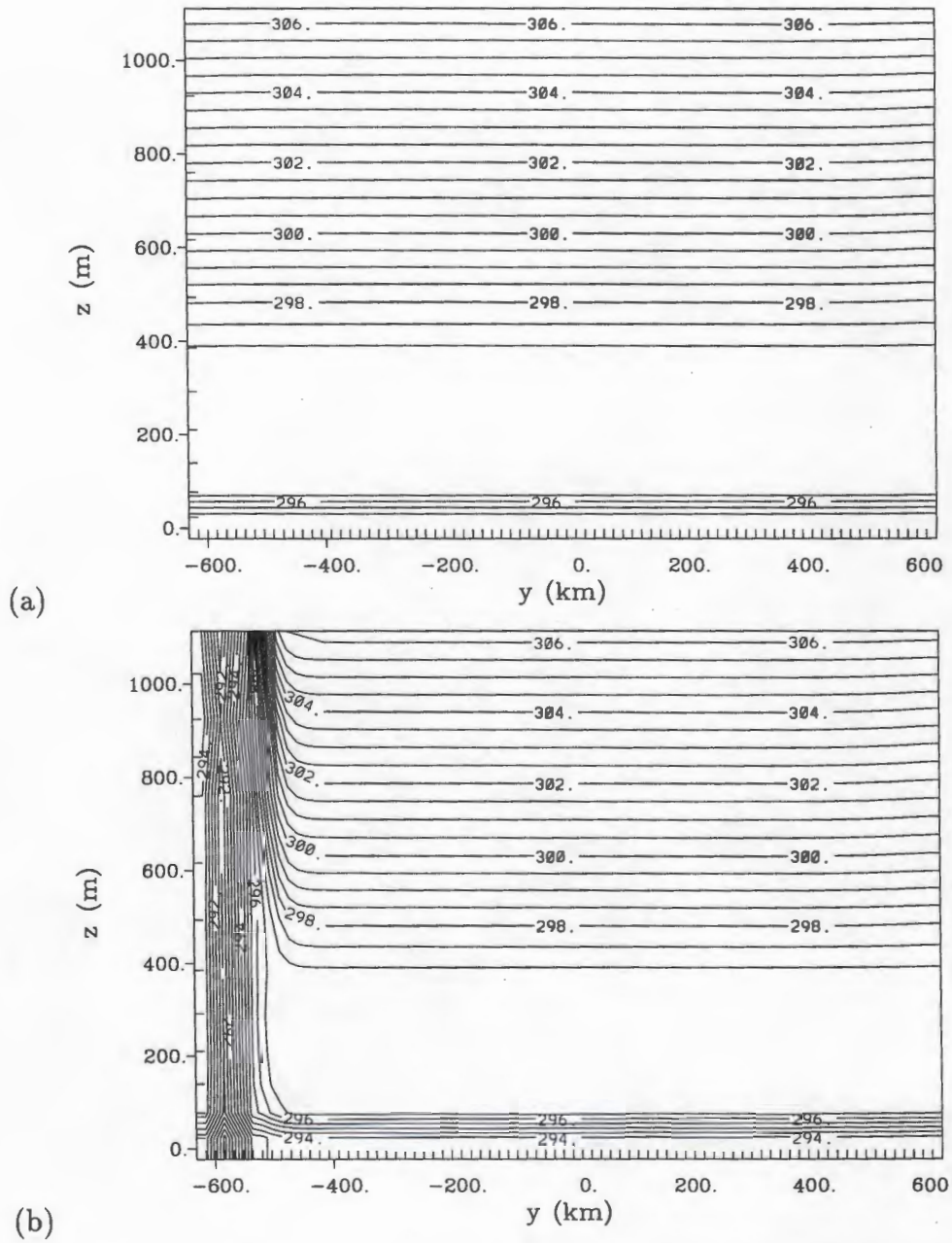

Figure 2.6: The vertical profile of the atmospheric temperature in the marine boundary layer (a) before the cooling and (b) after the cooling. The vertical cross-section is located in a west to east slice 80 km from the southern boundary of the model domains. Contour interval: 0.5K. Note: only the lowest 1100 m of the model's vertical grid are shown.

Chapter 3

Results

In this section the results of the sensitivity testings of various factors are discussed by analyzing the wind and temperature fields. The results are compared to observation data. Due to the limitation of the computational resources this approach is qualitative, and the number of simulations in each sensitivity testing is very limited. In the future when higher speed computers become available high resolution quantitative approach can be applied to the sensitivity testing.

3.1 Comparison between modelling results and observation

This section is to show the consistency of the idealised model with observations. Table 3.4 is a comparison of the modelling results and observation.

Item	Modelling results	Observation
wind speed change	10-20 m/s	10-20 m/s
surface pressure change	3 mb	4-8 mb
across-shore scale	300-400 km	300-400 km

Table 3.4: Comparison between the simulation results and observations of coastally trapped disturbances.

The observed data in Table 3.4 are adapted from the study of Bond et al. (1996), which are a climatological summary of CTD events. The surface pressure change of 3 mb is obtained

from the simulations with a maximum cooling amount between 6 and 15 ^{o}C, which is the range used in most of the simulations. In my simulations, surface pressure change is a factor related to cooling amount, which should be consistent with observed data. Thus the surface pressure change cannot be varied at will. The across-shore scale in my simulations is the off-shore scale of a CTD away from original cooling region. The comparison reveals that the modelling results match reasonably well the range of climatological observations (Bond et al., 1996). Other aspects of my modelling results also compare well with observations. In the modelling results, the ridge of high pressure propagates along the coastal mountains and this is consistent with observations (Bond et al., 1996). In all the simulations, the vertical structure of the observed disturbance is dominated by changes in the structure of the thick inversion capping the marine boundary layer, not simply by changes in the thickness of the boundary layer. This is consistent with the observation of the June 1994 event (Ralph et al., 1998). See Fig. 3.15(b) for the potential temperature field in the simulations and Fig. 3.16 for the potential temperature field in observations (Ralph et al., 1998). Note that in both the modeling results and the observations, the cooling mainly happens in the inversion layer while the structure of the MBL does not change significantly by the initiation and propagation of the CTDs. The potential temperature of the MBL is largely dependent on the SST because the air in the MBL exchanges heat with the sea through turbulence. However, since the turbulence in the inversion is small, air in the inversion exchanges heat very slowly with the lower layers. In the model, because the SST is colder than the potential temperature of the lower part of the CTD, the temperature of the MBL doesn't decrease after the transition to southerly wind. The potential temperature of the inversion layer of the

undisturbed atmosphere, which is less dependent on the SST, is warmer than the inversion layer in the CTD. Thus cooling occurs in the inversion. The same explanation may also be applied to the 1994 case. In some observations (Ralph, et al., 1998), there was even a temperature increase after the transition to southerly flow. This indicates that the SST was colder than the lower part of the CTD. Many of the sensitivity test results are consistent with observation. This will be discussed in detail later on but summarized briefly here:

In the sensitivity tests of gaps in coastal mountains and descending topography CTDs becomes weaker and the propagation speed decreases. It has been observed that CTDs can weaken near the strait of Juan de Fuca and Columbia River mouth (Reason and Dunkley, 1993). In the sensitivity tests of cooling amount, it is found that when the cooling amount is small, wind reversal may happen in the upper MBL first. This was observed in both the 1994 (Ralph et al., 1998) and 1996 events (Nuss, 1997), as well as in realistic simulations of Jackson, Reason and Guan (1999).

Thus idealised RAMS simulations are able to capture many CTD features. There is some limitation in this study in that the CTDs are represented by gravity currents. Not all observed CTDs are gravity currents and the simulation results may not be valid for CTDs that have the Kelvin waves characteristics of section 1.4.

See Fig. 3.7 for observations of CTD wind field and Fig. 3.8(a) for a simulated wind field. There is a zone of southerly wind near the shore in both the observed and simulated CTD wind fields. The offshore scale of both the simulated and observed CTD decrease gradually to the north.

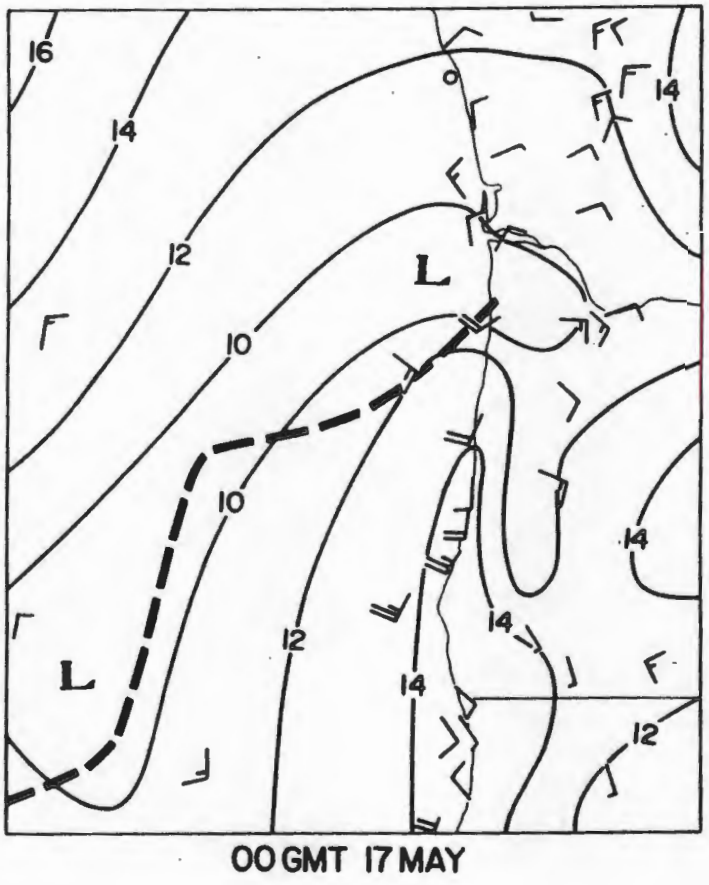

Figure 3.7: An observation of CTD wind field. The contour is mean sea level pressure in millibars (only last two digits shown. for example, 10 represents 1010 millibars.) and 10m winds in knots. Each full barb represents 10 kts. The heavy dashed line is the northern edge of stratus cloud associated with the CTD (reproduced from Mass and Albright, 1987).

3.2 The comparison between simulations of different resolutions

Although higher resolution simulations are more consistent with observations, current computational resources make it not feasible to use high resolution run in sensitivity testing. A high resolution run was used to resolve the detailed structure of CTD wind and temperature fields and is compared with the simulation results of a low resolution simulation run with a cooling area of 7 grid points x 7 grid points (hereafter ca-7*7). In the high resolution simulation, the resolution is 4 km. In the low resolution simulation, the resolution is 16 km. Because the high resolution runs are very time-consuming, the computational domain for the high resolution run is smaller than the low resolution run. Thus in the plots of the high resolutions and low resolutions, especially in the vertical cross-sections are of different shapes. But they have the same areas. From Fig. 3.8(a) and Fig. 3.8(b) the structures of the wind fields in the horizontal direction in the two simulations look similar. The main difference is that in the higher resolution run there is a local maximum wind speed near the wave front. This is more consistent with observations (Bond et al., 1996). Because of the high wind near the front the CTD in the higher resolution run propagates faster. Fig. 3.9(a) and Fig. 3.9(b) are the same comparison in the vertical cross-section in the alongshore direction. The horizontal wind field is more complicated in the high resolution simulation. There are some isolated wind reversals in north of the wave front. These isolated wind reversals may be linked to Kelvin waves since they don't have a front. According to the calculation of Reason and Steyn (1992), the propagation speed of Kelvin waves is usually faster than that of gravity currents. The high resolution simulation reveals the presence of Kelvin waves propagating in front of gravity currents. Fig. 3.10(a) and Fig. 3.10(b) are

the same comparison in the vertical cross-section in the across-shore direction. The wind fields of the high resolution and low resolution simulation in both vertical cross-sections look similar. The only significant difference is that the maximum wind speed is larger in the high resolution simulation. In the low resolution simulation the wind speed in each grid point is the average value over an area of 256 km^2 while in the high resolution simulation it is the average value over an area of 16 km^2. Some extreme wind speeds disapear when taking an average over a larger region.

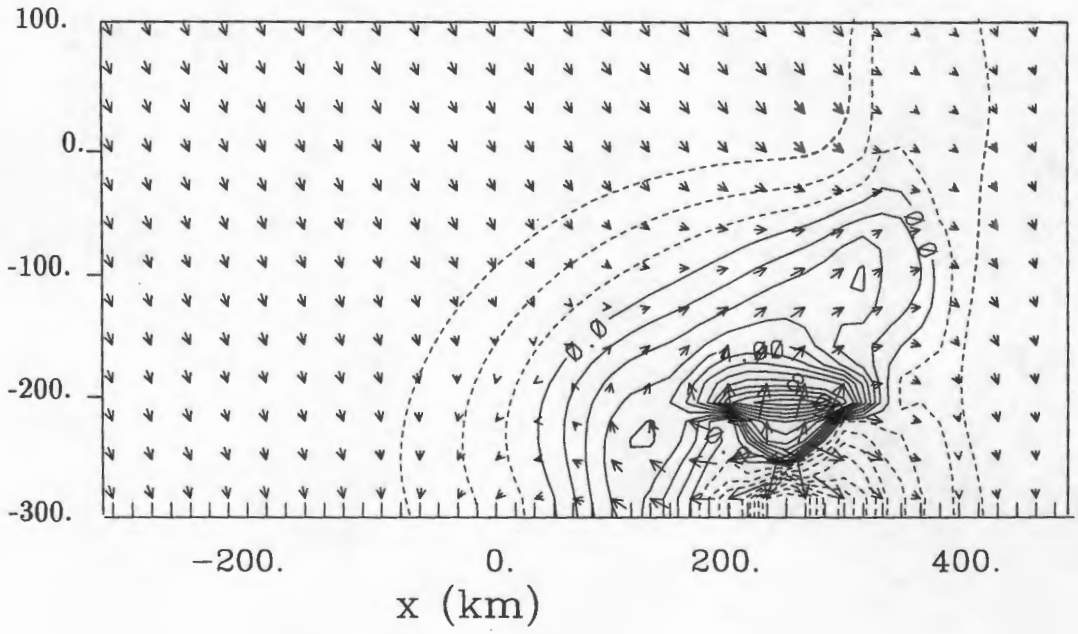

(a)

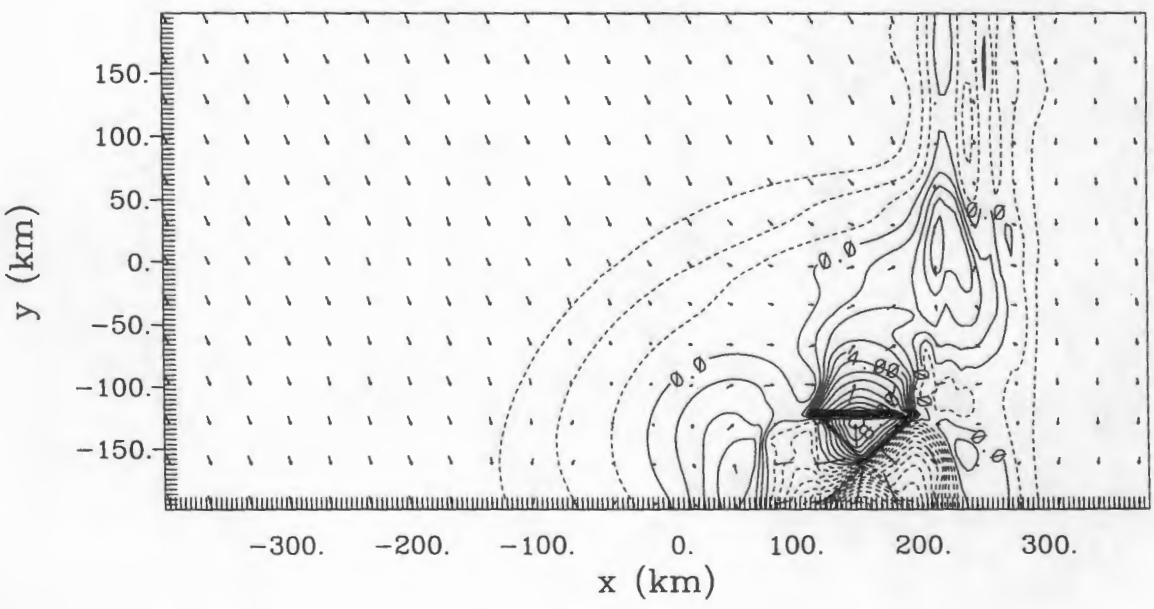

(b)

Figure 3.8: The alongshore wind speed in the horizontal cross-section 24.1 m above sea surface after 6.5 hours of simulation: (a) low resolution run (b) high resolution run. Contour interval: 1m/s. The arrows are the wind vectors.

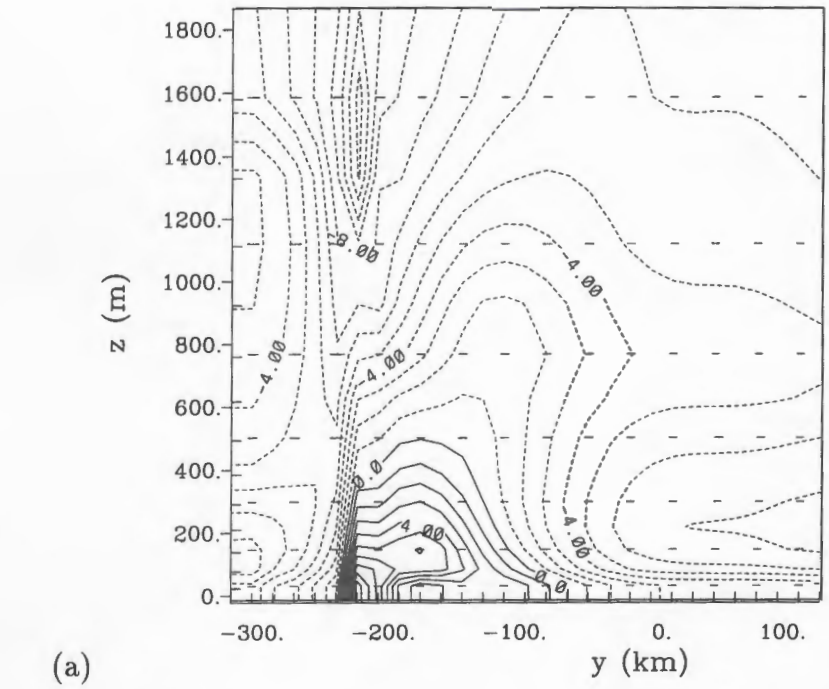

(a)

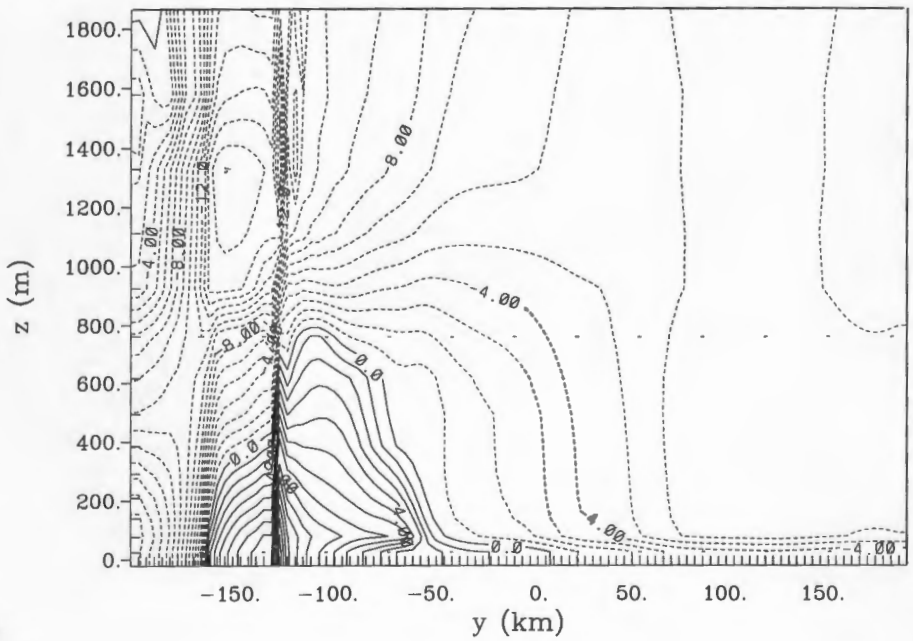

(b)

Figure 3.9: The alongshore wind speed in the vertical cross-section in the alongshore direction after 6.5 hours of simulation. The vertical cross-section is located in a south to north slice 264 km east of the center of the model domain (just off-shore). (a) low resolution run (b) high resolution run. Contour interval: 1m/s.

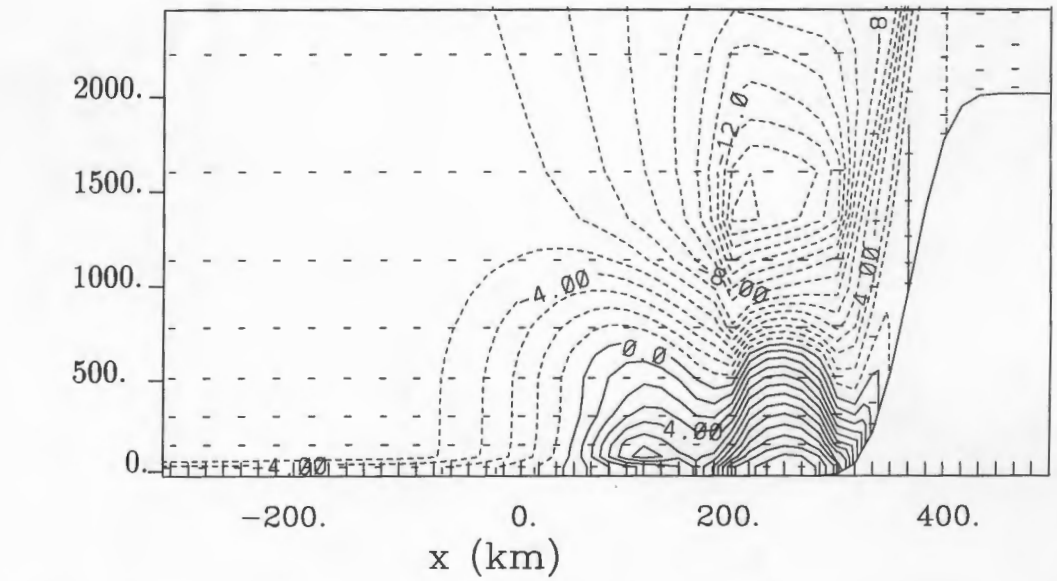

(a)

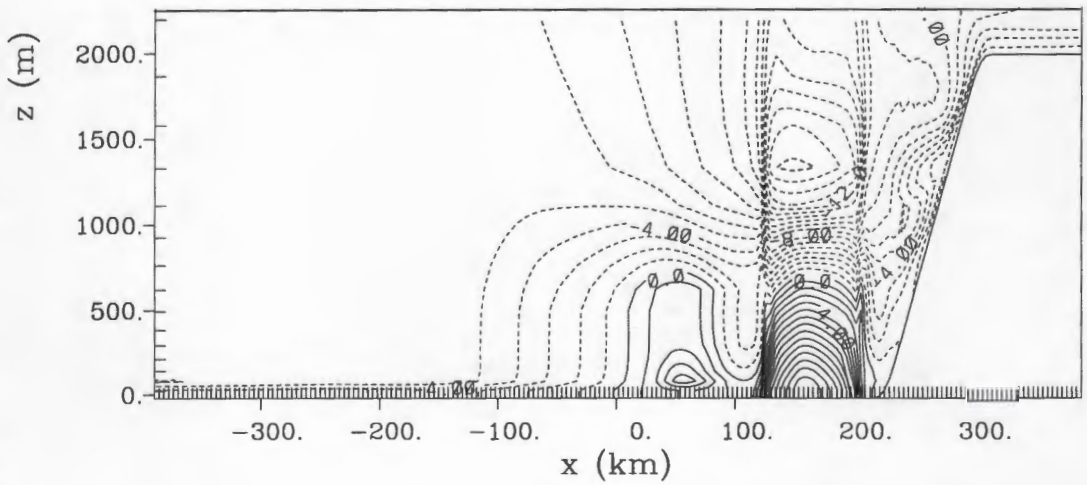

(b)

Figure 3.10: The alongshore wind speed in the vertical cross-section in the across-shore direction after 6.5 hours of simulation. The vertical cross-section is located in a west to east slice 232 km south of the model domain. (a) low resolution run (b) high resolution run. Contour interval: 1m/s.

3.3 The evolution of a CTD

In this section the wind and temperature fields of a CTD are discussed to show the time evolution of a simulated CTD. Also the structure of the CTD wind field is explained. In the following plots the alongshore wind speed and potential temperature fields in various cross-sections are shown. The cooling condition is applied after the second hour of simulation. After the cooling a pressure gradient with the high pressure to the south is created and the CTD begins to propagate to the north. Fig. 3.11, Fig. 3.12 and Fig. 3.13 are at the end of the cooling process. Fig. 3.14 and Fig. 3.15 are at 8th hour of simulation. At this time the CTD propagates around the middle of the domain. Because of the Coriolis force the offshore scale of the CTD is inside the Rossby radius. Fig. 3.17 is at the 16th hour of simulation. At this time the CTD propagates near the north boundary of the domain. The plots show that the off-shore scale of the CTD is decreased. As will be pointed out in section 3.6 this is because the initial wind speed is 6 m/s and large initial synoptic northerly wind usually decreases the off-shore scale of CTDs.

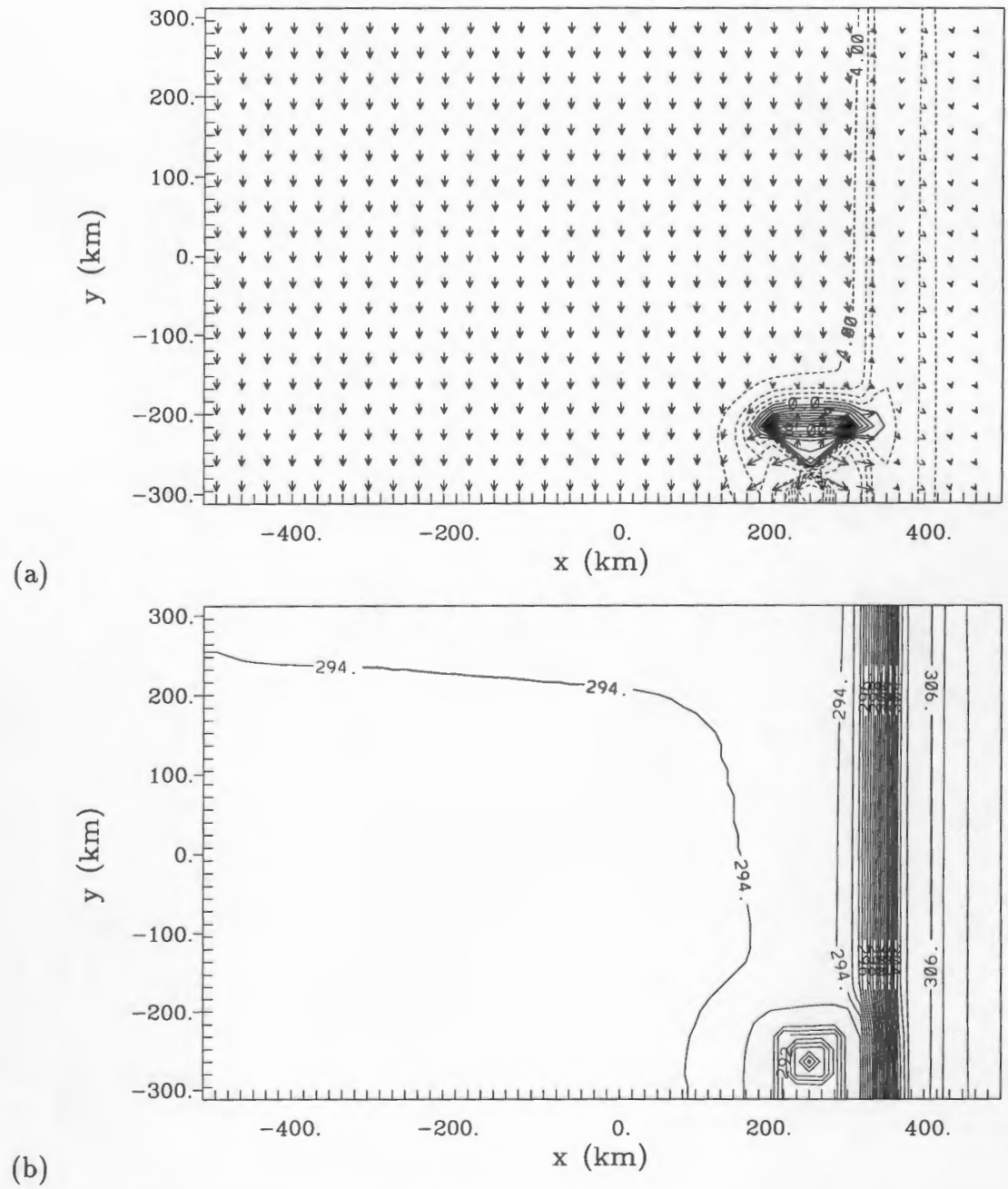

Figure 3.11: The alongshore wind and temperature fields in the horizontal cross-section after 3 hours of simulation (just following the application of the cooling condition. (a) alongshore wind speed in a horizontal cross-section 24.1 m above ground. Contour interval: 1 m/s. (b) temperature field in the same horizontal cross-section as in (a). Contour interval: 0.5K.

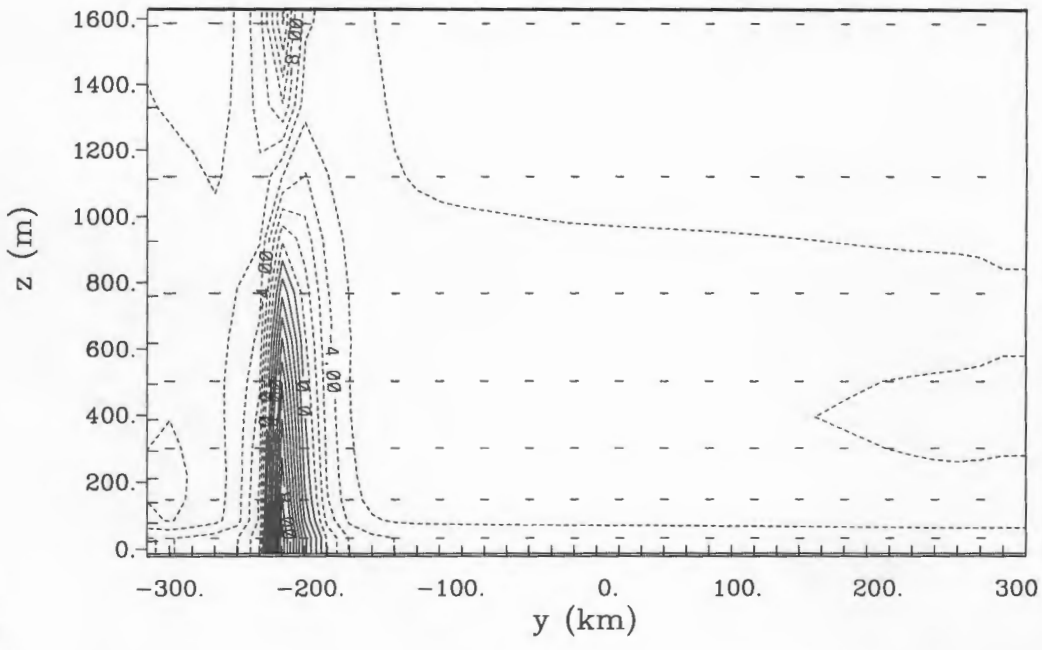

(a)

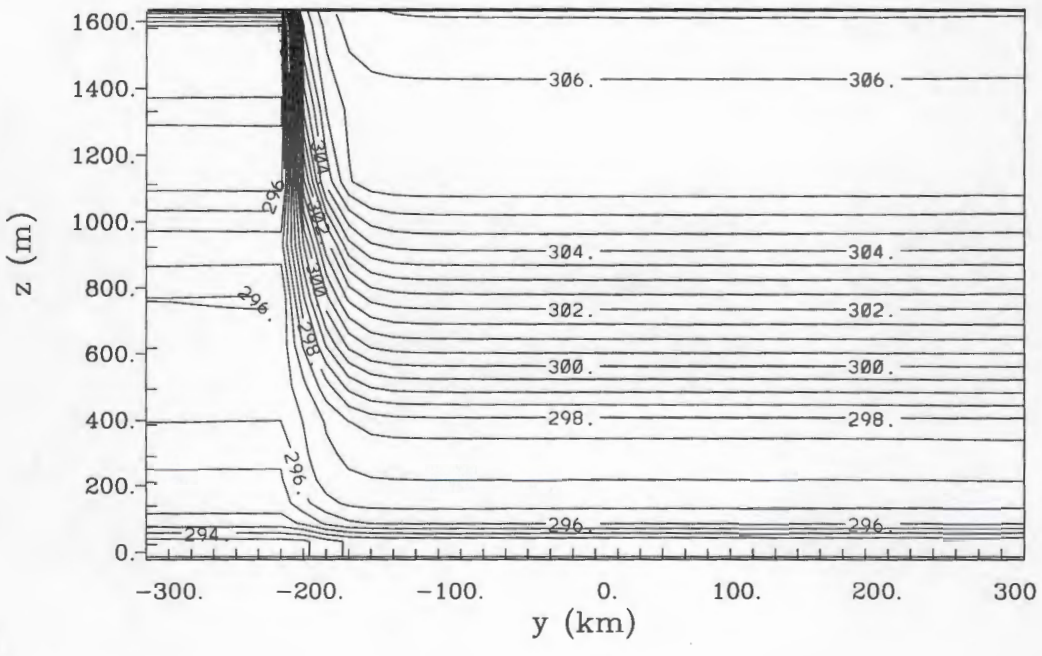

(b)

Figure 3.12: The alongshore wind and temperature fields in the alongshore vertical cross-section after 3 hours of simulation of a typical CTD evolution: (a) A vertical cross-section of the alongshore wind speed. The vertical cross-section is located in a south to north slice 264 km east of the center of the model domain. Contour interval: 1.0 m/s. (b) The vertical profile of potential temperature in the same vertical cross-section as in (a). Contour interval: 0.5 K.

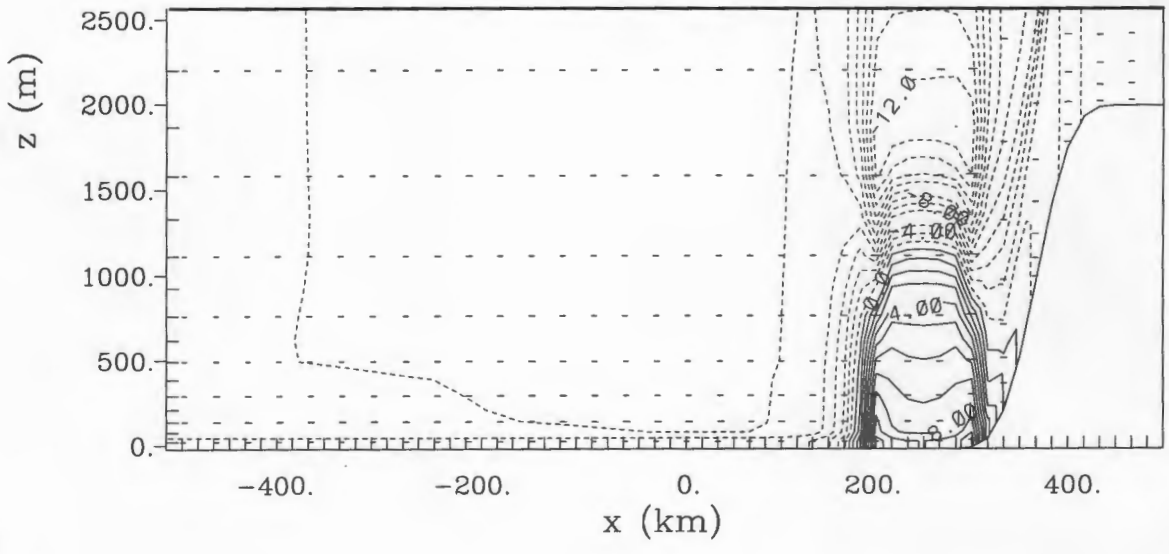

(a)

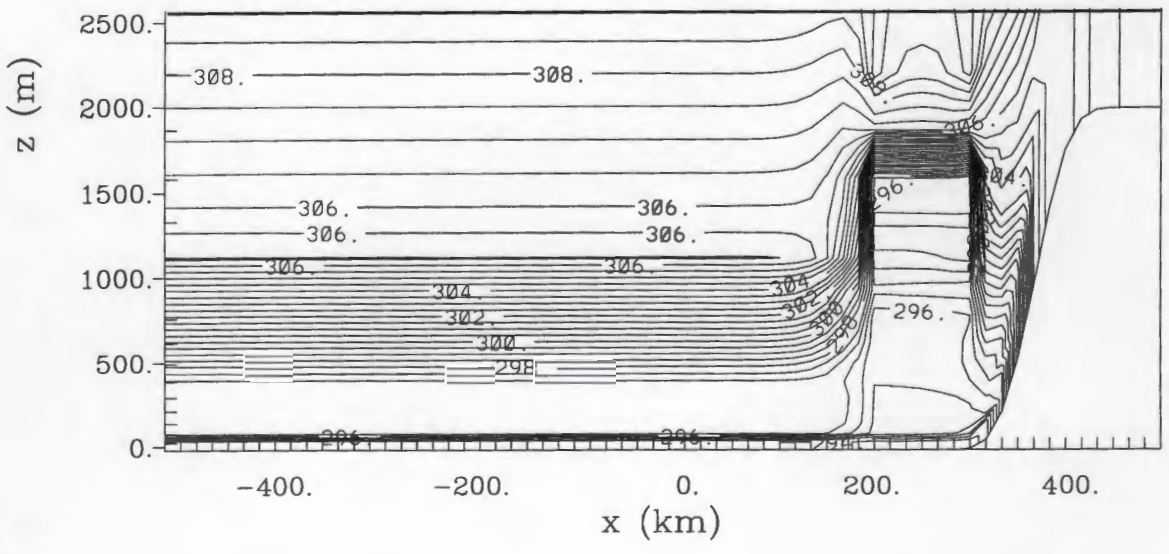

(b)

Figure 3.13: (a) A vertical cross-section of the alongshore wind speed after 3 hours of simulation. The vertical cross-section is located in a east to west slice 216 km south of the center of the model domain. Contour interval: 1.0 m/s. (b) The vertical profile of potential temperature after 3 hours of simulation in the same vertical cross-section as in (a). Contour interval: 0.5 K.

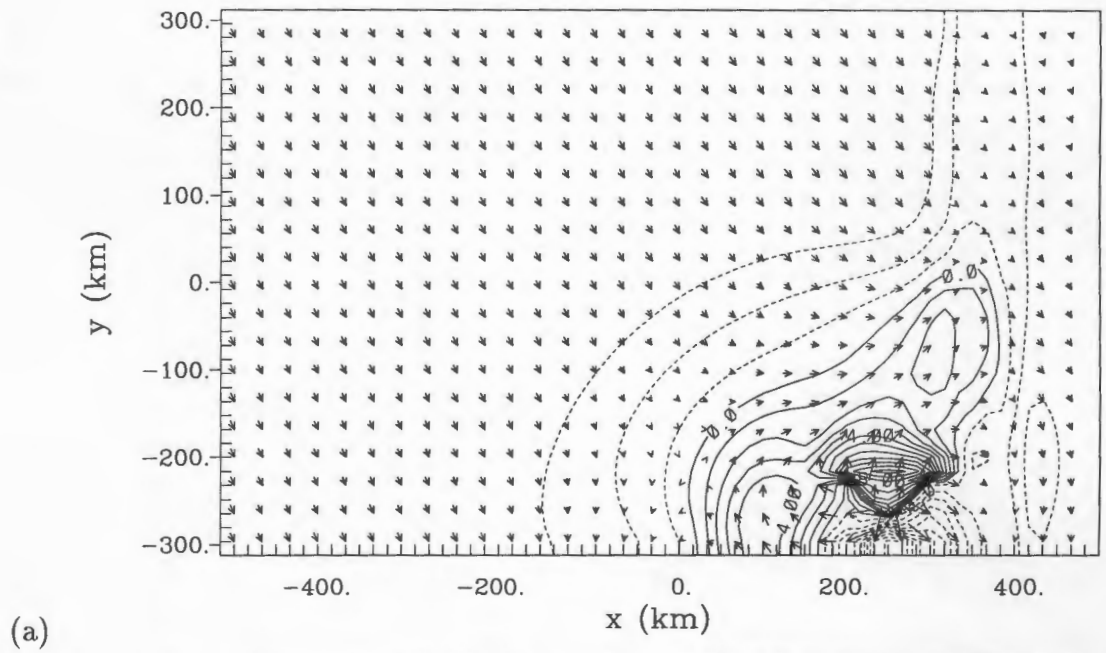

(a)

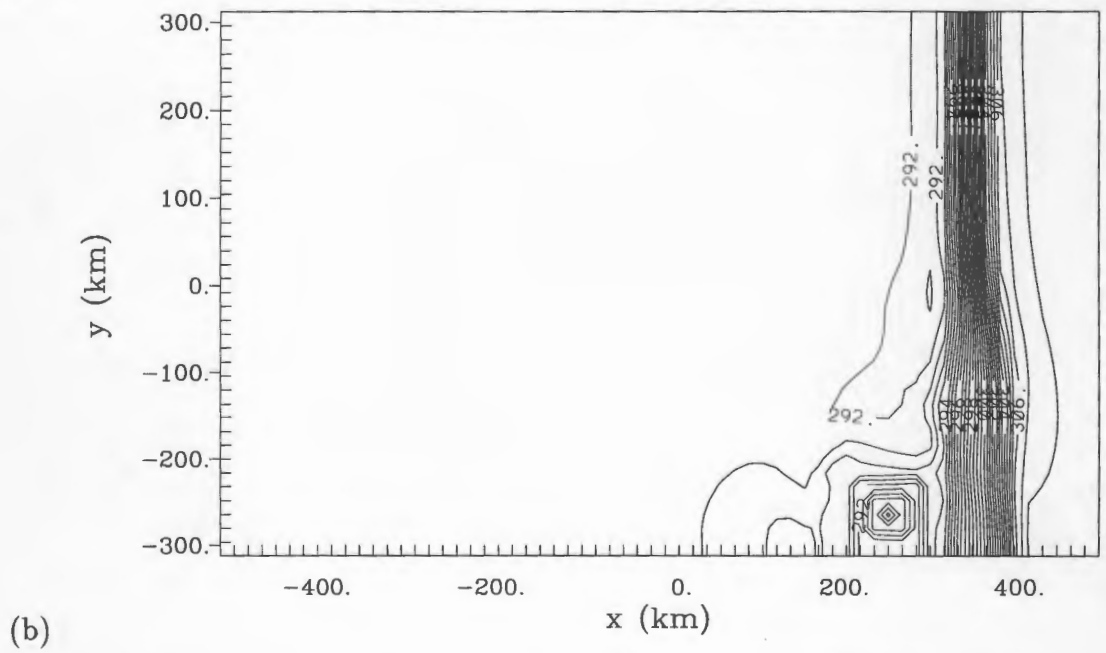

(b)

Figure 3.14: (a) alongshore wind speed in the horizontal cross-section 24.1 m above ground after 8 hours of simulation. Contour interval: 1 m/s. (b) temperature field in the same horizontal cross-section as in (a) after 8 hours of simulation. Contour interval: 0.5K.

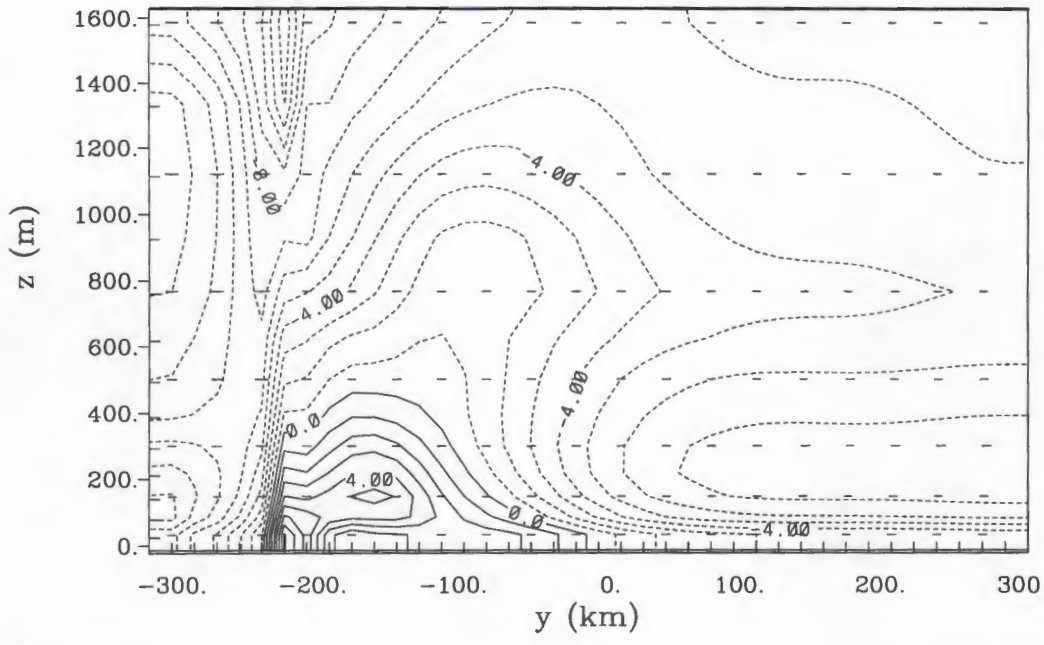

(a)

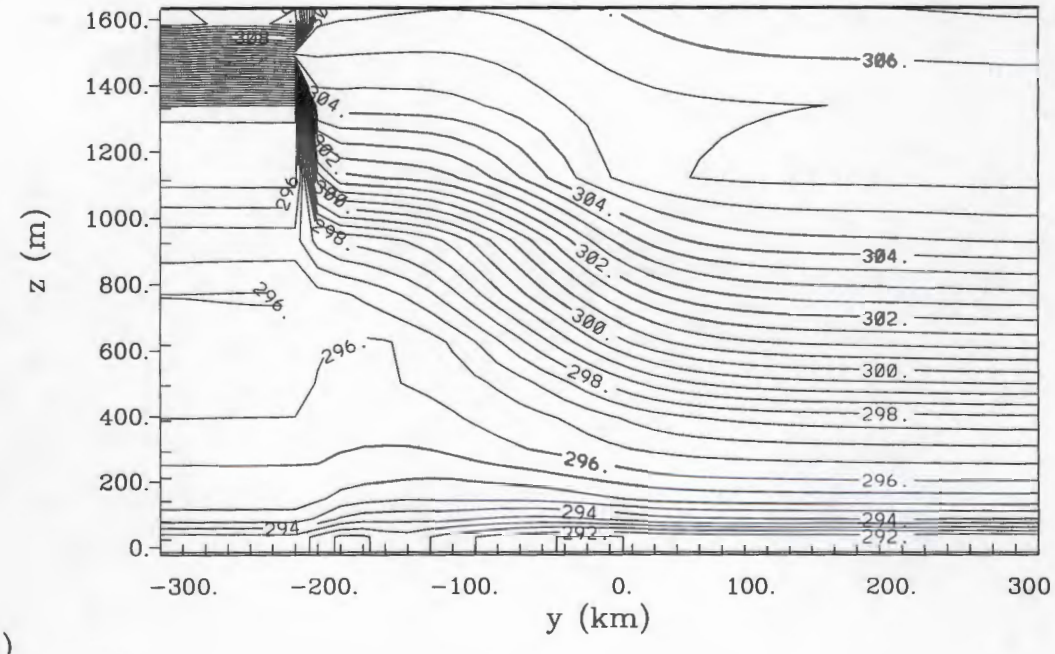

(b)

Figure 3.15: (a) A vertical cross-section of the alongshore wind speed after 8 hours of simulation. The vertical cross-section is located in a south to north slice 264 km east of the center of the model domain. Contour interval: 1.0 m/s. (b) The vertical profile of potential temperature in the same vertical cross-section as in a after 8 hours of simulation. Contour interval: 0.5 K.

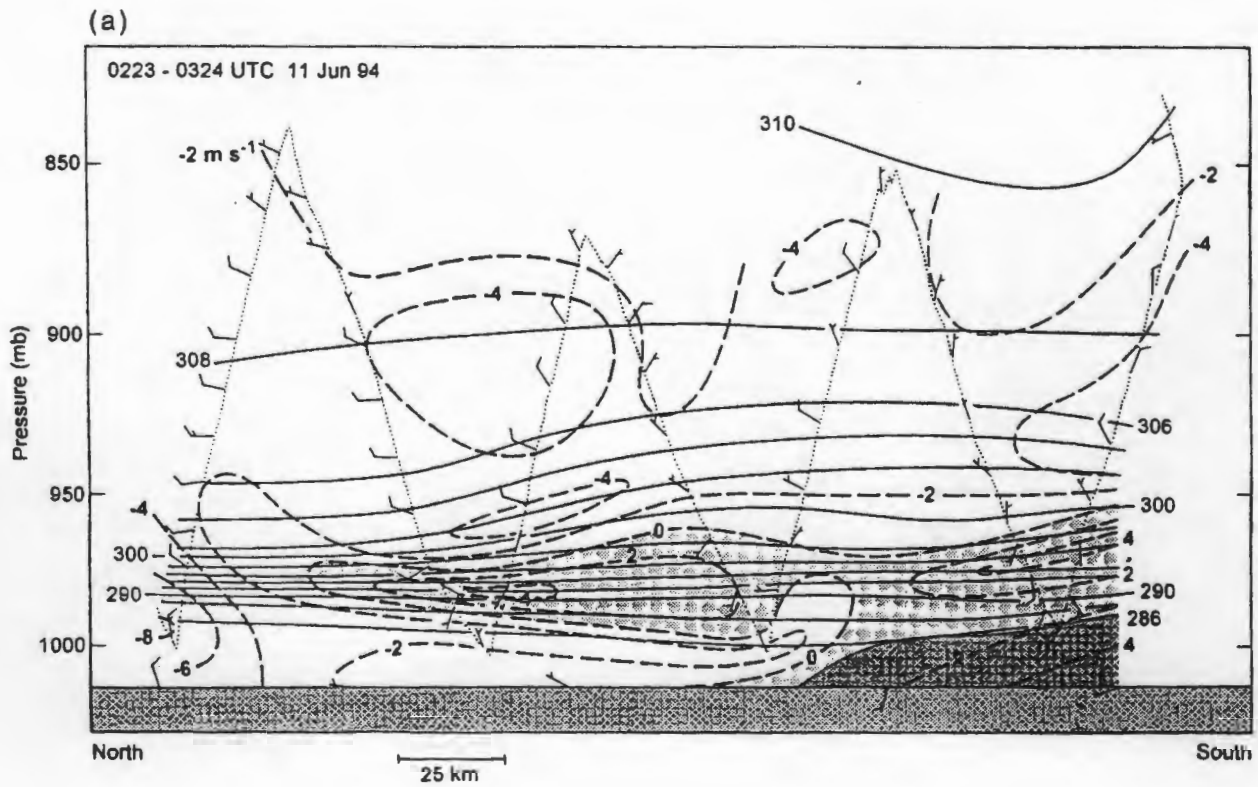

Figure 3.16: A real observation of the CTD potential temperature field. The solid lines represent potential temperature (K) and the bold dashed lines represent alongshore wind speed (m/s). The dark shading marks the region of low clouds (reproduced from Ralph et al., 1998).

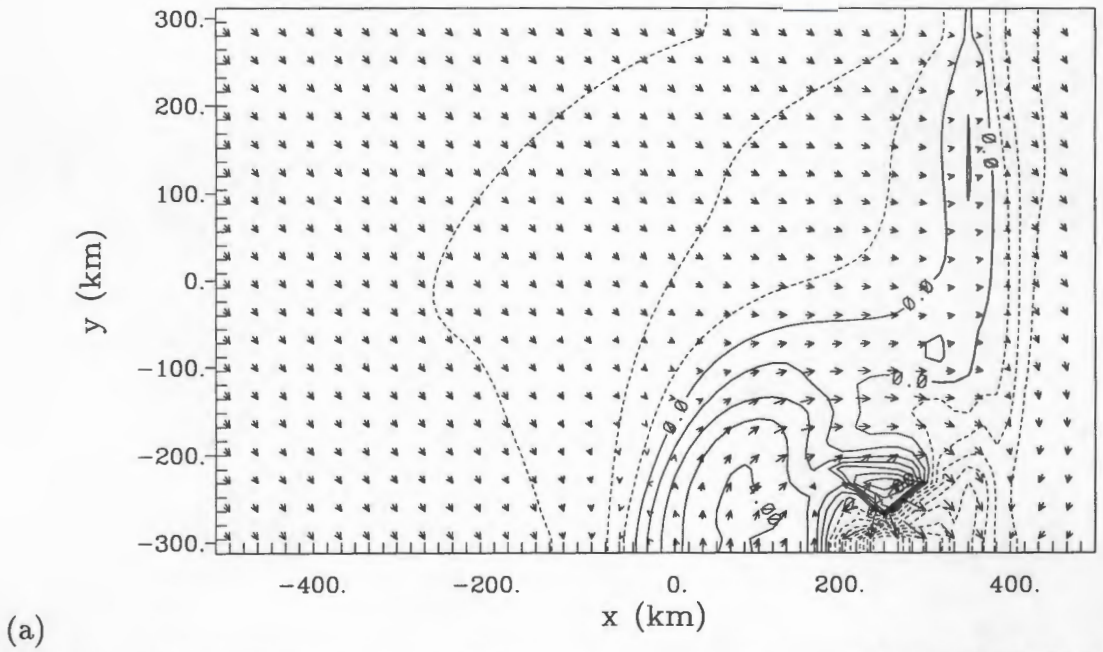

(a)

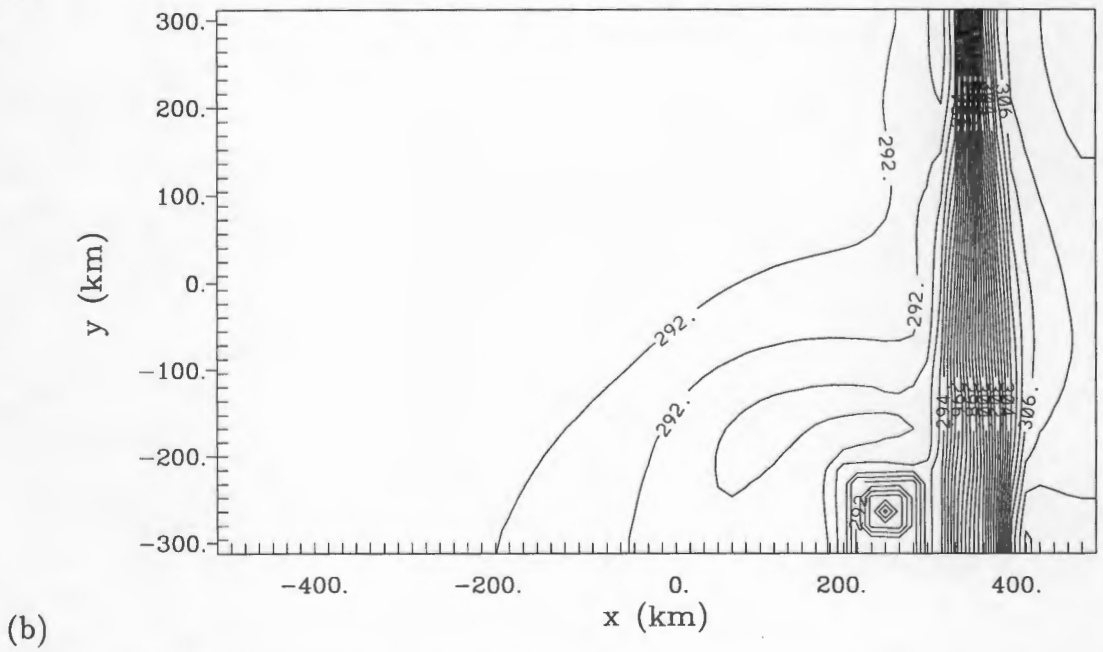

(b)

Figure 3.17: (a) The alongshore wind speed in the horitzantal cross-section 24.1 m above ground after 16 hours of simulation. Contour interval: 1.0 m/s. (b) The potential temperature field in the same horizontal cross-section as in a after 16 hours of simulation. Contour interval: 0.5 K

3.4 Sensitivity testing of different cooling areas.

According to Mass and Albright's analysis (1987), CTDs are initiated by cooling in the lower atmosphere. They speculated that a larger cooling area should be favorable for the CTD propagation. This section is to investigate the effects of different cooling areas. In the sensitivity testing of different cooling areas, the maximum cooling amount ranging from 6-15 ^{0}C in different vertical levels is the same in all 3 runs. There is a centre where the maximum cooling occurs. Away from the centre the cooling amount decreases evenly. Thus the larger the cooling area is, the smaller the pressure gradient will be, as the total pressure difference is nearly the same but occurs over a greater distance.

The following cooling areas are used in the sensitivity tests:

1. Run ca-5*5, cooling area : 80 km x 80 km (5 grid points x 5 grid points).

2. Run ca-7*7, cooling area : 112 km x 112 km. (7 grid points x 7 grid points)

   Thus in run ca-7*7 the cooling area is nearly doubled from run ca-5*5.

3. Run ca-10*10, cooling area : 160 km x 160 km (10 grid points x 10 grid points)

   Again the cooling area is doubled from run ca-7*7.

Judging from the northmost location of wind reversal between 0500 UTC (universal time coordinated) and 2000 UTC, the propagation speed in run ca-5*5 is 12.0 m/s. This speed is about the same as that of run ca-7*7, although the cooling area is nearly only one half that of run ca-7*7. The upper level southerly wind field of run ca-5*5 seems to be stronger than that of run ca-7*7 and the propagation speed in run ca-5*5 is also slightly faster than that in run ca-7*7. Figs. 3.18 (a) and 3.18 (b) display the alongshore wind field 292 m above sea

surface for run ca-5*5, run ca-7*7, respectively. In run ca-7*7, in some parts of the CTD, wind reverses back to northerly and then to southerly again. In run ca-5*5, the wind field does not reverse back to northerly. The maximum wind in run ca-5*5 is larger than that of run ca-7*7. For example, the maximum wind speed in Fig. 3.18(a) is 12 m/s while that in Fig. 3.18(b) it is 9 m/s.

In the third simulation ca-10*10 the cooling area is 10 grid points x 10 grid points and the cooling area nearly quadruples that in run ca-5*5. From the alongshore velocity plot we can see that the maximum southerly wind is rapidly decreasing and the CTD begins to retreat after 17 hours of simulation (Fig. 3.19). This is probably due to geostrophic adjustment. Geostrophic adjustment happens when the wind field is ageostrophic, or there is a wind component that is across the iso-bars. The time scale for geostrophic adjustment depends on the scale of the disturbance. The larger the off-shore scale is, the more time there is for the Coriolis force to turn the flow from southerly to westerly and finally northerly. When the flow becomes geostrophic, the alongshore flow, which is a downgradient ageostrophic flow, disappears.

To sum up, the simulation results seem to reveal that when the initial cooling area becomes larger, the CTD does not generally become stronger. Sometimes it could be just the contrary, the larger the initial cooling area is, the more quickly the flow will become geostrophic and the sooner the CTD will retreat.

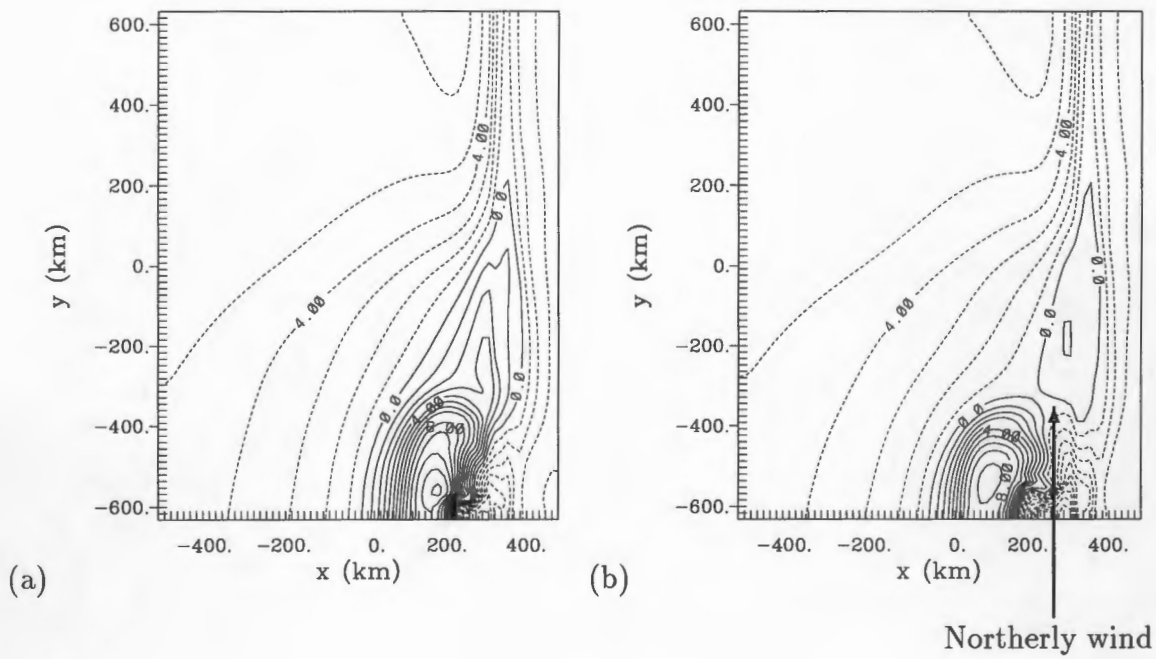

Figure 3.18: The alongshore wind speed in the horizontal cross-section 292 m above sea surface after 15 hours of simulation: (a) the simulation with a cooling area of 5 grid points x 5 grid points. (b) the simulation with a cooling area of 7 grid points x 7 grid points. Note that wind reverses back to northerly in some regions of the CTD. Contour interval: 1m/s.

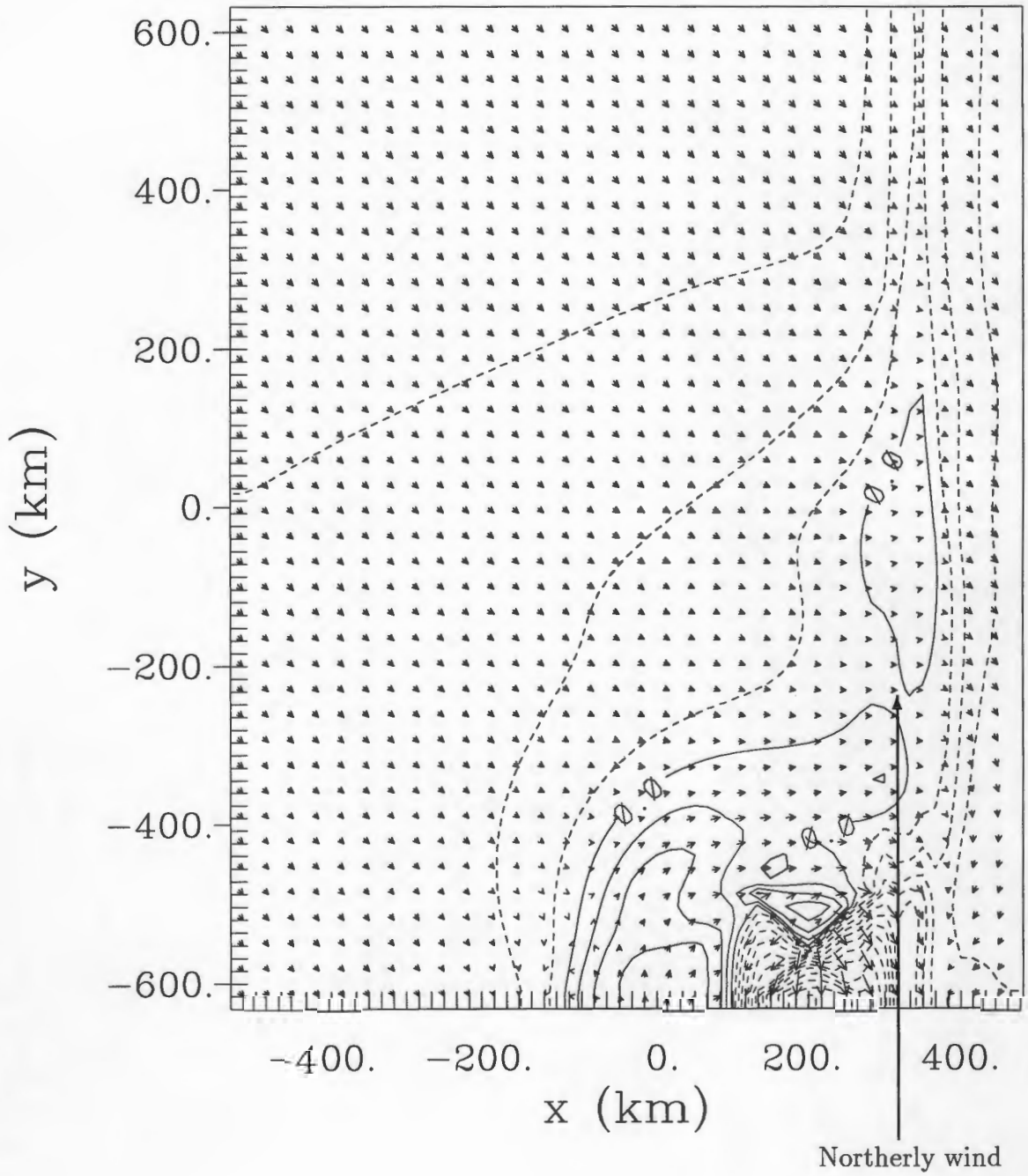

Figure 3.19: The alongshore wind speed in the horizontal cross-section 24.1 m above ground after 17 hours of simulation for run ca-10*10 (cooling area of 10 grid points x 10 grid points.) Note that wind reverses back to Northerly in some regions of the CTD. Contour interval: 1m/s.

3.5 Sensitivity testing of different cooling amount

Six simulations were made to test the sensitivity of CTDs to different cooling amount. Initial cooling amount is important in that it creates a horizontal temperature gradient near the coast. The horizontal pressure gradient is linked to this temperature gradient, which controls the evolution of the CTDs. Thus the effect of the cooling amount should be very important. In 3 runs the cooling area is 5 grid points x 5 grid points (80 km x 80 km) and in the other 3 runs the cooling area is 7 grid points x 7 grid points. The interaction between cooling amount and cooling area can therefore be studied in these runs. For each of the two different cooling areas, three runs were made:

1. With a maximum cooling amount ranging from 6-15 ^{0}C in different vertical levels. The temperature of the first 13 levels is held constant after the cooling.

2. With a maximum cooling amount ranging from 4-13 ^{0}C in different vertical levels. The temperature of the first 13 levels is held constant after the cooling.

3. With a maximum cooling amount ranging from 4-13 ^{0}C in different vertical levels. The temperature of the first 10 levels is held constant after the cooling. This significantly decreases the cooling depth as the altitude of the 13th level is 1330 m while that of the 10th level is only 760 m.

In the San Diego vertical sounding the maximum cooling amounts of 11-15 ^{0}C have all been observed (Dorman, 1985).

In the previous 2D simulations (not shown) of CTDs, it was found that cooling amount is a very sensitive factor. It can determine whether a CTD can exhibit Kelvin wave or gravity

current characteristics and what its propagation speed is. The 3D simulations presented here agree with the previous 2D simulation results.

In the simulation with a cooling region of 5 grid points x 5 grid points x 13 grid points (vertical) and a maximum cooling amount of 4-13 ^{0}C (hereafter run cra-5*5*13/13), the CTD began to retreat after 12 hours of simulation (Fig. 3.20). In some regions, the wind reverses back to northerly. In a very narrow strip near the coast, the wind is still southerly and it becomes narrower and narrower. The narrow strip is completely separated from the main southerly wind region in the original cooling area and show signs of propagating. Also, in upper levels the CTD is much weaker than in the run ca-7*7 although cooling amount is just 2 ^{0}C less.

In the simulation with a cooling region of 5 grid points x 5 grid points x 10 grid points and a maximum cooling amount of 4-13 ^{0}C (hereafter run cra-5*5*10/13), CTD retreats after 7 hours of simulation (Fig. 3.21). As in run cra-5*5*13/13, there is also a region of southerly wind that is separated from the region of southerly wind in the original cooling area. It is also propagating to the north. In this simulation the region with wind reversal is much smaller than that in run cra-5*5*13/13. The CTD mainly reduces the northerly wind and southerly wind is insignificant. Previous 2D simulations demonstrate some similar phenonema. When the amount of cooling is very small, there is no wind reversal. However, there exists propagating small (in comparison with the amplitude of CTDs in other simulations) amplitude "bumps" in the potential temperature profile. The propagating "bump" is linked to decreasing northerly wind. In the above two simulations wind is sometimes reversed to southerly in the upper level of the disturbance but is still northerly at the surface (Fig. 3.23).

The 1994 CTD event is a weak case exhibiting a similar feature (Ralph et al., 1995). In the 1996 CTD, wind reversal also occurs in the upper level first (Nuss, 1997). In Jackson et al.'s (1999) realistic simulation there is a similar occurance.

Wind reversal might not be an indispensible feature of CTD. When cooling amount is small (For example, when the maximum cooling amount is less than 4-13 ^{0}C) the southerly wind is insignificant, even nonexistent. Although in conventional CTD theory wind reversal is an important feature of CTD, the propagating small (here small means much smaller than a CTD initiated with a maximum cooling amount of 6-15 ^{0}C) disturbance trapped by the coastal mountain should also be a CTD by definition since it is also trapped horizontally by the Coriolis force and coastal mountains and vertically by the temperature inversion. It is suspected this kind of weak CTD happens more often. Weak CTDs usually do not propagate for a long time. This is shown by Bond et al.'s (1996) discussion of the climatology of CTD. Most coastal trapped wind reversals are very weak and are not recorded by all the 4 stations in the North American west coast used in the Bond et al (1996) study. In the simulation with a cooling region of 7 grid points x 7 grid points x 10 grid points and a maximum cooling amount of 4-13 ^{0}C (hereafter run cra-7*7*10/13) (Fig. 3.22), the CTD seems to be somewhat stronger than that in run cra-5*5*10/13. The southerly wind region of the CTD split into 2 regions 1 hour later than that in run cra-5*5*10/13.

It seems that a larger cooling area is favorable to CTD propagation when the cooling amount is small, For example, when the maximum cooling amount is less than 4-13 ^{0}C. Comparing to the typical time scale of 1-1.5 days, CTDs which retreat in 0.5 day will be defined as retreating CTDs.

At this stage, a hypothesis about the relationship between geostrophic adjustment and scale of the cool air pool is proposed. When the cooling area is larger the effect is double-edged. On one hand the larger the cooling area is, the more cold air is available. On the other hand, the larger the cooling area, the more likely geostrophic adjustment will occur and the sooner a CTD will retreat. The larger the cooling area, the greater the offshore scale of the CTD, since the Rossby radius is actully calculated from the east edge of the cooling region. The larger the offshore scale, the more time is allowed for the Coriolis force to turn the flow from southerly to easterly, then northerly. When the cooling amount is small (For example, when the cooling amount is less than 4-13 ^{0}C), the main problem is the lack of continuous significant supply of cold air and this causes the separation of the southerly wind region. However, when the cooling amount is large (For example, when cooling amount is 6-15 ^{0}C) and the cold air supply is enough to make up for the warming of CTDs, the main obstacle for CTD propagation is geostrophic adjustment.

To test the validity of this hypothesis two more runs are made, one is with a cooling region of 5 grid points x 5 grid points x 13 grid points and a maximum cooling of 1.2-10.2 ^{0}C (hereafter run cra-5*5*13/10.2) (Fig. 3.24(a)), the other is 7 grid points x 7 grid points x 13 grid points (hereafter run cra-7*7*13/10.2) with the same maximum cooling (Fig. 3.24(b)). As expected the CTD with a larger cooling area (run cra-7*7*13/10.2) is stronger than that initiated with a smaller cooling area (run cra-5*5*13/10.2). The CTD in run cra-7*7*13/10.2 does not only seem to split 1.5 hours later but also the southerly wind is stronger. Thus the above hypothesis is supported.

To sum up, cooling amount is a very sensitive factor for the evolution of CTDs. When cooling amount is small (for example, when the maximum cooling amount is less than 1.2-10.2 ^{0}C), a type of CTD without a wind reversal is found. The cooling amount has a large interactions with cooling area, since the effect of cooling area may be just the opposite under different cooling amounts. When the cooling amount is small (for example, when the maximum cooling amount is less than 4-13 ^{0}C) and CTDs begin to retreat after 12 hours of simulation, a larger cooling area tends to be favorable for the CTD propagation. When the cooling amount is large (For example, when the maximum cooling amount is 6-15 ^{0}C) and CTDs can propagate for at least 20 hours, smaller cooling area tends to be favorable for CTD propagation.

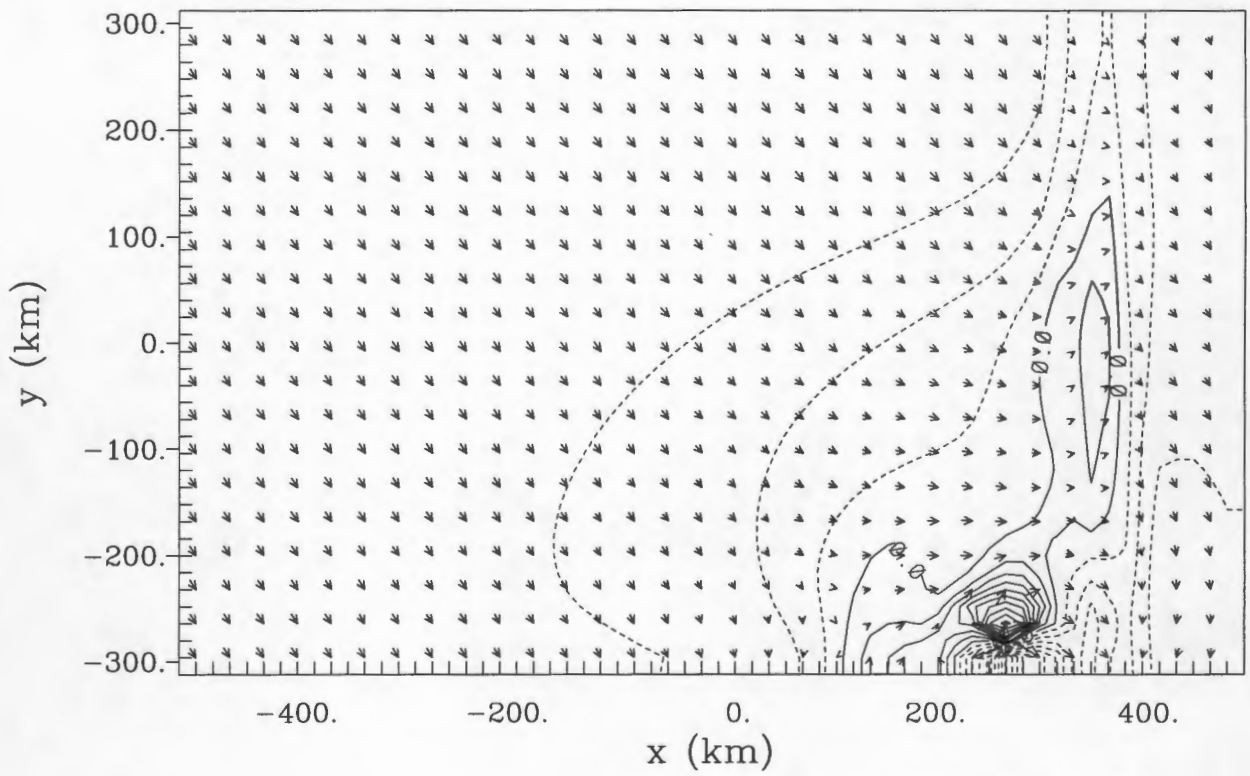

Figure 3.20: The alongshore wind speed in the horizontal cross-section 24.1 m above ground after 11.5 hours of simulation in run with a cooling area of 5 grid points x 5 grid points x 13 grid points and a maximum cooling amount of 4-13 ^{0}C. Contour interval: 1m/s.

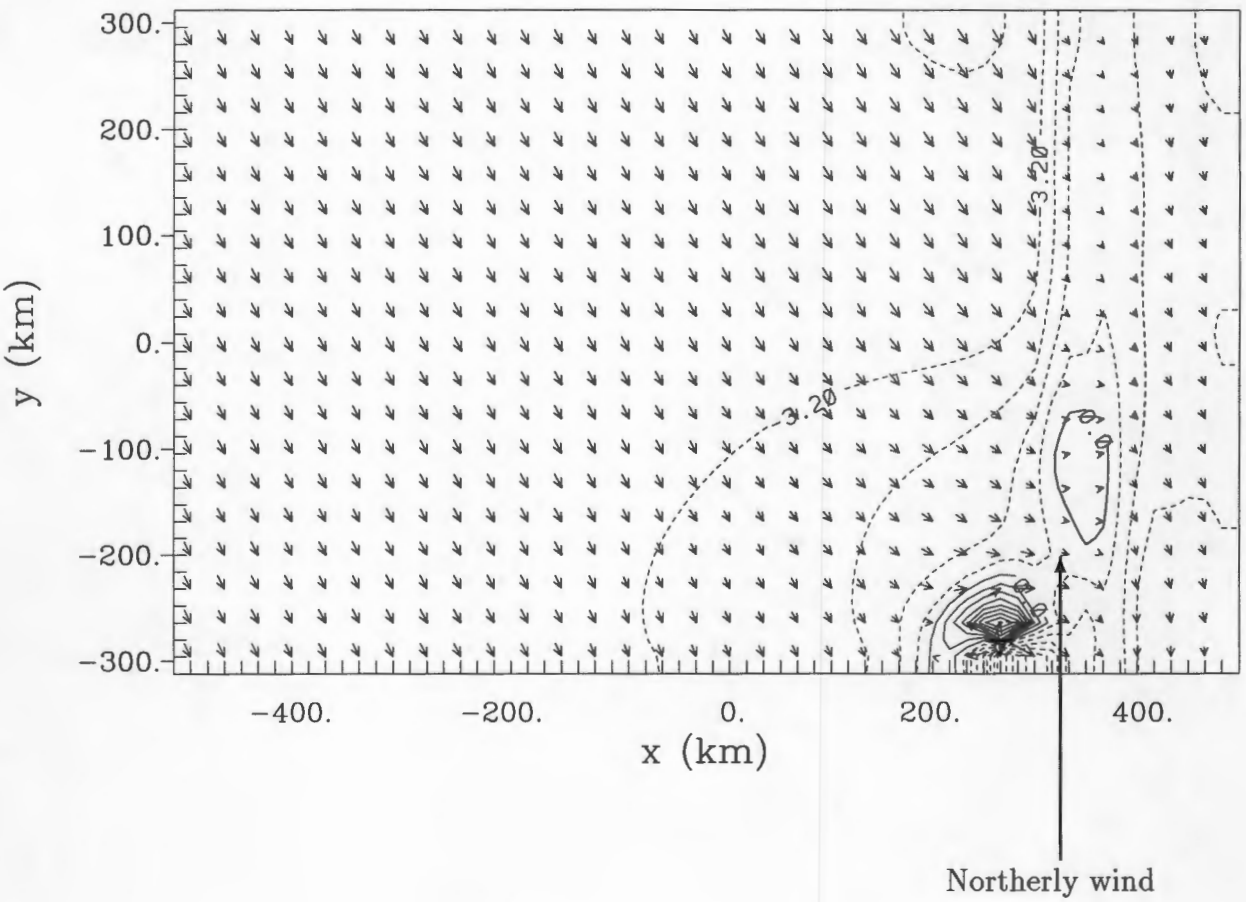

Figure 3.21: The alongshore wind speed in the horizontal cross-section 24.1 m above ground after 8 hours of simulation in run with a cooling area of 5 grid points x 5 grid points x 10 grid points and a maximum cooling amount of 4-13 ^{0}C. Note that in some regions of the CTD wind reverses back to northerly. Contour interval: 0.8 m/s.

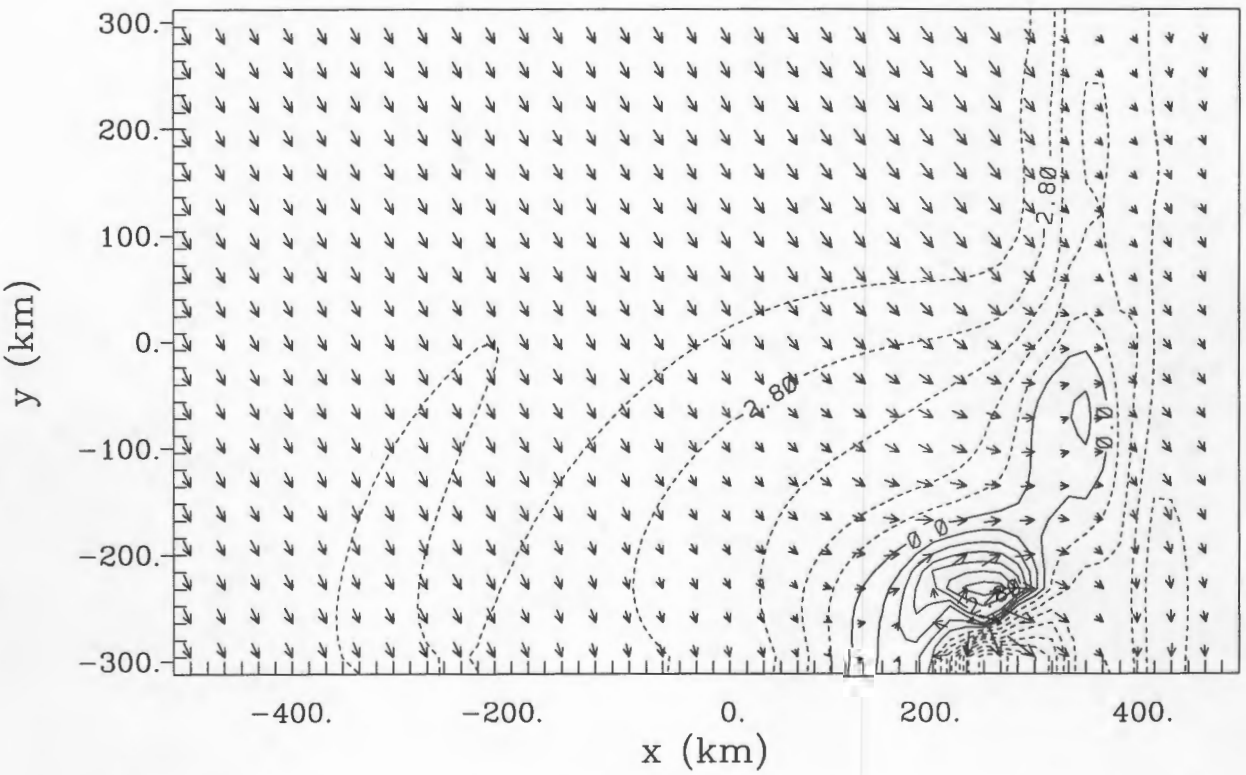

Figure 3.22: The alongshore wind speed in the horizontal cross-section 24.1 m above ground after 8 hours of simulation in the run with a cooling area of 7 grid points x 7 grid points x 10 grid points and a maximum cooling amount of 13 ^{0}C. Contour interval: 0.7m/s.

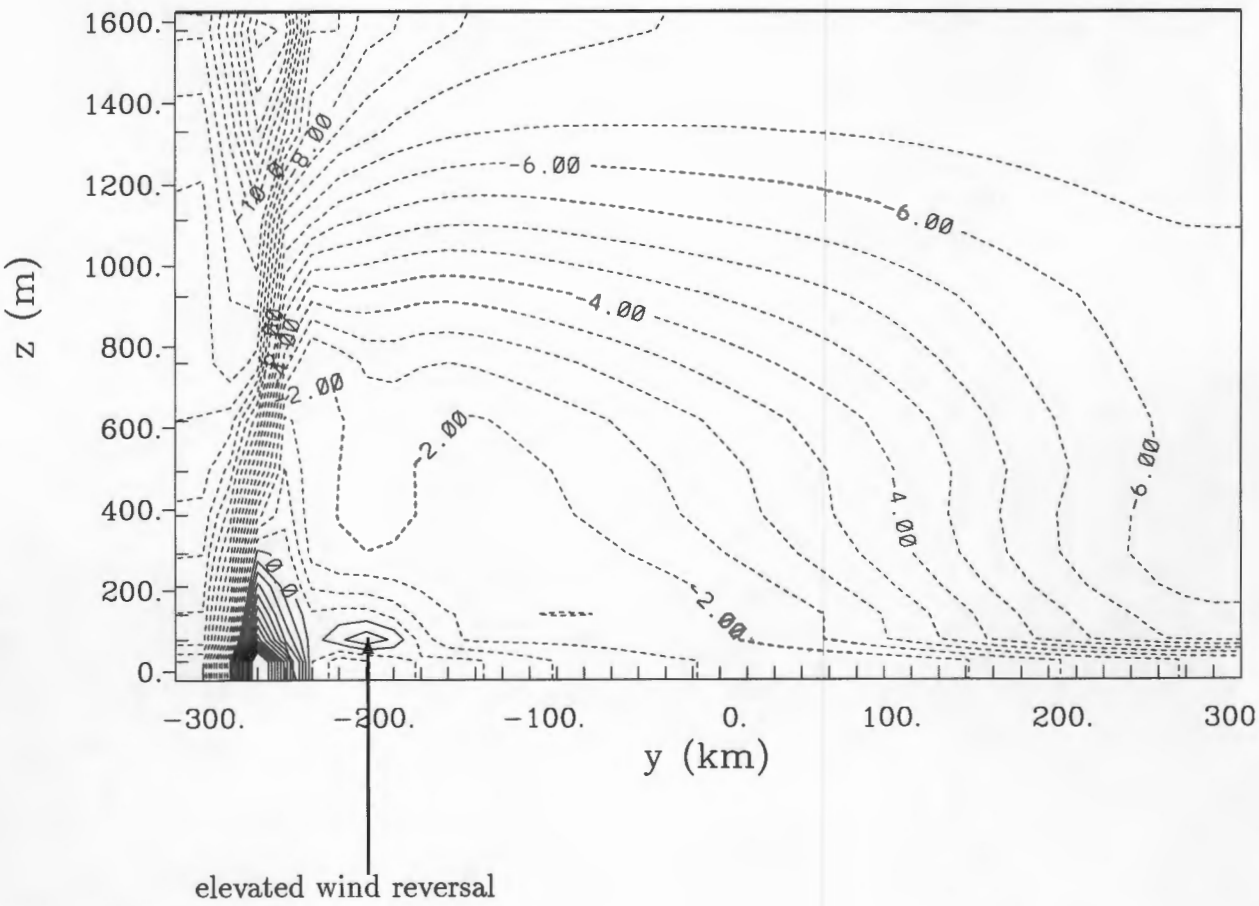

Figure 3.23: The vertical cross-section of alongshore wind speed after 15 hours of simulation in the run with a cooling area of 5 grid points x 5 grid points x 10 grid points and a maximum cooling amount of 13 ^{0}C. The cross-section is located in a south to north slice 296 km east of the middle of the model domain. Note that there is an elevated wind reversal near the original cooling region. Contour interval: 1m/s.

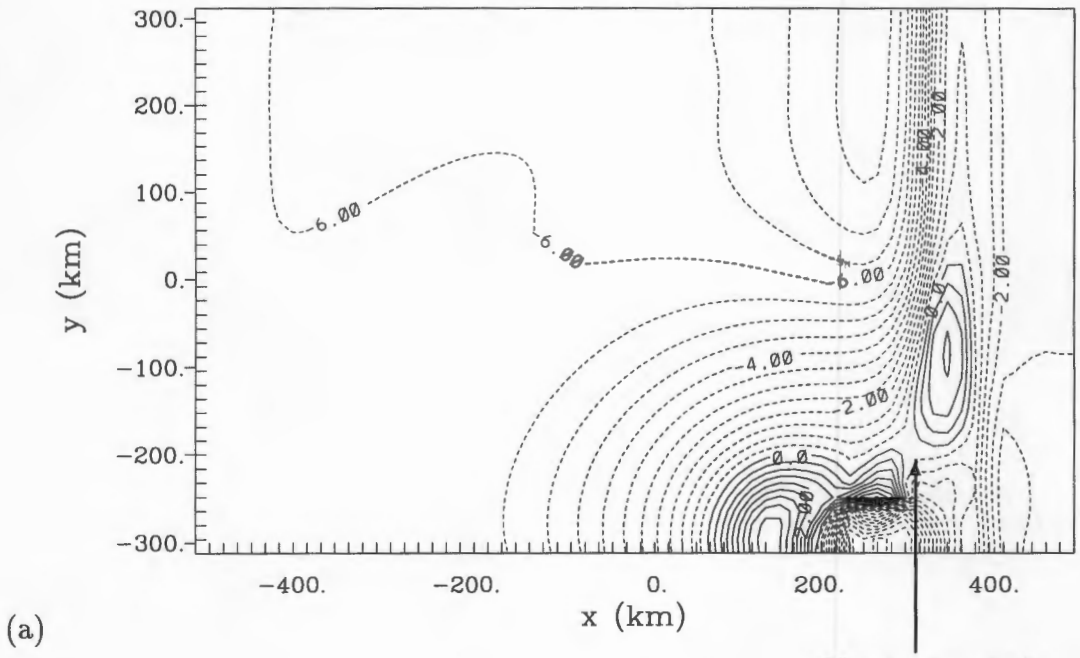

(a)

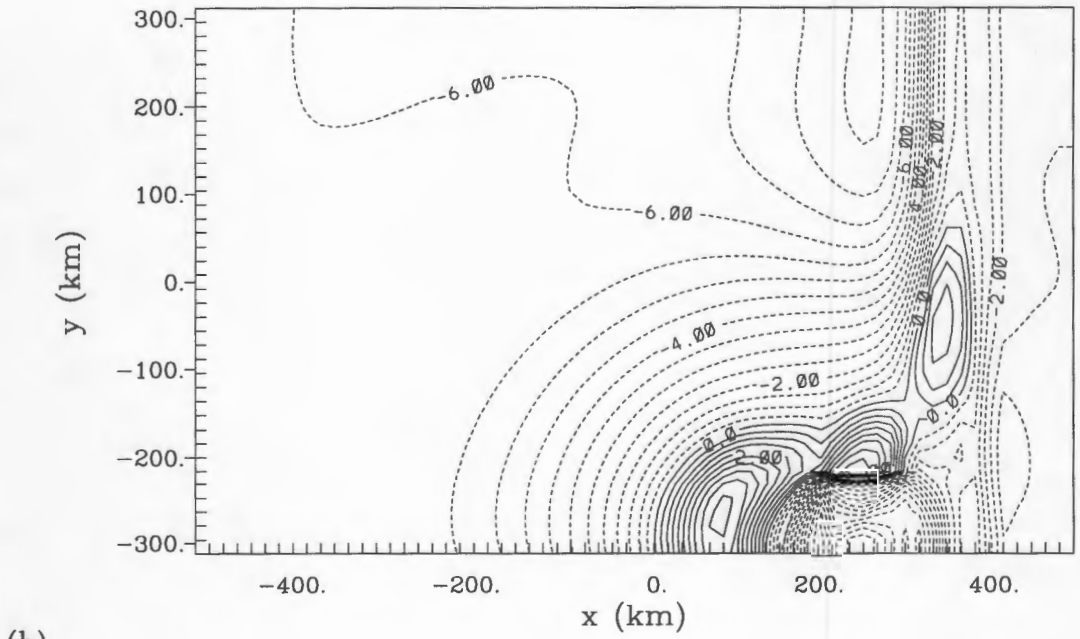

(b)

Figure 3.24: The alongshore wind speed in the horizontal cross-section 24.1 m above ground after 9 hours of simulation in (a)the run with a cooling area of 5 grid points x 5 grid points x 13 grid points and a maximum cooling of 1.2-10.2 ^{0}C. Note that in some regions of the CTD wind reverses back to northerly. (b) The run with a cooling area of 7 grid points x 7 grid points x 13 grid points and a maximum cooling amount of 1.2-10.2 ^{0}C. Contour interval: 1m/s.

3.6 Sensitivity testing of the initial synoptic wind speed

Three runs are made to test the significance of initial opposing synoptic wind speed. During each CTD event the opposing initial synoptic wind speed is different. The effect of the synoptic northerly flow on the structure of CTDs is not well known. This section tries to find the importance of initial opposing synoptic flow on CTD evolution. Initial alongshore northerly wind speed is set as 2 m/s (hereafter run v2), 4 m/s (hereafter run v4) and 6 m/s (hereafter run v6) (northerly wind). The across-shore wind speed is set as 1 m/s (offshore) in all the simulations because this is an average across-shore wind speed (Bond et al., 1996). All the synoptic wind fields are homogeneous. According to Bond et al.'s (1996) climatological analysis, northerly alongshore wind speeds vary between 0 m/s to 10 m/s. Thus my choices of wind speeds are reasonable. Simulation results reveal that there exist very large differences, especially in the offshore scale. The simulations with smaller northerly wind have a larger offshore scale. The contrast between run v2 (Fig. 3.25(a)) and run v6 (Fig. 3.25(b)) is very large. When the northerly wind speed is small (For example, when it is less than 2m/s), the ageostrophic flow caused by the disturbance is large enough to cause wind reversal. In this case, the offshore scale can be as large as the Rossby radius. When the opposing synoptic wind speed is large the wind reversal will be mainly limited to a narrow zone near the shore. However, a decrease in the northerly flow can be observed nearly to the Rossby radius. This is due to the fact that, over the land, friction is greater and the northerly flow is decreased. Further away from the shore the northerly wind is too large to be reversed into southerly by the disturbance. Judging the location of the northmost wind reversal between 0500 UTC and 1300 UTC, the average propagation speed is 10.8 m/s in

run v6. In the simulation with an initial northerly wind of 4 m/s, the average propagation speed is 11.2 m/s in the same interval. In the simulation with an initial wind speed of 2 m/s, the propagation speed is 12.0 m/s. The difference in propagation speed is much less than the difference in initial alongshore wind speed. This is because surface friction over land decreases the contrasts in the initial wind speed. This result is not the same as that in the previous 2D simulations. The difference is due to the fact that, in 2D simulations, the surface everywhere is ocean and there is no decreasing of northerly flow due to the friction over land and there is no off-shore scale. This demonstrates the advantage of 3D simulations again.

To sum up, the sensitivity tests of initial opposing synoptic wind speed reveal that when the initial opposing synoptic wind speed is large (for example, 6 m/s), the off-shore scale of CTDs is greatly reduced. This is mainly due to the friction of the land, which decreases the synoptic northerly flow and makes wind reversal possible in the case of large initial synoptic wind speed (for example, 6 m/s). Over the ocean there is no wind reversal. However, there is a decrease in the northerly flow.

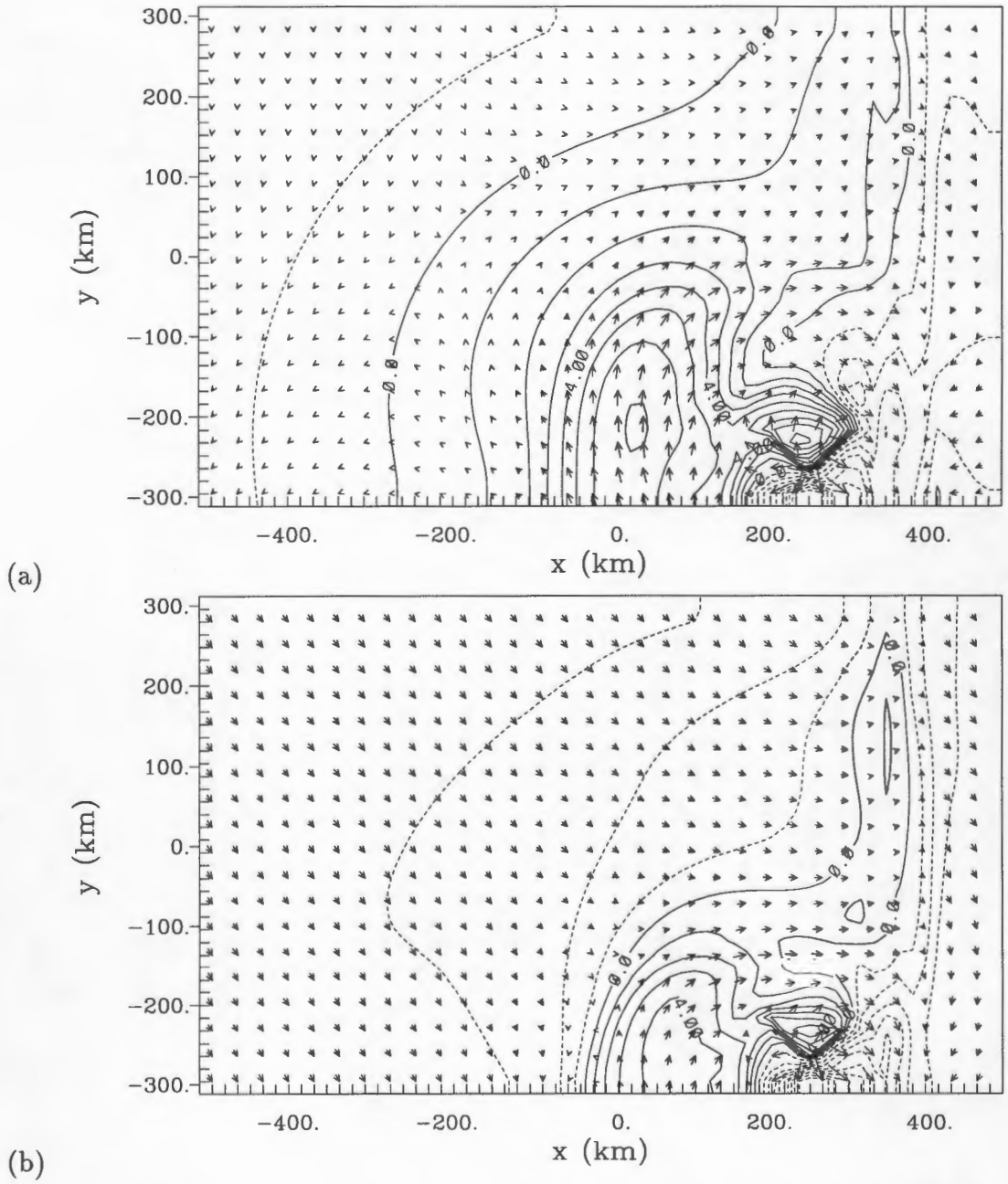

Figure 3.25: The alongshore wind speed in the horizontal slice 24.1 m above ground after 15 hours of simulation. (a) in the run with an opposing wind speed of 2 m/s (b) in a run with an opposing wind speed of 6 m/s. Contour interval: 1m/s.

3.7 Sensitivity testing of sea surface temperature (SST)

In each CTD event the SST is different. In the summer the SST is usually lower than the atmospheric temperature. The ocean exchanges heat with the atmosphere. Thus different SST may have different effects on the structure and propagation of CTDs, especially in the lower atmosphere. In the sensitivity testing of SST three simulations are made. The SSTs are homogeneously set as 16 ^{0}C (hereafter run SST-16-3D), 21 ^{0}C (hereafter run SST-21-3D), 23 ^{0}C (hereafter run SST-23-3D), respectively. These SSTs are all possible around the North American west coast summer. In the NCEP reanalysis project (NOAA, 1997), the monthly average SST over the North American west coast ranges from 10-15 ^{0}C in May, 11-18 ^{0}C in June and 15-23 ^{0}C in July. The simulation results reveal that the propagation speed of the CTD with a SST of 21 ^{0}C, is slightly faster than that with a SST of 16 ^{0}C. I have also made 2D simulations to test the effect of SST. In the 2D simulations the grid spacing is 2 km, sounding data are the same as those used in the 3D run, and other parameters are also the same as used in the 3D simulations. The two SSTs are 16 ^{0}C (hereafter run sst-16-2D) and 21 ^{0}C (hereafter run SST-21-2D), respectively. When the SST is colder than the original cooling region, there is usually a very stable layer immediately above sea surface. This is because the air temperature is cold near the sea surface due to the heat exchange between the sea and air (Fig. 3.25(b)). In the 2D simulation the CTD with an SST of 16 ^{0}C propagates slightly faster. This appears to be a dilemma. Careful comparison between the 2D and the 3D simulations resolves the problem. In 2D simulations, the cooling is homogeneous and the cooling amount is more than that in the 3D simulations. Sixteen degrees is quite close to the potential temperature (or the lowest level atmospheric

temperature) of the original cooling area after the cooling. In the potential temperature plot of the 2D simulation with a SST of 16 ^{0}C, there is no horizontal temperature gradient in the lower level within the CTD. However, at the edge there is a large temperature gradient that separates the CTD from the environmental air (Fig. 3.26(b)). In the 2D simulation with a SST of 21 ^{0}C, the temperature gradient is spread evenly in the CTD and there is no distinct front in the lower atmosphere (Fig. 3.26(a)). In the 3D simulations, 21 ^{0}C is closer to the lowest level atmospheric temperature of the original cooling region. The potential temperature plot reveals the same thing as in the 2D simulations. There is no horizontal temperature gradient inside the CTD and there is a front above the surface separating the CTD from environmental air (Fig. 3.26(7)). In the 3D simulation with a SST of 16 ^{0}C, there is a horizontal temperature gradient inside the CTD while there is no front in the lower atmosphere (Fig. 3.27(a)). The existence of the front enhances existing pressure differences between the head of the disturbance and the ambient air. The enhanced pressure gradient increases the propagation speed. Thus, when SST is close to the lowest level atmospheric temperature after the cooling, the CTD seems to become stronger. The 3D simulation with a SST of 23 ^{0}C further confirms the theory. The SST in this simulation splits into two after 11 hours of simulation (Fig. 3.28). There is no front in the lower atmosphere either (Fig. 3.27(c)).

To sum up, when the SST is close to the temperature of the lower atmosphere after cooling, a front comes into being. The pressure gradient at the head is enhanced by the front and the propagation speed is faster than those of the CTDs with a SST higher or lower than the temperature of the lowest atmosphere after cooling.

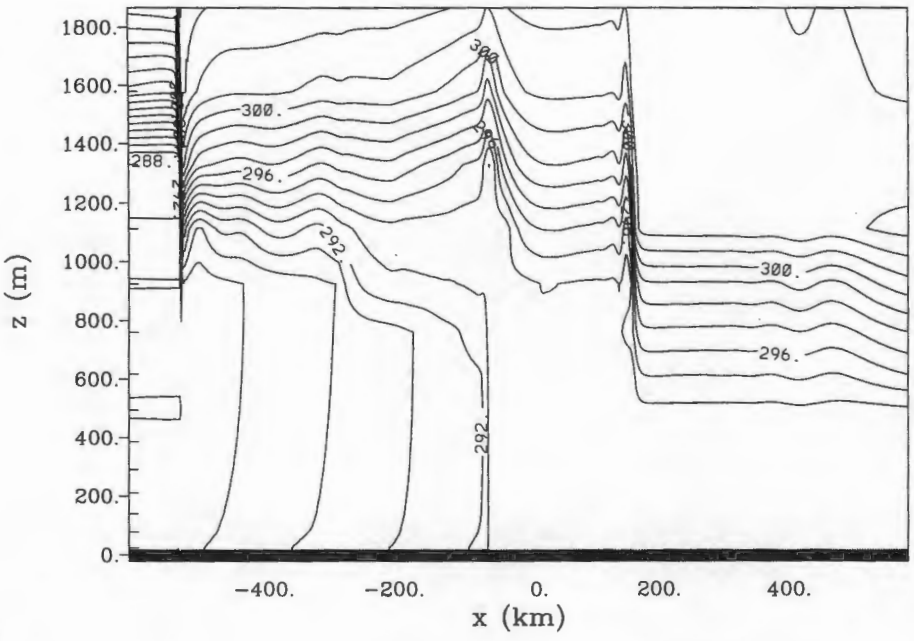

(a)

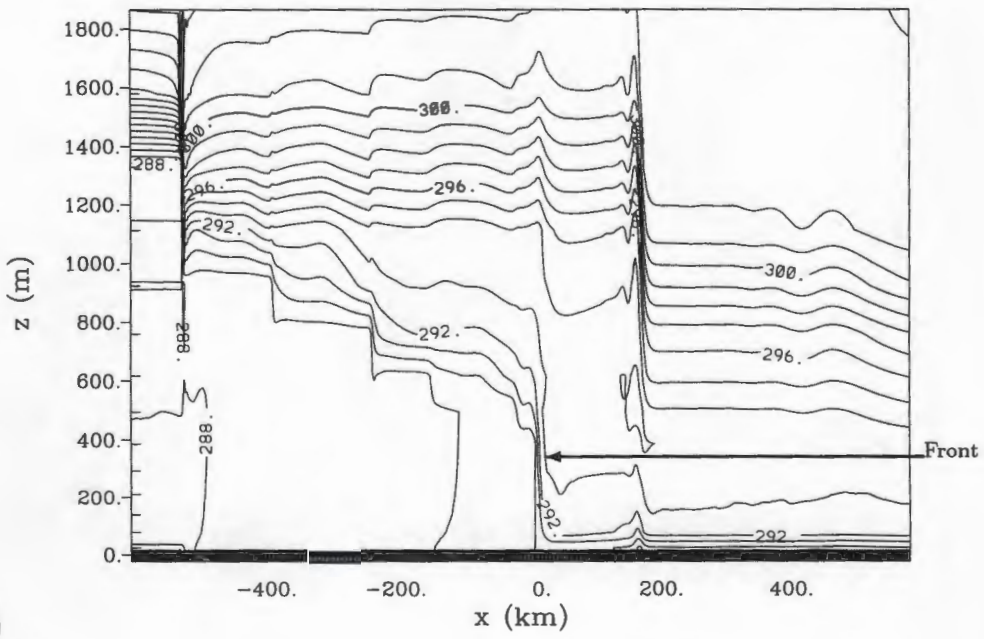

(b)

Figure 3.26: The vertical profile of potential temperature in 2D simulation after 15 hours of simulation.(a) sea surface temperature=21 ^{0}C. (b) sea surface temperature=16 ^{0}C. Note that there is a front in the lower atmosphere. Contour interval: 1K

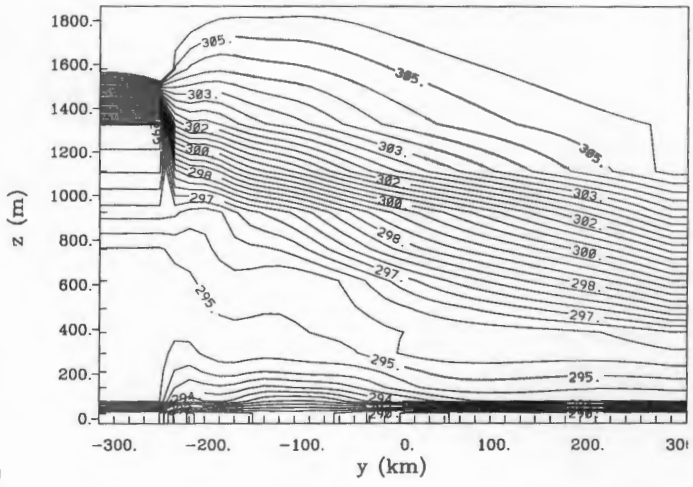

(a)

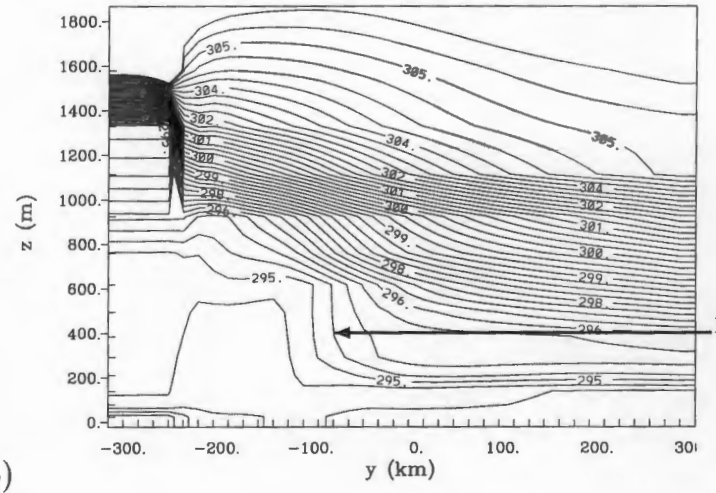

(b)

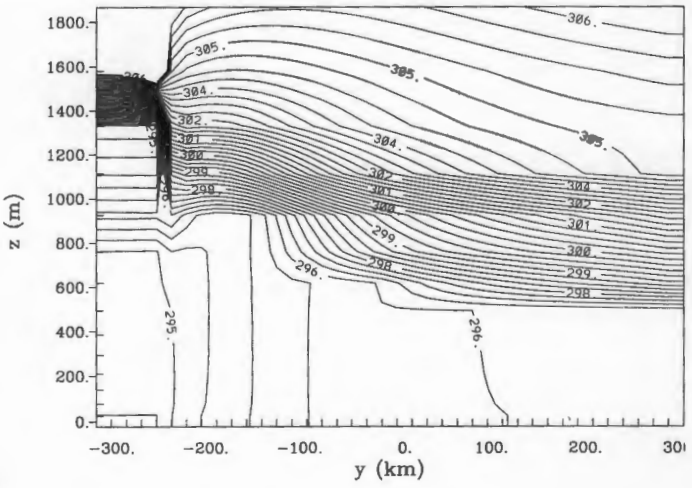

(c)

Figure 3.27:

Fig. 3.26. The vertical profile of potential temperature in 3D simulation after 15 hours' simulation in the 3D simulations. The vertical cross-sections is located in a south-north slice 248 km east of the center of the model domain. (a) sea surface temperature=16 ^{0}C (b) sea surface temperature=21 ^{0}C. Note that there is a front in the lower atmosphere. (c) sea surface temperature=23 ^{0}C. Contour interval:0.3K

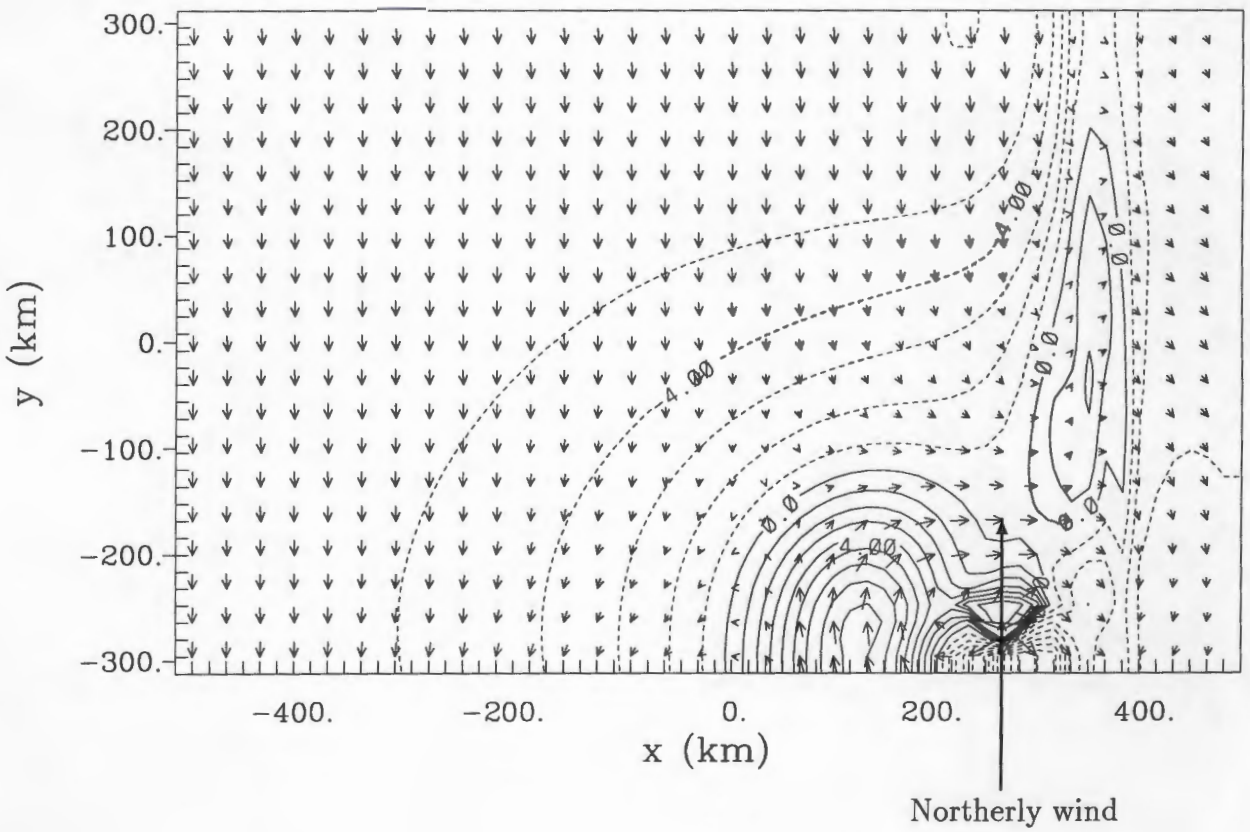

Figure 3.28: The alongshore wind speed in the horizontal cross-section 24.1 m above ground after 11.5 hours' simulation in the 3D simulation with a sea surface temperature of 23 ^{0}C. Note that in some regions of the CTD wind reverses back to northerly. Contour interval: 1m/s.

3.8 Sensitivity testing of gaps in the coastal mountains

Along the North American west coast there are many valleys which dissect the coastal mountains. According to observations (Reason and Dunkley, 1993), valleys tend to slow CTDs. In this section the effects of different depths of gaps on CTD evolutions are studied. In this study, four valleys (Fig. 3.29(a), Fig. 3.30(a), Fig. 3.31(a), Fig. 3.32(a)) are used. The valleys range from one whose lowest altitude is 500 m with the altitude descending from 2000 m to 500 m over a distance of 50 km and the bottom of the valley (500 m high) is 50 km wide, to a narrow valley whose altitude descends from 2000 m to 1400 m over a distance of 30 km. There are many valleys in the North American Pacific coastal mountains and Southeastern Australian mountains. In the Hunter river valley around Newcastle, Australia, the altitude decreases from 1000 m to below 400 m over a distance of 50 km. In North America there are also many valleys such as the Columbia river valley. In the Columbia river valley, the altitude drops from over 1000 m to below 200 m. In some locations, the Columbia valley is 30 km wide while in other locations it can be as wide as 160 km. In the Sacramento river valley the altitude decreases from over 1000 m to below 100 m over a distance of 50 km (Rado et al., 1993). Thus the valleys selected are realistic in width.

The simulation results reveal that valleys have a large (in comparison with the effect of different SST) impact on CTD propagation (Fig. 3.29(b), Fig. 3.30(b), Fig. 3.31(b) and Fig. 3.32(b)). The offshore scale of the CTD is greatly reduced after they passed the valleys. In fact, in valley 1-3 the offshore scale of the CTD is so small that it can be very easily missed by the observations, since there are only a few boats and aircraft observations of CTDs. Thus researchers may think that the CTD stops at the valley. Satellite images show that the

coastal stratus stalled or even stopped propagating at the Columbia River mouth during one event(Reason and Dunkley, 1993). According to Reason (1989), CTDs are usually greatly influenced by coastal valleys. Sometimes a CTD may retreat after it reaches a valley and sometimes it may stop at the valley. Thus observations support the simulation results.

The across-shore wind speed in the valley is high (4 m/s) and this dissipates the CTD greatly (Fig. 3.33). At the bottom of the valley, topography is lower than the disturbed stable layer above the MBL and topographic trapping is not efficient.The energy leaks through the valley and CTD becomes weaker. When the height of the bottom of the valley is close to that of disturbed stable layer above the MBL, the influence on the CTD propagation becomes smaller. In valley 4, the maximum altitude of the valley is 1400 m, which is close to the maximum height of cooling, the off-shore scale of the CTD is significantly larger after it passes the valley than those in the simulation of valley 1-3. The simulation results are consistent with Reason and Dunkley's (1993) observation of the September 1988 event. In that event a CTD stalled 8 hours at Columbia River mouth. It was also found that the CTD slowed near the strait of Juan De Fuca.

To sum up, the propagation speed and off-shore scale of CTDs are decreased by the valleys. This is due to the fact that energy is leaking through the valleys and the pressure gradient between the wave front and environmental air is decreased. When the depth of the valley is close to that of of the disturbed stable layer above the MBL, the effect on CTD evolution becomes smaller.

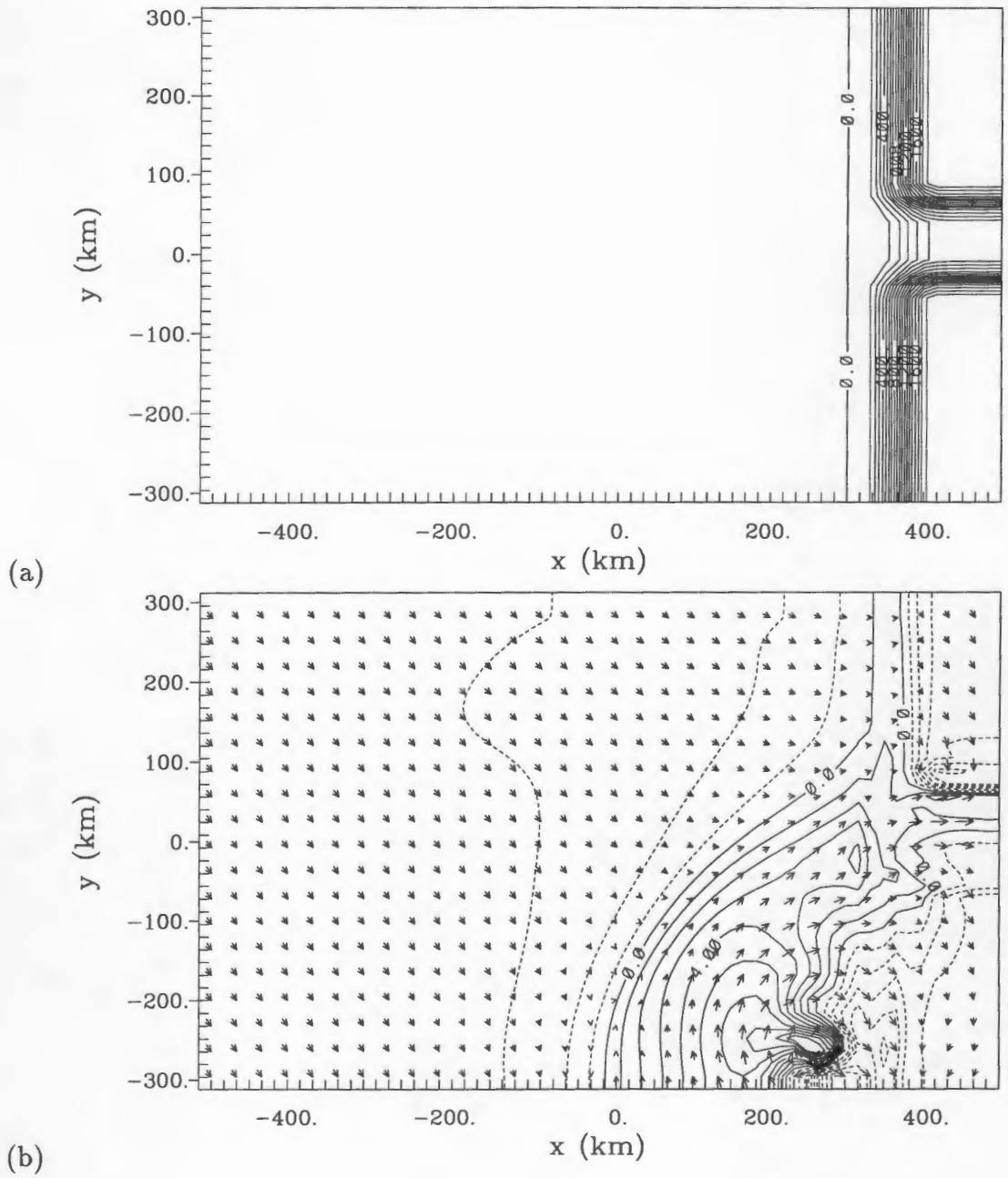

Figure 3.29: (a)Valley 1. Valley depth: 1500 m; Valley width: 65 km; Contour interval: 100m. (b)The alongshore wind speed in the horizontal cross-section 24.1 m above ground after 20 hours of simulation with valley 1. Contour interval: 1m/s.

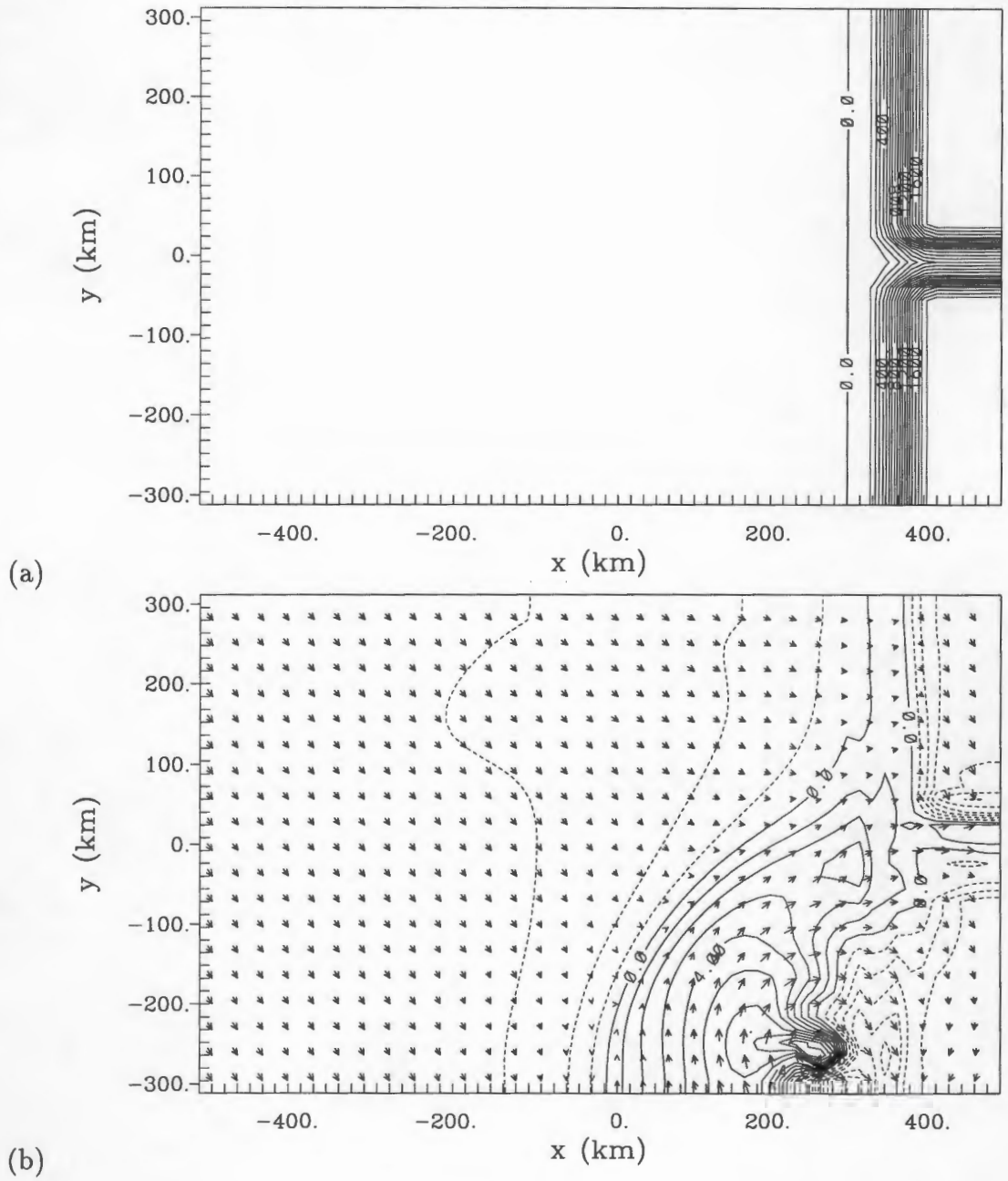

Figure 3.30: (a)Valley 2. Valley depth: 1200 m; Valley width: 65 km; Contour interval: 100m. (b)The alongshore wind speed in the horizontal cross-section 24.1 m above ground after 20 hours of simulation with valley 2. Contour interval: 1m/

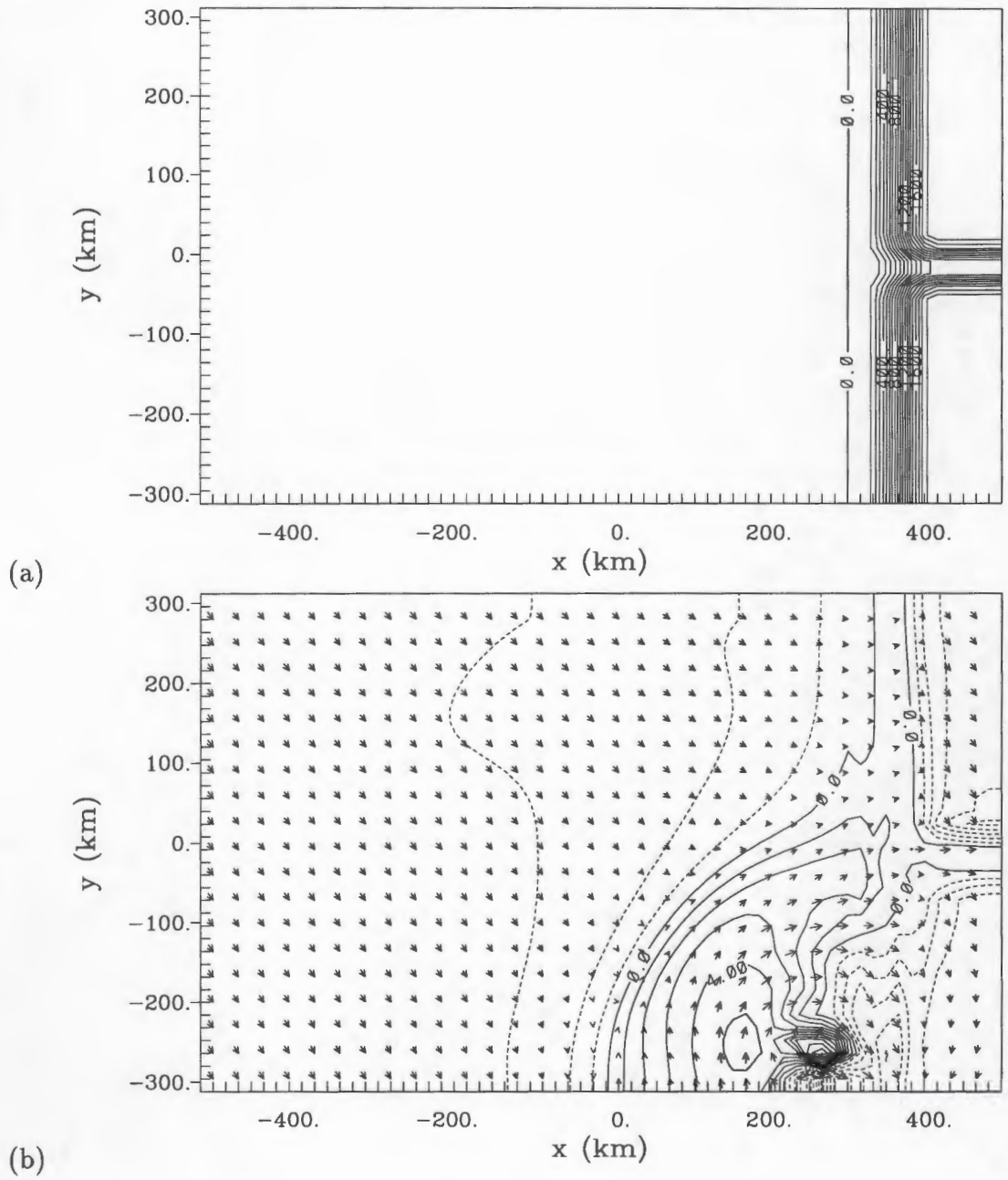

Figure 3.31: (a)Valley 3. Valley depth: 900 m; Valley width: 65 km; Contour interval: 100m. (b)The alongshore wind speed in the horizontal cross-section 24.1 m above ground after 20 hours of simulation with valley 3. Contour interval: 1m/s.

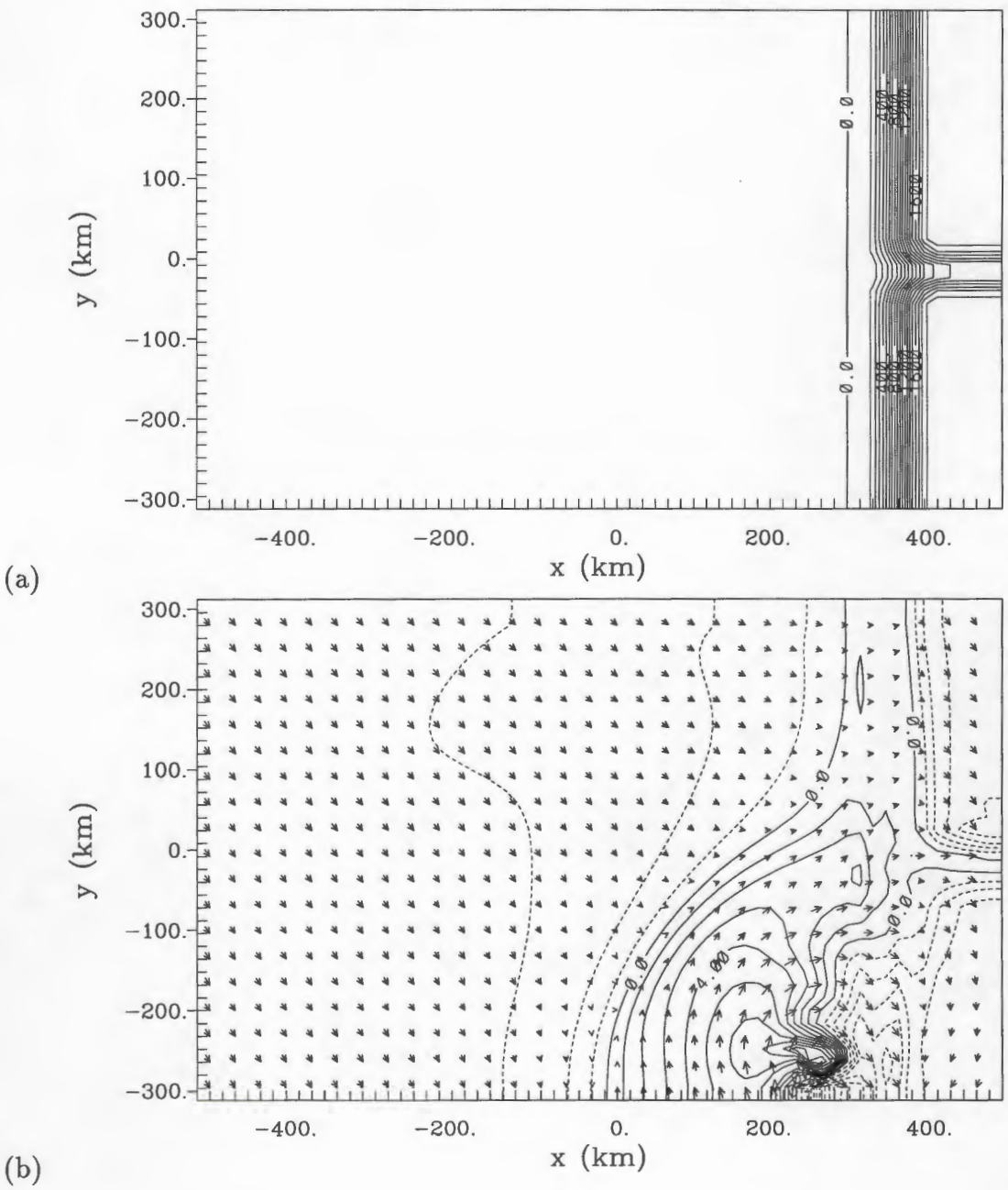

Figure 3.32: (a)Valley 4. Valley depth: 600 m; Valley width: 65 km; Contour interval: 100m. (b)The alongshore wind speed in the horizontal cross-section 24.1 m above ground after 20 hours of simulation with valley 4. Contour interval: 1m/

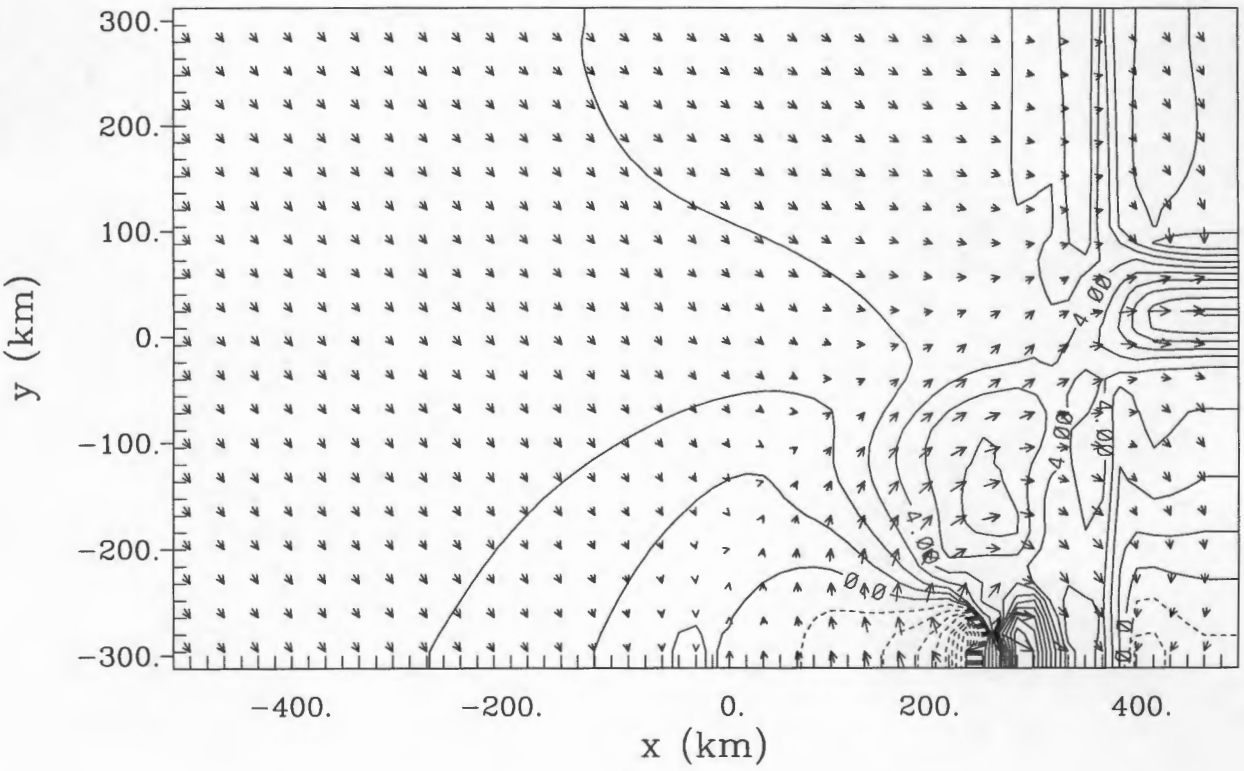

Figure 3.33: The across-shore wind speed in the horizontal cross-section 24.1 m above ground after 20 hours of simulation of valley 1. Contour interval: 1m/s.

3.9 Sensitivity testing of mountain slope and descending topography

In the testing of a descending topography the coastal mountain height evenly descends from 2000 m to 500 m over a distance of 100 km in the alongshore direction. In North America and Australia the topography is broken. There are many valleys and regions of descending topography, especially north of Brisbane (Reason, 1989). Descending topography exist in South America and Northwest Africa, where CTDs are speculated to occur. Also there are many coastal regions where CTDs may occur once the synoptic condition becomes favourable. The general results obtained from the testing will help to study other CTDs. Along the North American west coast the steepness of mountains varies greatly. In some regions the altitude increases from sea level to 2000 m over a distance of 120 km in the alongshore direction. In some other regions the same lapse occurs over a distance of 50 km (Rado, et al., 1993). In all the simulations, except the sensitiviy testing of slope angle, the altitude increases from 0 to 2000 m over a distance of 64 km. In the sensitivity testing of slope angle, another slope in which the same lapse occurs over 128 km is set. In the descending topography tests, mountain steepness becomes less as the altitude decreases while in the original cooling region the mountain is still steep. Thus, the two problems can be linked together: how a less steep mountain influences the initiation of CTDs and how it influences the propagation of CTDs. See Fig. 3.34(a) for the descending topography and Fig. 3.35(a) for the less steep mountain.

Two simulations are made to test the effect of the steepness of the slope on the propagation of CTD. In one of the simulations, the altitude increase from 0 m at the shore to 2000 m at the mountain top over a distance of 128 km (hereafter run ag). In the control run ca-7*7 the same lapse happens over a distance of 64 km. In run ag, the offshore scale is much smaller than that in the control simulation. See Fig. 3.35(b) for the wind field in run ag and Fig. 3.36(b) for that in the control simulation. Note in the control simulation the propagation speed is faster as it travels a longer distance during the same time interval. Here the offshore scale of a CTD is defined by the distance from the shore to the westmost point of wind reversal in the same latitude. Along the North American west coast, in some areas the topography increases to 2000 m just 60 km from the shore while in some other region it happens over a distance of 100 km or more. In the simulation with descending topography (hereafter run ht) the CTD propagates with a greatly reduced speed (Fig. 3.34(b)).

Southerly flow is dominant near the initial cooling region. However, the Coriolis force gradually turns the southerly flow into westerly as an air parcel travels to the north. Thus the southerly component of the wind changes into the westerly component. The westerly onshore component is blocked by the coastal mountains and gradually reduces to 0.

The influence of slope angle on CTD propagation can be explained by the following facts:

- When the mountain is higher than the raised MBL height and the slope is steep (such as the idealised mountains used in the control simulation), the westerly component is quickly blocked and southerly component hasn't been decreased much during the blocking process. In this case, the southerly wind is large and the CTD is strong (such as the CTD in the control simulation).

- When the mountain is higher than the raised MBL height but the slope is not steep (such as the mountain in the run ag), it takes longer for the westerly component to be blocked. More time is available for the Coriolis force to turn the southerly flow into westerly. Moreover, as an air parcel travels longer over the mountain, friction also has more time to reduce the wind speed. Thus in this case southerly wind is small and the CTD is weak (such as the CTD in the run ag).

- When the mountain height is less than the raised MBL height, across-shore flow cannot be completely blocked. The disturbance penetrates deep into the continent and energy leaks through the mountain. In this case the trapping mechanism is not working properly and a CTD will become weaker.

To sum up, small slope angle (in comparison with a larger slope angle) and descending topography are not favorable to the CTD propagation. Propagation speed of CTDs is decreased in the above situations. This is due to surface friction, a longer time is available for the Coriolis force to act on the air.

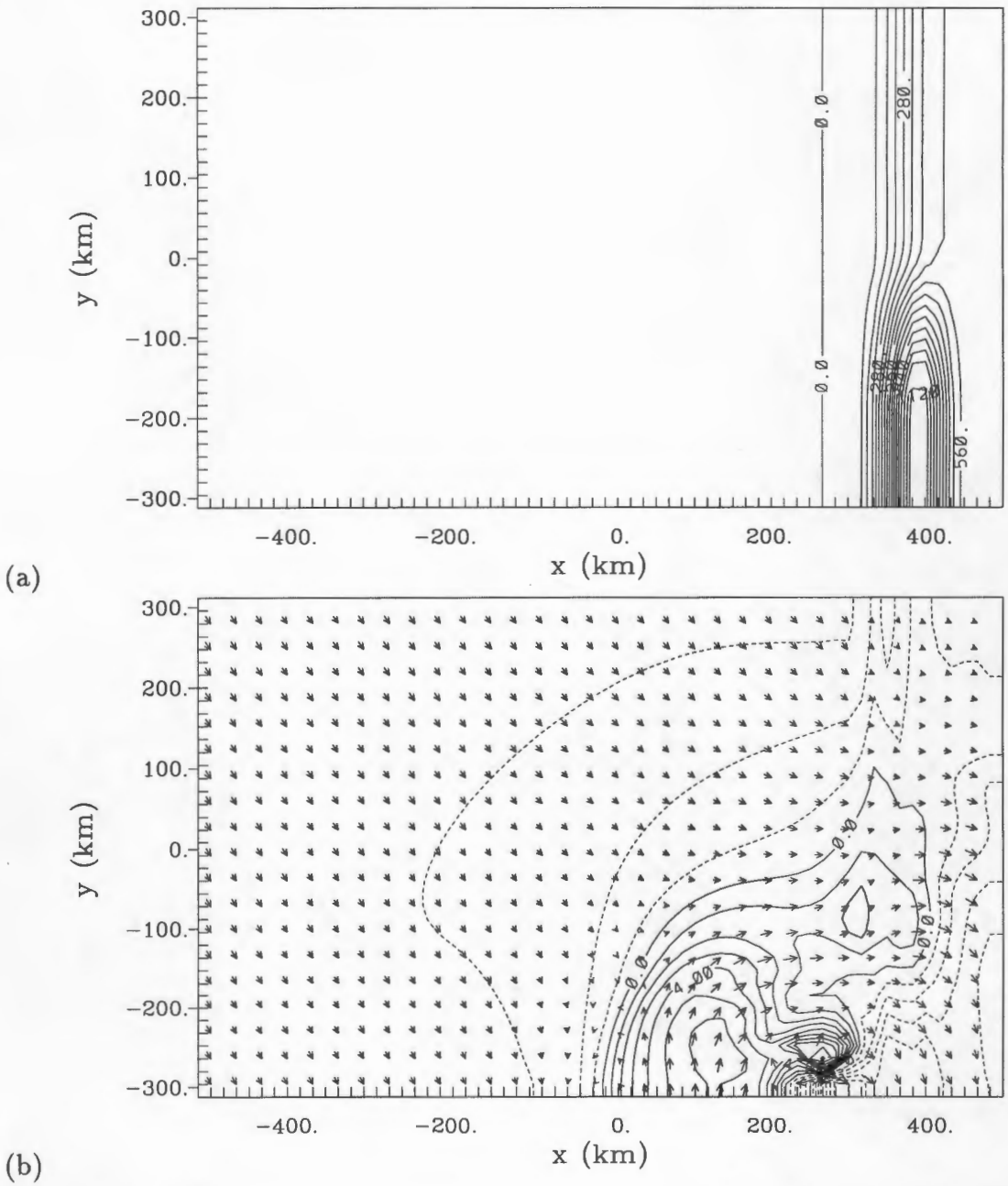

Figure 3.34: (a) The descending topography used in run ht. Contour interval: 70m. (b) The alongshore wind speed in the simulation of descending topography after 15 hours of simulation. The horizontal cross-section is located 24.1 m above ground. Contour interval: 1m/s.

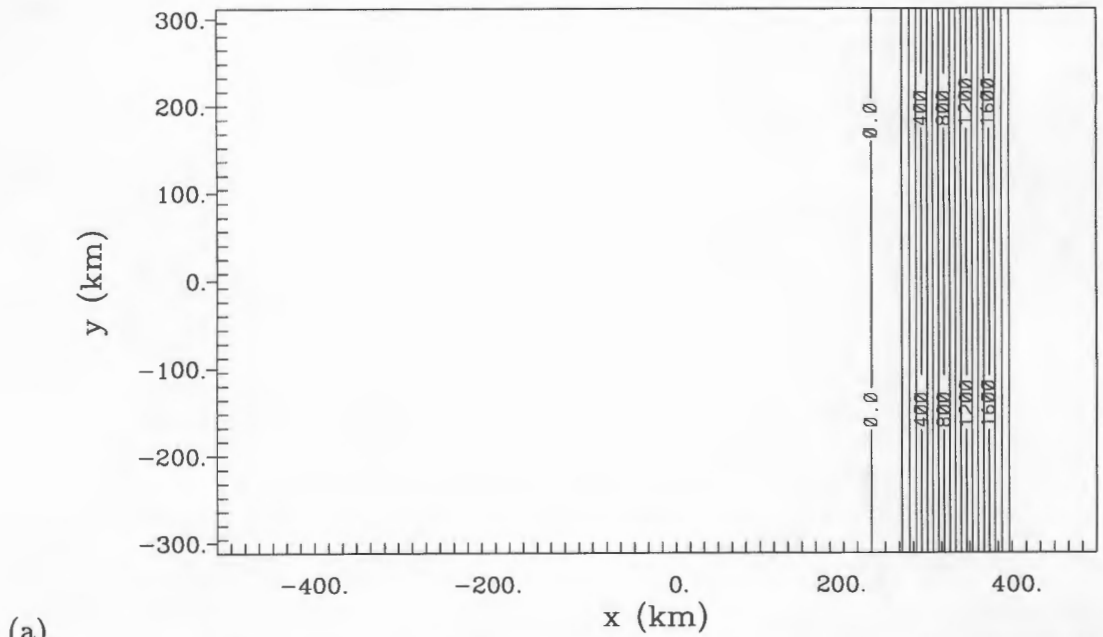

(a)

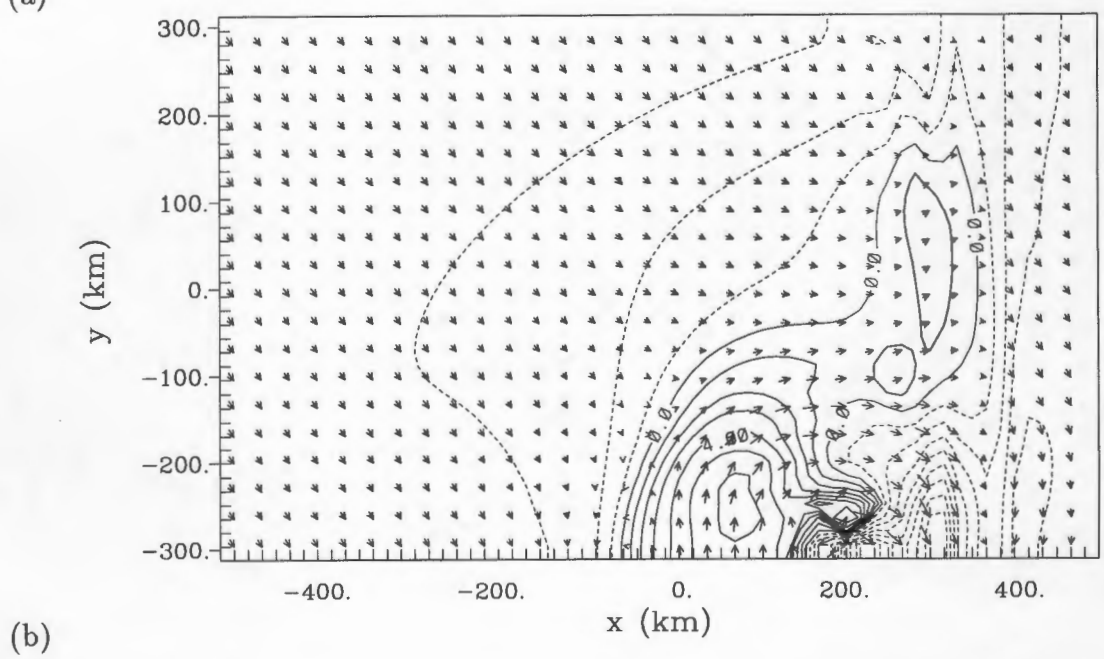

(b)

Figure 3.35: (a)The less steep mountain used in run ag. Contour interval: 100m. (b) The alongshore wind speed in the simulation with a less steep mountain after 15 hours of simulation. The horizontal cross-section is located 24.1 m above ground. Contour interval: 1m/s.

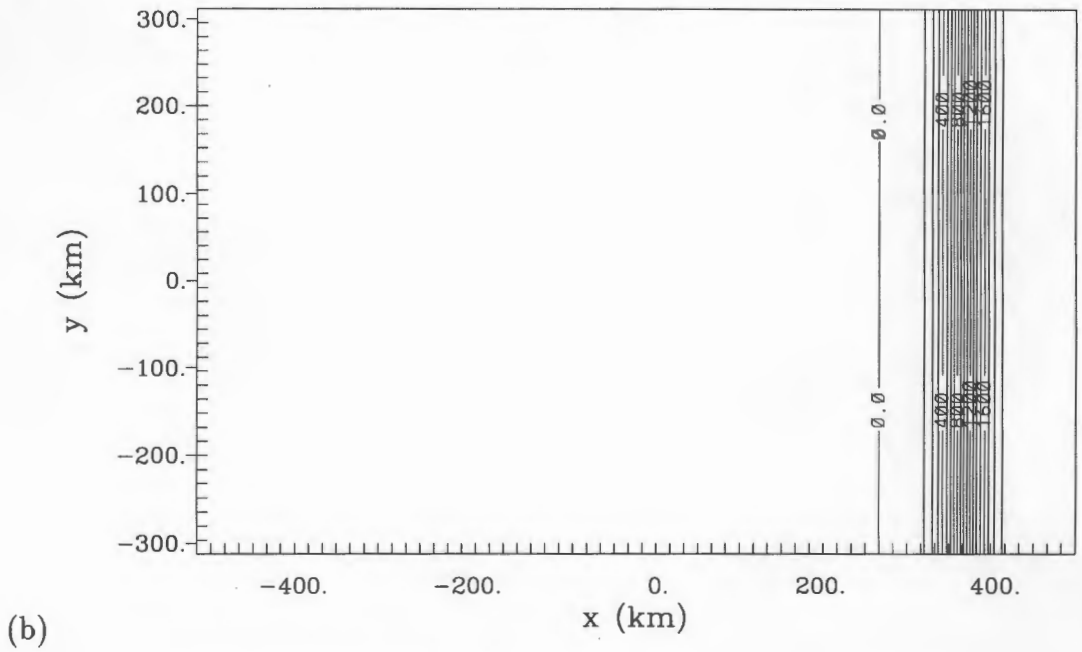

(b)

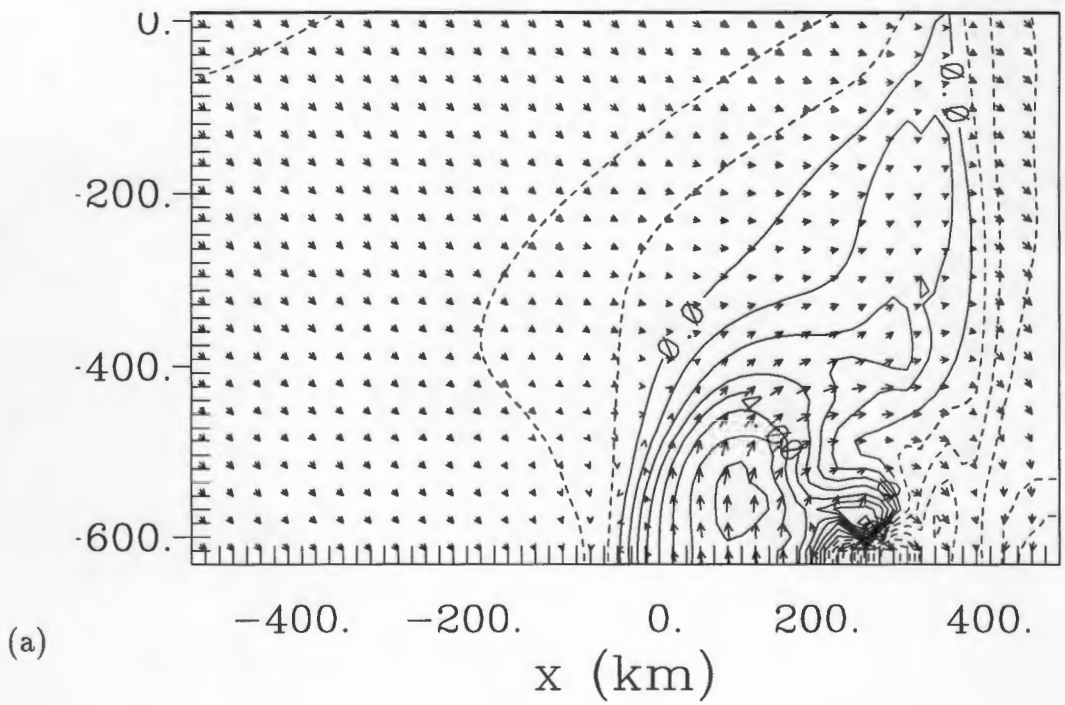

(a)

Figure 3.36: (a) The control topography used. Contour interval: 100m. (b) The alongshore wind speed in the control simulation after 15 hours of simulation. The horizontal cross-section is located 24.1 m above ground. Contour interval: 1m/s.

3.10 An idealised simulation of CTD propagating past a near-shore island

There are some coastal islands near the North American west coast, such as Vancouver Island. According to observation (Reason and Dunkley, 1993), they have significant effects on CTD propagation. In testing the effect of a near-shore island, a simplified version of Vancouver Island was used for 2 runs. In the first the simplified topography of Vancouver Island, British Columbia and Washington State is used. In the other run Vancouver Island is removed. The difference will be the influence of Vancouver Island. See Fig. 3.37(c) for the simplified topography of Washington State, B.C. and Vancouver Island.

The modelling results show that the CTD splits into two, one trapped by the coastal mountain of the mainland and the other trapped by the mountain on the island. The wind field over the simplified topography of Washington state resembles observations. The CTD penetrates into Washington state because of valleys around the Olympic Pennisula (Reason and Dunkley, 1993). See Fig. 3.37(d) for the simulation without Vancouver Island, Fig. 3.37(e) for the idealised topography without Vancouver Island, Fig. 1.2 for the real topography of Vancouver Island, B.C. and Washington State, Fig. 3.37(c) for the idealised topography of Vancouver Island, B.C. and Washington State. Fig. 3.37(b) for the simulation with Vancouver Island and Fig. 3.37(a) for an observation of a CTD near Vancouver Island (Mass and Albright, 1987). Note the ridge of high pressure splits into two due to the existence of Vancouver Island. With the arrival of a CTD, the across-shore wind becomes onshore near Vancouver Island. The onshore flow brings cold marine air into the idealised strait of Juan de Fuca and this leads to cooling in the lower atmosphere. Another branch of the trapped disturbance comes into being and propagates along the mountains in the Vancouver Island.

To sum up, a near-shore island may split a CTD into two, one trapped by the coastal mountains of the continent and the other by the mountains of the island. This probably will occur when the CTD is very strong and plenty of cold air advects through the strait of Juan De Fuca.

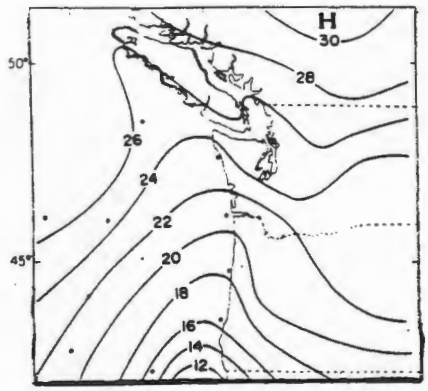

(a)

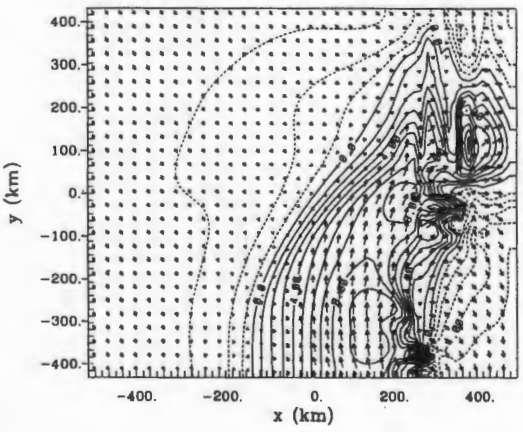

(b)

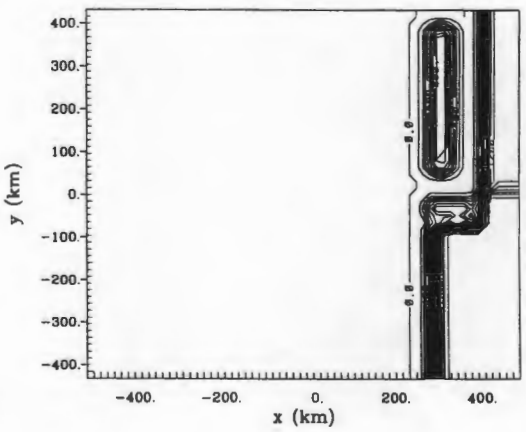

(c)

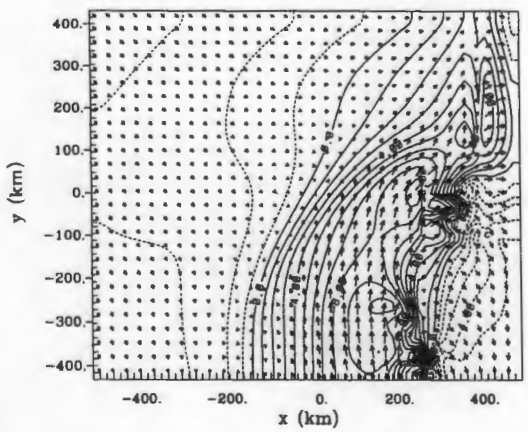

(d)

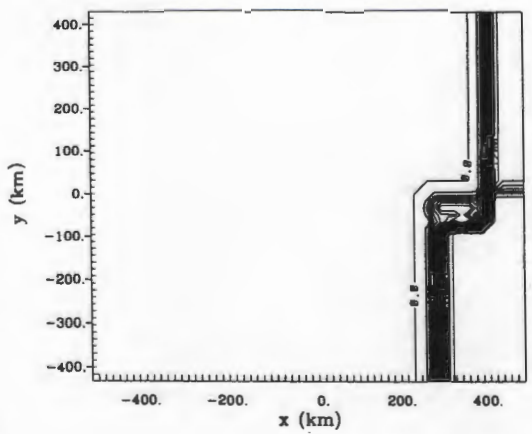

(e)

Figure 3.37:

Figure 3.36: The idealised testing of the effect of Vancouver island on the propagation of a CTD:(a) The observation of a CTD event near Vancouver island. Mean sea level pressure in millibars (only last two digits shown) (reproduced from Mass and Albright, 1987) (b) The alongshore wind speed in the horizontal cross-section 24.1 m above sea surface after 20 hours of simulation with Vancouver Island; (c) The idealised topography in the simulation with Vancouver island; (d) The alongshore wind speed over sea surface after 20 hours of simulation without Vancouver island; (e) The idealised topography used in the simulation without Vancouver island. Contour interval is 100m for topography and 1m/s for wind speed.

Chapter 4

Summary and Conclusion

RAMS is used in a sensitivity testing mode to study various synoptic and topographic effects such as the initial cooling area and the cooling amount, the initial wind speed, valleys in coastal mountains, descending topography, near-shore islands, and SST, on the propagation of CTDs. The CTDs are initiated as gravity currents by cooling the model lower atmosphere near the shore. After the cooling there is a zone near the shore in which the northerly wind reverses into southerly wind. The CTDs propagate northward along the coastal barrier. The simulations are summed up in Table 4.5.

Interactions between cooling amount and cooling area are studied. The CTD is very sensitive to the initial cooling condition. A small change of initial cooling amount might result in very different wind reversal characteristics. When the cooling amount is small the CTD might even retreat after a few hours. The interactions between cooling amount and other factors are of particular importance. Simulation results reveal that

- With small amounts of initial cooling (for example, when the maximum cooling amount is less than 4-13 ^{0}C), CTD begin to retreat and wind direction to reverse back to northerly before 12 hours of simulation. It is found that when cooling amount is small, wind reversal may happen in the upper level first. This is consistent with observation of the 1994 (Ralph, et al., 1995) and 1996 cases (Nuss, 1997). In both cases there is a

weak CTD with an elevated wind reversal.

- When small amounts of initial cooling (for example, when maximum cooling amount is less than 4-13 ^{0}C) are combined with larger cooling areas, there are more intense and rapidly propagating CTD since the supply of cold air is the main limitation.

- When the cooling amount is large (for example, when the maximum cooling amount is 6-15 ^{0}C) and the CTD can propagate for at least 20 hours (which is close to the typical lifespan of CTD, 1-1.5 days), larger cooling areas will result in more rapid CTD decay. This is because when the area of cold air is large (for example, when the cooling area is larger than 10 grid points x 10 grid points), there is sufficient time for geostrophic adjustment to occur. In other words the larger off-shore scale allows more time for the Coriolis force to turn the southerly flow into westerly. Therefore, as long as the supply of cold air is not a limitation, disturbances initiated by larger cooling areas will retreat sooner.

- When the opposing flow is strong, the across-shore CTD scale tends to be less. This is mainly due to the frictional effect of the land. It decreases the initial northerly flow. Thus wind reversal may happen over the land but over the ocean there is still no wind reversal. This causes the off-shore scale of the CTD to be much less than the Rosssby radius. However, the magnitude of the northerly wind may still be reduced offshore. If the CTD is strong enough there may also be a wind reversal over the ocean.

- The sensitivity tests of SST variations show that when the SST is close to the lowest level atmospheric temperature after the cooling, there will be a front near the surface.

The pressure gradient between the wave front is enhanced and the propagation speed of CTD is slightly enhanced.

- Valleys or gaps which dissect the coastal mountains are found to affect CTD propagation. When the depth of the valley is significantly lower (for example 25% lower) than the maximum height of the disturbed lower atmosphere, the across-shore scale of the CTD is much smaller after it passes the gap. On-shore flow within a valley is enhanced. In the observation of the CTD event of September 1988 (Reason and Dunkley, 1993) it was found that the CTD stalled at the Columbia river valley.

- Simulations in which an island is placed near the coast reveal that the CTD may split, with one part trapped by the coastal mountain of the mainland and the other trapped by the mountain on the island. This may happen when a CTD is very strong and a cold air reservoir can be built in the coast of B.C..

There is some limitation in our approach in that there is no warming in the north, unlike in observed cases. Instead, the cooling amount in the south is set 4-6 degrees higher to make up for the lack of a warming condition in the north. A warming condition is more difficult to set in an idealised model, because the maximum warming moves northward along the shore (Guan et al., 1998) and this maximum warming is linked to the initiation mechanism. However it is difficult to set complicated conditions that will lead to the warming in an idealised model. In comparison, the maximum cooling does not move along the shore (Guan et al., 1997) and is easier to specify in the model. Due to the lack of a warming condition, the maximum southerly wind is near the initial cooling region instead of near the wave front as in the observations. This problem might be solved in the future by initiating the CTD with

a low pressure migrating across the Rocky Mountains. The wind field and pressure field can be adopted from climatological mean value. This approach is similar to the shallow water equations approach (Rogerson and Samelson, 1996). The difference is that a 3-D model can be used and the thermal advection equation can be included. In this case, both thermal advection and momentum terms will act to create a pressure gradient near the shore. In the south of the migrating low there is onshore flow and cooling effect; in the north of the migrating low there is offshore flow and warming effect.

Some phenomena predicted in the model have not been observed so far. This is possibly due to the fact that there are not many detailed observations of actual events. For example, in the model it is predicted that a CTD may split into two near Vancouver Island. But until now there has been no CTD observed along the B.C. inner coast. In the future when there are better observations there may be CTDs found along the inner B.C. coast under favorable synoptic conditions. Also the cooling area and amount is not easily observed and their effect is difficult to study with observed data. This problem may be solved when there are better realistic simulations that can reveal the cooling condition.

Another limitation of my sensitivity tests is that it is a qualitative approach. Due to computational resources, the model is coarse. It is hard to do the sensitivity tests quantitatively without precise propagation and wind speeds. A higher resolution run was found to change the propagation speed. However it is clear which CTD is stronger qualitatively. In the future when faster computers become available, it will be possible to do the sensitivity testing quantitatively. Another constraint with my research that is also due to the limitation of computational resources, is that not enough time is available to do more sensitivity tests

in studying each factor. Sometimes adjectives such as large, small are used without precise values. Although some examples of large or small are given most of time, it is still not precise. This question can also be solved in the future when higher-speed computers become available.

4.1 Suggestion for future research

In some idealised simulations of CTD such as those of Rogerson and Samelson (1995), convergence/divergence of the onshore/offshore flow is the only factor that lead to the initiation of CTDs. In their shallow water equations there is no thermal advection equation. According to Mass and Albright (1987) the CTD is mainly initiated by the cooling in the lower atmosphere near the shore of California. It is suggested that in the future the relative importance of the convergence/divergence factor and thermal advection factor should be studied to understand the initiation mechanism of CTDs. There have been no detailed observations of CTD wind field that can reveal the convergence/divergence effect of the coastal mountains. In the future when observations of the detailed wind field are available it may be possible to resolve this problem.

Name	Purpose/Configuration	Results
ca-7*7	cooling area of 7 gps x 7 gps	control run for run ca-5*5, ca-10*10
ca-5*5	cooling area of 5 gps x 5 gps	propagation speed increased
ca-10*10	cooling area of 10 gps x 10 gps	CTD retreats
cra-5*5*13/13	cooling region: 5 gps x 5 gps x 13 gps mca: 4-13 ^{0}C	CTD retreat
cra-5*5*10/13	cooling region: 5 gps x 5 gps x 10 gps; mca: 4-13 ^{0}C	CTD retreat sooner comparing with run 2
cra-7*7*10/13	cooling region: 7 gps x 7 gps x 10 gps mca: 4-13 ^{0}C	CTD stronger comparing with run 3
cra-5*5*13/10.2	cooling region: 5 gps x 5 gps x 13 gps; mca: 1.2-10.2 ^{0}C	as a control run for run 6
cra-7*7*13/10.2	cooling region: 7 gps x 7 gps x 13 gps mca: 1.2-10.2 ^{0}C	CTD stronger comparing with run 5
v2	synoptic wind = 2m/s	as a control run for run v4, v6
v4	synoptic wind = 4m/s	propagation speed decreased off-shore scale decreased
v6	synoptic wind = 6m/s	propagation speed further decreased off-shore scale greatly decreased
sst-16-2D	SST=16 ^{0}C 2D simulation	control run for run SST-21-2D; front in the lower atmosphere
SST-21-2D	SST=21 ^{0}C 2D simulation	propagation speed decreased comparing to run 1
SST-16-3D	SST=16 ^{0}C 3D simulation	as a control run for run SST-21-3D,SST-23-3D
SST-21-3D	SST=21 ^{0}C 3D simulation	propagation speed increased comparing with run SST-16-3D; front in the lower atmosphere
SST-23-3D	SST=23 ^{0}C 3D simulation	propagation speed decreased comparing with run 3
v-1500/65	valley depth = 1500 m valley width = 65 km	propagation speed and offshore scale futher decreased comparing to run v-1500/50
v-1500/50	valley depth = 1500 m valley width = 50 km	control run for run v-1500/65
V-900/32	valley depth = 900 m valley width = 32 km	control run for run V-600/32
V-600/32	valley depth = 600 m valley width = 32 km	propagation speed and off-shore scale comparing with run 3
ag	the angle of slope is half of that in run ca-7*7	propagation speed decreased
ht	the altitude of mountains is decreasing	propagation speed decreased
novan	simulation without Vancouver Island	control run
van	simulation with Vancouver Island	CTD split into two

Table 4.5: Summary of all the simulations of coastally trapped disturbances

References

Bond, N., C. F. Mass and J. Overland, 1996: Coastally trapped wind reversals along the U.S. West Coast during the warm season. Part I: Climatology and temporal evolution, *Mon. Wea. Rev.*, 124, 430-445

Dorman, C., 1985: Evidence of Kelvin waves in California's marine layer and related eddy generation. *Mon. Wea. Rev.,* 113, 827-839

Dorman, C.,1987: Possible Role of Gravity Currents in Northern California's Coastal Summer Wind Reversals. *Journal of Geophysical Research,* 92(C2), Pages 1497-1500

Dorman, C., L. Armi, J.M. Bane and D.P. Rogers, 1998: Sea surface mixed layer during the 10-11 June 1994 California Coastally Trapped Event. *Mon. Wea. Rev.,* 126, 600-619

Fu, H., 1993: Numerical simulations of global ocean currents. Undergraduate thesis, Nanjing University, 60pp

Gill, A.E., 1977: Coastally trapped waves in the atmosphere, *Q.J.R. Meteorol. Soc.,* 103, 431-440.

Guan, S., P.L. Jackson and C.J.C. Reason, 1998: Numerical modelling of a Coastally Trapped Disturbance. Part I: Comparison with observations. *Mon. Wea. Rev.* 126(4), 972-990

Holton, J.R., 1979: *Introduction to dynamic meteorology.* Academic Press, 507 pp

Jackson, P.L. and C.J.C. Reason, 1995: Numerical modelling of coastally trapped disturbances. *Preprints of 7th conference on Mountain Meteorology*, Breckenridge, CO, 17-21 July 1995, 189-190.

Jackson, P.L., C.J.C. Reason and S. Guan, 1999: Numerical modeling of a Coastal Trapped Disturbance. Part II: Structure and dynamics. *Mon. Wea. Rev.*, 126, 972-990

Klemp, J.B., R. Rotunno and W.C. Skamarock, 1995: Shallow water simulation of coastally trapped disturbances. *Preprints of the 7th conference on Mountain Meteorology,* Breckenridge, CO, 17-21 July 1995, 197-202

Kubu, C., 1997. Evidence of Coastally Trapped Disturbances Along the Beaufort Sea Coastline. M.S. thesis, University of Western Ontario, 322 pp.

Mass, C.F. and M.D. Albright, 1987: Coastally southerlies and alongshore surges of the West Coast of North America: Evidence of mesoscale topographically trapped response to synoptic forcing. *Mon. Wea. Rev.,* 115, 1707-1738

Mass, C., and N. Bond, 1995: Coastally trapped wind reversals along the U.S. west coast during the warm season. Part II: Synoptic evolution, *Mon. Wea. Rev.,* 124, 446-461

NOAA, cited 1997: NCEP reanalysis project. [Available on-line from http://cdc.noaa.gov/ncep_ reanalysis.]

Nuss, W.A., cited 1997: Coastal Meteorology. [Available on-line from

http://www.met.nps.navy.mil/ nuss/coast.html.]

Persson, P.O.G., P.J. Neiman and F.M. Ralph, 1995: Topographically generated potential vorticity anomalies: A proposed mechanism for initiating orographically trapped disturbances. *Preprint of the 7th Conference on Mountain Meteorology,* Breckenridge, CO, 17-21 July 1995

Pielke, R.A., W.R. Cotton, R. Walko, C.J. Tremback, W.A. Lyons, L.D. Grasso, M.E. Nicholls, M.D. Moran, D.A. Wesesley, T.J. Lee, and J.H. Copeland, 1992: A comprehensive meteorological modelling system - RAMS. *Meteor. Atmos. Phys.*, 49, 69-91.

Rado, S. et al, 1993 *The New International Atlas.* Rand McNally & Company,256 pp

Ralph, F.M., L. Armi, J.M. Bane, C. Dorman, W.D. Neff, P.J. Neiman, W. Nuss and P.O.G. Persson, 1998: Observations and analysis of the 10-11 June 1994 Coastally Trapped Disturbance. *Mon. Wea. Rev.,* 126, 2435-2465.

Ralph, F.M., P.J. Neiman, P.O.G. Persson, W. Neff, J. Miletta, L. Armi, and J. Bane, 1995: Observations of an orographically trapped disturbance along the California coast on 10-11 June 1994. *Preprint of the 7th Conference on Mountain Meteorology,* Breckenridge, CO, 17-21 July 1995, 204-211.

Reason, C.J.C., 1989: Coastally Trapped Disturbances in lower atmopshere. Ph.D. thesis, University of British Columbia, 214pp

Reason, C.J.C., R. Dunkley, 1993: Coastally Trapped Stratus Events in British Columbia, *Atmosphere-Ocean*, 31(2) 1993, 235-258

Reason, C.J.C. and D.G. Steyn, 1992: The dynamics of coastally trapped mesoscale ridges in the lower atmosphere, *J. Atmos. Sci.,* 49, 1677-1692

Rogerson, A.M. and R.M. Samelson, 1995: Synoptic forcing of coastally trapped disturbance in the atmospheric marine boundary layer. *J. Atmos. Sci.,* 52, 2025-2040.

Samelson, R.M. and A.M. Rogerson, 1996: Life-Cycle of a Linear Coastal-Trapped Disturbance. *Mon. Wea. Rev.*,124, 1853-1863

Simpson, J.E., 1987: Gravity Currents: In the Environment and the Laboratory. Ellis Horwood Limited, 244 pp.

Tricker, R.A.R., 1964: Bores, Breakers, Waves and Wakes. Elsevier Publishing Co., 250 pp.

Skamarock, W.C., J.B. Klemp, and R. Rotunno, 1995: Propagation of coastally trapped wave around coastal bends, *Preprints of the 7th conference on Mountain Meteorology*, Breckenridge, CO, 17-21 July 1995, 191-196

Thompson, W.T., T. Haack, J.D. Doyle and S.D. Burk, 1998: A Nonhydrostatic Mesoscale Simulation of the 10-11 June 1994 Coastally Trapped Wind Reversal, *Mon. Wea. Rev.*, 125(12), 3211-3230

Appendix: Some acronyms used in the thesis

Some acronyms used in the thesis are as follows:

CTD: Coastally trapped disturbance

MBL: Marine boundary layer

RAMS: Regional atmospheric modeling system

SST: Sea surface temperature

UTC: Universal time coordinated